Summer 2007

Nonlinear control of nonholonomic mobile robot formations

Travis Alan Dierks

Department:

NONLINEAR CONTROL OF NONHOLONOMIC MOBILE ROBOT FORMATIONS

by

TRAVIS DIERKS

A THESIS

Presented to the Faculty of the Graduate School of the

UNIVERSITY OF MISSOURI-ROLLA

In Partial Fulfillment of the Requirements for the Degree

MASTER OF SCIENCE IN ELECTRICAL ENGINEERING

2007

Approved by

_____	_____
Dr. Jagannathan Sarangapani, Advisor	Dr. Kelvin T. Erickson

_____

Dr. Scott C. Smith

PUBLICATION THESIS OPTION

This thesis consists of the following two articles that have been submitted for publication as follows:

Pages 3 - 47 are intended for submission to 2007 IEEE Transactions on Robotics and Automation.

Pages 48 - 92 are intended for submission to 2007 IEEE Transactions on Neural Networks.

ABSTRACT

In this thesis, the framework developed to control a single nonholonomic mobile robot is expanded to include the control of formations of multiple nonholonomic mobile robots. A combined kinematic/torque control law is developed for leader-follower based formation control using backstepping in order to accommodate the dynamics of the robots and the formation in contrast with kinematic-based formation controllers typically found in literature.

A novel approach is taken in the development of the dynamical controller such that the torque control inputs for the follower robots include the dynamics of the follower robot as well as the dynamics of its leader, and the case when all robot dynamics are known is considered. The asymptotic stability of each robot as well as the entire formation is shown using Lyapunov methods and numerical results are provided. Additionally, a novel obstacle avoidance scheme is introduced that allows each follower robot to navigate around obstacles while simultaneously tracking its leader. The stability of the follower robots as well as the entire formation during an obstacle avoidance maneuver is demonstrated using Lyapunov theory.

Subsequently, an adaptive neural network (NN) is introduced to remove the assumption on the availability of robot dynamics. The inherent NN universal approximation property is used to estimate the dynamics of the follower robot and its leader online, and a kinematic controller is integrated with a NN computed-torque controller. The errors for the entire formation are shown to be uniformly ultimately bounded even in the presence of obstacles.

ACKNOWLEDGMENTS

I would first like to thank my advisor Dr. Jagannathan Sarangapani for his guidance and support over the course of my Master's Program. It has been an honor working with him, and I look forward to continue working with him as I pursue a Ph.D. I also would like to thank Dr. Kelvin T. Erickson and Dr. Scott C. Smith for serving on my committee. I thank the Department of Education for providing financial support through the GAANN Fellowship program. I would also like to thank my parents and my fiancé, Laura, for their support and encouragement. Finally, I would like to thank God for the opportunities I have been presented with.

TABLE OF CONTENTS

Page

PUBLICATION THESIS OPTION……...iii

ABSTRACT……...iv

ACKNOWLEDGMENTS……...v

LIST OF ILLUSTRATIONS……..ix

LIST OF TABLES……..xi

SECTION

1. INTRODUCTION……..…1

PAPER

1. Control of Nonholonomic Mobile Robot Formations: Backstepping Kinematics into Dynamics…… …….3

Abstract...…….....3

I. INTRODUCTION……...……..3

II. NONHOLONOMIC MOBILE ROBOTS.……6

III. LEADER-FOLLOWER FORMATION CONTROL……....8

A. Backstepping Controller Design……..10

B. Leader-Follower Tracking Control……13

C. Dynamics Controller……....19

D. Leader Control Structure……..22

E. Formation Stability……..23

IV. LEADER-FOLLOWER OBSTACLE AVOIDANCE..……..25

A. Obstacle Avoidance……27

B. Formation Stability in the Presence of Obstacles……31

V. SIMULATION RESULTS……..…….....34

A. Scenario I: Obstacle Free Environment ……35

B. Scenario II: Obstacle Ridden Environment……36

VI. CONCLUSIONS……..45

VII. REFERENCES……..46

2. Neural Network Control of Nonholonomic Mobile Robot Formations …….48

Abstract……..…...48

I. INTRODUCTION……..…….48

II. LEADER-FOLLOWER FORMATION CONTROL……..……...51

A. Backstepping Controller Design……..52

B. Leader-Follower Tracking Control……..55

C. Dynamic Controller…….60

D. Leader Control Structure…….…66

E. Formation Stability……..68

III. LEADER-FOLLOWER OBSTACLE AVOIDANCE……70

A. Obstacle Avoidance…….72

B. Formation Stability in the Presence of Obstacles……76

IV. SIMULATION RESULTS……78

A. Scenario I: Obstacle Free Environment ……80

B. Scenario II: Obstacle Ridden Environment…….82

V. CONCLUSIONS……90

VI. REFERENCES……...90

SECTION

2. CONCLUSIONS AND FUTURE WORK……93

VITA……..95

LIST OF ILLUSTRATIONS

Figure Page

PAPER 1

1. Nonholonomic Mobile Robot……...…6
2. Follower *j* Controller Structure ……..……14
3. Leader-Follower Formation Control……...15
4. Obstacle Encounter…….....27
5. Formation Structure……35
6. Trajectory when Dynamics are Included and when Only Kinematics are Considered……..……37
7. Bearing Errors for Dynamical Controller..…….37
8. Separation Errors for Dynamical Controller……..…….38
9. Formation Trajectories with Obstacles…..…….39
10. Zoomed Formation Trajectories with Obstacles…….40
11. Desired Separation for Follower 2……..40
12. Desired Bearing for Follower 2……..41
13. Separation Errors……41
14. Bearing Errors…….42
15. Formation Trajectories in a Dynamic Obstacle Environment……42
16. Zoomed Formation Trajectories in a Dynamic Obstacle Environment……..…43
17. Desired Separation in a Dynamic Obstacle Environment……..43
18. Desired Bearing in a Dynamic Obstacle Environment……...44
19. Separation Tracking Errors in a Dynamic Obstacle Environment.....44

20. Bearing Errors in a Dynamic Obstacle Environment…….45

PAPER 2

1. Follower *j* Controller Structure..…….56
2. Leader-Follower Formation Control..…...…….58
3. Obstacle Encounter..……..72
4. Formation Structure..…….....80
5. Formation Trajectories for Case 1 and Case 2……..81
6. Separation Tracking Errors……..……...81
7. Bearing Tracking Errors…….82
8. Formation Trajectories with Obstacles……...84
9. Zoomed Formation Trajectories with Obstacles…….84
10. Desired Separation for Follower 2 …….85
11. Desired Bearing for Follower 2……..85
12. Separation Errors……86
13. Bearing Errors…….86
14. Formation Trajectories in a Dynamic Obstacle Environment……87
15. Zoomed Formation Trajectories in a Dynamic Obstacle Environment……..87
16. Desired Separation in a Dynamic Obstacle Environment……..88
17. Desired Bearing in a Dynamic Obstacle Environment……88
18. Separation Tracking Errors in a Dynamic Obstacle Environment……...89
19. Bearing Errors in a Dynamic Obstacle Environment……..89

LIST OF TABLES

Table Page

PAPER 1

I. Controller Gains……...……35

II. Obstacle Avoidance Gains……...36

PAPER 2

I. Controller Gains...……80

II. Obstacle Avoidance Gains……...82

SECTION

1. INTRODUCTION

Over the past decade, the attention has shifted from the control of a single nonholonomic mobile robot to the control of multiple mobile robots because of the advantages a team of robots offers. The control of formations of nonholonomic mobile robots typically involves coordinating a group of mobile robots to maintain a specified geometric shape. There are several methodologies to robotic formation control which include behavior-based, generalized coordinates, virtual structures, and leader-follower to name a few. Perhaps the most popular and intuitive approach is the leader-follower method. In this method, a follower robot stays at a specified separation and bearing from a designated leader robot.

A characteristic that is common in many formation control papers is the design of a kinematic controller only. Thus, the dynamics of the robots and the formation are ignored and a perfect velocity tracking assumption is required. In Paper 1, the frameworks developed for controlling single nonholonomic mobile robots are examined and expanded upon to be used in leader-follower formation control. The dynamics of the robots themselves are considered thus incorporating the formation dynamics in the controller design and removing the perfect velocity tracking assumptions. The dynamical extension introduced in this paper provides a rigorous method of taking into account the specific vehicle dynamics to convert a steering system command into control inputs via the backstepping approach. Both feedback velocity control inputs and velocity following control laws are presented for asymptotic stability of the formation. The case when all robot dynamics are known is considered.

Furthermore, a simple but effective obstacle avoidance scheme is proposed that allows each follower robot to navigate around obstacles while simultaneously tracking its leader. The obstacle avoidance method is designed to utilize the ability of each follower robot to maintain a desired location with respect to its leader. In the proposed approach, both the desired separation and desired bearing are altered to ensure the follower robot navigates safely around the encountered obstacle. The proposed obstacle avoidance scheme is shown to achieve stability in the sense of Lyapunov for each follower as well as the entire formation during an obstacle avoidance maneuver.

In Paper 2, an adaptive neural network (NN) is introduced to remove the assumption on the availability of the robot dynamics made in Paper 1. The inherent NN universal approximation property is used to estimate the dynamics of the follower robot and its leader online, and a kinematic controller is integrated with a NN computed-torque controller. The errors for the entire formation are shown to be uniformly ultimately bounded even in the presence of obstacles.

PAPER 1

Control of Nonholonomic Mobile Robot Formations: Backstepping Kinematics into Dynamics[1]

Travis Dierks* and S. Jagannathan

***Abstract*—*In this paper, a combined kinematic/torque control law is developed for leader-follower based formation control using backstepping in order to accommodate the dynamics of the robots and the formation in contrast with kinematic-based formation controllers. The asymptotic stability of the entire formation is guaranteed using Lyapunov theory, and numerical results are provided. The kinematic controller is developed around control strategies for single mobile robots and the idea of virtual leaders. The virtual leader is replaced with a physical mobile robot leader and the assumption of constant reference velocities is removed. An auxiliary velocity control is developed in order to prove the asymptotic stability of the followers which in turn allows the asymptotic stability of the entire formation. A novel approach is taken in the development of the dynamical controller such that the torque control inputs for the follower robots include the dynamics of the follower robot as well as the dynamics of its leader, and the case when all robot dynamics are known is considered. Additionally, a novel obstacle avoidance scheme for leader-follower based formation control is introduced which allows each follower robot to navigate around obstacles while simultaneously tracking its leader. The stability of the follower robots as well as the entire formation during an obstacle avoidance maneuver is demonstrated using Lyapunov methods and numerical results are provided.*

Keywords: Mobile Robot Formation Control, Nonholonomic System, Backstepping Control, Lyapunov Stability, Obstacle Avoidance

I. INTRODUCTION

Over the past decade, the attention has shifted from the control of a single nonholonomic mobile robot [1-5] to the control of multiple mobile robots because of the advantages a team of robots offer such as increased efficiency and more systematic approaches that a team can offer to tasks like search and rescue operations, mapping unknown or hazardous environments, and security and bomb sniffing.

[1] Research Supported in part by GAANN Program through the Department of Education and Intelligent Systems Center. Authors are with the Department of Electrical and Computer Engineering, University of Missouri-Rolla, 1870 Miner Circle, Rolla, MO 65409. Contact author Email: tad5x4@umr.edu.

There are several methodologies [6-18] to robotic formation control which include behavior-based [6][7][8], generalized coordinates [9], virtual structures [10][11], and leader-follower [12][13] to name a few. Perhaps the most popular and intuitive approach is the leader-follower method. In this method, a follower robot stays at a specified separation and bearing from a designated leader robot.

In [12] and [14], local sensory information and a vision based approach to leader-following is undertaken, respectively. In both approaches, the sensory information was used to calculate velocity control inputs. In [15], another kinematic controller is presented making use of a virtual operator multi-agent system (VOMAS) to assist formation control in joining robots into a team or removing robots from a team. A modified leader follower control is introduced in [13] where Cartesian coordinates are used rather than polar. A characteristic that is common in many formation control papers [7-16] is the design of a kinematic controller, thus requiring a perfect velocity tracking assumption.

In [16], it is acknowledged that the separation-bearing methodologies of leader-follower formation control closely resemble a tracking controller problem, and a reactive tracking control strategy that converts a relative pose control into a tracking problem by defining a virtual robot for each follower to track using separation-bearing techniques is presented. A drawback of this controller is the need to define a virtual robot and the fact that dynamics are not considered.

In this paper, we examine frameworks developed for controlling single nonholonomic mobile robots and seek to expand them to be used in leader-follower formation control. Specifically, we examine tracking controllers in the form of [1], [2], and [3]. Like [16],

we seek to convert a relative pose problem into a tracking control problem, but without the use of a virtual robot for the follower. We also seek to bring in the dynamics of the robots themselves thus incorporating the formation dynamics in the controller design. In [17], the dynamics of the follower robot are considered, but the effect the leader's dynamics has on the follower (formation dynamics) is not incorporated. The leader's dynamics become part of the follower robot's control torque input through the derivative of the follower's kinematic velocity control, which is a function of the leader's velocity. In other words, the dynamical extension introduced in this paper provides a rigorous method of taking into account the specific vehicle dynamics to convert a steering system command into control inputs via the backstepping approach. Both feedback velocity control inputs and velocity following control laws are presented for asymptotic stability of the formation.

Furthermore, a simple but effective obstacle avoidance scheme is proposed that allows each follower robot to navigate around obstacles while simultaneously tracking its leader. The obstacle avoidance method is designed to utilize the ability of each follower robot to maintain a desired location with respect to its leader. When an obstacle is encountered, the desired location of the follower robot with respect to its leader is modified so that the follower navigates around the obstacle. In [16], the desired location of a follower with respect to its leader is modified by using separation-bearing [18] based formation control wherein the desired bearing is modified while steering the follower robot around an obstacle. The drawback of only varying the desired bearing is that the new reference point for the follower to track may lie behind the follower robot's current

position which is the case when the magnitude of the new desired bearing is greater than the magnitude of the current one making it undesirable.

By contrast in our approach, both the desired separation and desired bearing are altered to ensure the above scenario does not occur. Our proposed obstacle avoidance scheme is shown to achieve stability in the sense of Lyapunov for each follower as well as the entire formation during an obstacle avoidance maneuver. Simulation results are provided illustrating the effectiveness of the approach in both a static and dynamic environment.

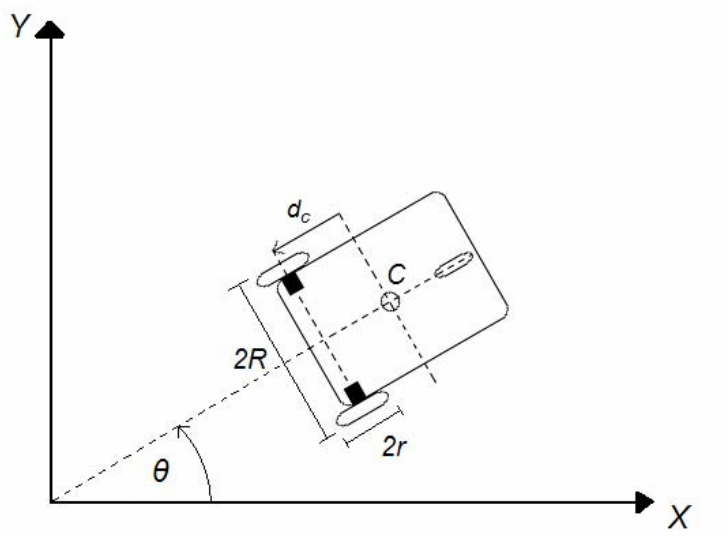

Figure 1: Nonholonomic Mobile Robot

II. NONHOLONOMIC MOBILE ROBOTS

Robotic systems, including the mobile robot depicted in Figure 1, can be characterized as a robotic system having an *n*-dimensional configuration space $\mathcal{C}$ with generalized coordinates $(q_1,...q_n)$ and subject to m constraints can be described by [3]

$$M(q_c)\ddot{q}_c + V_m(q_c,\dot{q}_c)\dot{q}_c + F(\dot{q}_c) + G(q_c) + \tau_d = B(q_c)\tau - A^T(q_c)\lambda \qquad (1)$$

where C denotes a reference point located a distance d_c from the rear axle, $M(q_c) \in \Re^{nxn}$ is the inertial matrix and is positive definite, $V_m(q_c, \dot{q}_c) \in \Re^{nxn}$ is the centripetal/coriolis matrix, $F(\dot{q}_c) \in \Re^{nx1}$ includes the surface friction terms, $G(q_c) \in \Re^{nx1}$ is the gravitational vector, τ_d represents unknown bounded disturbances, $B(q_c) \in \Re^{nxr}$ is an input transformation matrix, $\tau \in \Re^{nx1}$ is the input torque vector, $A(q_c) \in \Re^{mxn}$ is a matrix associated with the system constraints, and $\lambda \in \Re^{mx1}$ is a vector of force constraints.

The nonholonomic constraint of the mobile robot states that the robot can only move in direction normal to the axis of the driving wheel, or mathematically [1] it can be given by

$$\dot{y}_c \cos\theta - \dot{x}_c \sin\theta - d_c\dot{\theta} = 0 . \tag{2}$$

The kinematic constraints of C are considered to be independent of time, and expressed as [1]

$$A(q_c)\dot{q}_c = 0 \tag{3}$$

where $\dot{q}_c$ represents the kinematic equations for the reference point C of the robot in Figure 1. Let $S(q_c)$ be a full rank matrix $(n-m)$ formed by the set of smooth and linearly independent vector fields spanning the null space of $A(q_c)$ such that

$$S^T(q_c)A^T(q_c) = 0 . \tag{4}$$

From (3) and (4), it is possible to find an auxiliary vector time function $v(t) \in \Re^{n-m}$ such that [1][3]

$$\dot{q}_c = \begin{bmatrix} \dot{x}_c \\ \dot{y}_c \\ \dot{\theta} \end{bmatrix} = \begin{bmatrix} \cos\theta & -d_c \sin\theta \\ \sin\theta & d_c \cos\theta \\ 0 & 1 \end{bmatrix} \begin{bmatrix} v \\ \omega \end{bmatrix} \tag{5}$$

where $|v| \le V_{\max}$ and $|\omega| \le \omega_{\max}$ and $V_{\max}$ and $\omega_{\max}$ are the maximum linear and angular velocities of the mobile robot. It is straight forward to verify that (5) satisfies the nonholonomic constraint for C.

The dynamics of the mobile robot can be derived using Lagrangian methods [3] and written in the form (1) where

$$M(q_c) = \begin{bmatrix} m & 0 & md_c \sin\theta \\ 0 & m & -md_c \cos\theta \\ md_c \sin\theta & -md_c \cos\theta & I \end{bmatrix}$$

$$B(q_c) = \frac{1}{r}\begin{bmatrix} \cos\theta & \cos\theta \\ \sin\theta & \sin\theta \\ R & -R \end{bmatrix} \qquad A^T(q_c) = \begin{bmatrix} -\sin\theta \\ \cos\theta \\ -d_c \end{bmatrix}$$

$$V_m(q_c, \dot{q}_c) = \begin{bmatrix} 0 & 0 & md_c\dot{\theta}\cos\theta \\ 0 & 0 & md_c\dot{\theta}\sin\theta \\ 0 & 0 & 0 \end{bmatrix} \qquad G(q_c) = 0$$

$$\lambda = -m(\dot{x}_c \cos\theta + \dot{y}_c \sin\theta)\dot{\theta} \tag{6}$$

The mobile robot dynamics from (1) satisfy [3][19] the following properties:

1. *Boundedness:* $M(q_c)$, the norm of $V_m(q_c, \dot{q}_c)$, and τ_d are all bounded.
2. *Skew Symmetric:* The matrix $\dot{M} - 2V_m$ is skew symmetric such that $\dot{M} - 2V_m = 0$.

III. Leader-Follower Formation Control

The two popular techniques in leader-follower formation control include separation-separation and separation-bearing [12][18]. The goal of separation-bearing formation control is to find a velocity control input such that

$$\lim_{t\to\infty}(L_{ijd} - L_{ij}) = 0 \text{ and } \lim_{t\to\infty}(\Psi_{ijd} - \Psi_{ij}) = 0 \tag{7}$$

where L_{ij} and ψ_{ij} are the measured separation and bearing of the follower robot with L_{ijd} and ψ_{ijd} represent desired distance and angles respectively [12][18]. Only separation-bearing techniques are considered in this paper, but our approach can be extended to separation-separation control.

To avoid collisions, separation distances are measured from the back of the leader to the front of the follower, and the kinematic equations for the front of the j^{th} follower robot can be written as

$$\dot{q}_j = \begin{bmatrix} \dot{x}_j \\ \dot{y}_j \\ \dot{\theta}_j \end{bmatrix} = \begin{bmatrix} \cos\theta_j & -d_j \sin\theta_j \\ \sin\theta_j & d_j \cos\theta_j \\ 0 & 1 \end{bmatrix} \begin{bmatrix} v_j \\ \omega_j \end{bmatrix} = S_j(q_j) v_j \tag{8}$$

where d_j is the distance from the rear axle to the to front of the robot, x_j, y_j, and θ_j are actual Cartesian position and orientation of the physical robot, and v_j, and ω_j are linear and angular velocities, respectively. Using (8), the dynamics from (1) can be rewritten in a transformed form that will be considered throughout this paper for the controller design [1][3]. Substituting the derivative of (8) into (1) as well as multiplying both sides of (1) by S_j^T renders

$$\begin{aligned} S_j^T M_j S_j \dot{v}_j + S_j^T (M_j \dot{S}_j + V_{m_j} S_j) v_j + \overline{F}_j + S_j{}^T \tau_{d\,j} \\ = S_j^T B_j(q_j) \tau_j - S_j^T A_j^T \lambda_j \end{aligned} \tag{9}$$

After appropriate variable redefinitions and applying (4), system (9) takes the form of

$$\overline{M}_j(q_j)\dot{v}_j + \overline{V}_{mj}(q_j, \dot{q}_j) v_j + \overline{F}_j(v_j) + \overline{\tau}_{d_j} = \overline{B}_j(q_j)\tau_j . \tag{10}$$

where $\overline{M}_j \in \Re^{rxr}$ is a symmetric positive definite inertia matrix, $\overline{V}_{mj} \in \Re^{rxr}$ is the bounded centripetal and coriolis matrix, $\overline{F}_j \in \Re^{rx1}$ is the friction vector, $\overline{\tau}_{dj}$ represents unknown

bounded disturbances, and $\bar{\tau}_j = \bar{B}_j \tau \in \Re^{rx1}$ is the input vector. It is important to note the *skew symmetric property* , $\dot{\bar{M}}_j - 2\bar{V}_{mj}(q_j, \dot{q}_j) = 0$, mentioned above still holds [1].

A. Backstepping Controller Design

The complete description of the behavior of a mobile robot is given by (8) and (10). Standard approaches to leader follower formation control deal only with (8) and assume that perfect velocity tracking holds. This paper seeks to remove that assumption by defining the nonlinear feedback control input

$$\tau_j = \bar{B}_j^{-1}(\bar{M}_j u_j + \bar{V}_{mj} v_j + \bar{F}_j(v_j) + \bar{\tau}_{dj}) \tag{11}$$

where u_j is an auxiliary input. Applying this control law to (10) allows one to convert the dynamic control problem into the kinematic control problem [1] such that

$$\begin{aligned} \dot{q}_j &= S_j(q_j) v_j \\ \dot{v}_j &= u_j . \end{aligned} \tag{12}$$

Tracking controller frameworks have been derived for controlling single mobile robots, and there are many ways [1-5] to choose velocity control inputs $v_{jc}(t)$ for steering system (8). To incorporate the dynamics of the mobile platform, it is desirable to convert $v_{jc}(t)$ into a control torque, $\tau_j(t)$ for the physical robot. Contributions in single robot frameworks are now considered and expanded upon in the development a kinematic controller for the separation-bearing formation control technique. Our aim to design a conventional computed torque controller such that (8) and (10) exhibit the desired behavior for a given control $v_{jc}(t)$ thus removing perfect velocity tracking assumptions.

Consider the tracking controller error system presented in [1] used to control a single robot as

$$\begin{bmatrix} e_{j1} \\ e_{j2} \\ e_{j3} \end{bmatrix} = T_{ej}(q_{jr} - q_j) = \begin{bmatrix} \cos\theta_j & \sin\theta_j & 0 \\ -\sin\theta_j & \cos\theta_j & 0 \\ 0 & 0 & 1 \end{bmatrix} \begin{bmatrix} x_{jr} - x_j \\ y_{jr} - y_j \\ \theta_{jr} - \theta_j \end{bmatrix} \tag{13}$$

$$\dot{x}_{jr} = v_{jr}\sin\theta_{jr},\ \ \dot{y}_{jr} = v_{jr}\sin\theta_{jr},\ \ \dot{\theta}_{jr} = \omega_{jr},\ \dot{q}_{jr} = \begin{bmatrix} \dot{x}_{jr} & \dot{y}_{jr} & \dot{\theta}_{jr} \end{bmatrix}^T \tag{14}$$

where x_{jr}, y_{jr}, and θ_{jr} are the positions and orientation of a virtual reference robot j seeks to follow [1].

In a single robot control, a steering control input $v_{jc}(t)$ is designed to solve three basic problems: path following, point stabilization, and trajectory following such that $\lim_{t\to\infty}(q_{jr} - q_j) = 0$ and $\lim_{t\to\infty}(v_{jc} - v_j) = 0$ [1]. If the mobile robot controller can successfully track a class of smooth velocity control inputs, then all three problems can be solved with the same controller [1].

The three basic tracking control problems can be extended to leader-follower based formation control as follows. The virtual reference cart is replaced with a physical mobile robot acting as the leader i, and x_{jr} and y_{jr} are defined as points at a distance L_{ijd} and a desired angle ψ_{ijd} from the lead robot. Now the three basic navigation problems can be introduced for leader-follower formation control as follows.

Tracking: Let there be a leader i for follower j such that

$$\dot{q}_i = \begin{bmatrix} \dot{x}_i \\ \dot{y}_i \\ \dot{\theta}_i \end{bmatrix} = \begin{bmatrix} \cos\theta_i & -d_i\sin\theta_i \\ \sin\theta_i & d_i\cos\theta_i \\ 0 & 1 \end{bmatrix} \begin{bmatrix} v_i \\ \omega_i \end{bmatrix} \tag{15}$$

$$\overline{M}_i(q_i)\dot{v}_i + \overline{V}_{mi}(q_i,\dot{q}_i)v_j + \overline{F}_i(v_i) + \overline{\tau}_{d_i} = \overline{B}_i(q_i)\tau_i \tag{16}$$

$$\begin{aligned} x_{jr} &= x_i - d_i \cos\theta_i + L_{ijd} \cos(\Psi_{ijd} + \theta_i) \\ y_{jr} &= y_i - d_i \sin\theta_i + L_{ijd} \sin(\Psi_{ijd} + \theta_i) \\ \theta_{jr} &= \theta_i \end{aligned} \tag{17}$$

and

$$v_{jr} = [|v_i| \quad |\omega_i|]^T \tag{18}$$

where v_{jr} is the time varying linear and angular speeds of the leader such that $v_{jr} \geq 0$ for all time. Then define the actual position and orientation of follower j as

$$\begin{aligned} x_j &= x_i - d_i \cos\theta_i + L_{ij} \cos(\Psi_{ij} + \theta_i) \\ y_j &= y_i - d_i \sin\theta_i + L_{ij} \sin(\Psi_{ij} + \theta_i) \\ \theta_j &= \theta_j \end{aligned} \tag{19}$$

where L_{ij} and ψ_{ij} are the actual separation and bearing of follower j. In order to solve the formation tracking problem with one follower, find a smooth velocity input $v_{jc} = f(e_{jp}, v_{jr}, K)$ such that $\lim_{t\to\infty}(q_{jr} - q_j) = 0$, where e_{jp}, v_{jr}, and K are the tracking position errors, reference velocity for follower j robot, and gain vector, respectively. Then compute the torque $\tau_j(t)$ for the dynamic system of (10) so that $\lim_{t\to\infty}(v_{jc} - v_j) = 0$. Achieving this for every leader i and follower $j = 1,2,...N$ ensures that the entire formation tracks the formation trajectory.

Path Following: Given a path P_i for leader i as well as the entire formation to follow, define a path P_j relative to P_i as the points at a distance L_{ijd} and an angle ψ_{ijd} for the follower robot j to follow with a linear velocity $v_j(t)$. Find a smooth velocity control input $v_{jc} = f(e_{j\theta}, v_{jr}, b_{ji}, K)$, where $e_{j\theta}$ and b_{ji} are the orientation and distance errors between a reference point of the follower robot j and path P_j, respectively, such that

$\lim_{t\to\infty}(e_{j\theta}) = 0$ and $\lim_{t\to\infty}(b_{ji}) = 0$. Then compute the torque $\tau_j(t)$ for the dynamic system given by (10) so that $\lim_{t\to\infty}(v_{jc} - v_j) = 0$. Achieving this for every leader *i* and follower $j = 1,2,...N$ ensures that the entire formation follows a formation path P_i with a bounded error that is a function of L_{ijd} and ψ_{ijd}.

Point Stabilization: Given an arbitrary configuration of leader *i* denoted as q_i, define a relative reference configuration for follower *j* as q_{jr}. Then find a smooth control velocity input $v_{jc} = f(e_{jp}, v_{jr}, K)$ such that $\lim_{t\to\infty}(q_{jr} - q_j) = 0$. Next, compute the torque $\tau_j(t)$ for the dynamic system of (10) so that $\lim_{t\to\infty}(v_{jc} - v_j) = 0$. Achieving this for every leader *i* and follower $j = 1,2,...N$ ensures the entire formation is stabilized about a reference point at the geometric center of the formation which is defined as the formation trajectory.

B. Leader-Follower Tracking Control

Many solutions [12-16] to the leader-follower formation control problem of (7) and the kinematic model (8) have been suggested and smooth velocity control inputs for the follower have been derived. Unfortunately, dynamical models are rarely studied, and the effect of the dynamics of mobile robot leader *i* on follower *j* has not been well understood in the process of incorporating the dynamics of the formation. This paper will now address these issues.

The contribution in this paper lies in deriving an alternative control velocity, $v_{jc}(t)$, for separation-bearing leader follower formation control, and calculating the specific torque $\tau_j(t)$ to control (10) which accounts for the dynamics of leader *i* as well as the dynamics of follower *j*. It is common in the literature to assume perfect velocity tracking

which does not hold in real applications. To remove this assumption, integrator backstepping is applied. A general control structure for mobile robot follower *j* is presented in Figure 2.

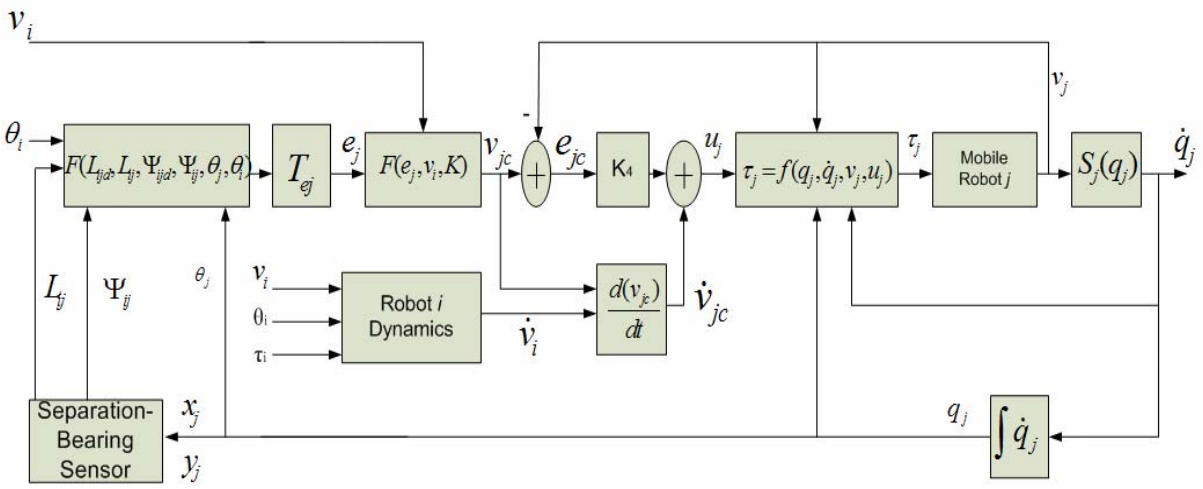

Figure 2: Follower *j* Controller Structure

Using (17), (19) and simple trigonometric identities, the error system (13) can be rewritten as

$$\begin{bmatrix} e_{j1} \\ e_{j2} \\ e_{j3} \end{bmatrix} = \begin{bmatrix} \cos\theta_j & \sin\theta_j & 0 \\ -\sin\theta_j & \cos\theta_j & 0 \\ 0 & 0 & 1 \end{bmatrix} \begin{bmatrix} L_{ijd}\cos(\Psi_{ijd}+\theta_i) - L_{ij}\cos(\Psi_{ij}+\theta_i) \\ L_{ijd}\sin(\Psi_{ijd}+\theta_i) - L_{ij}\sin(\Psi_{ij}+\theta_i) \\ \theta_i - \theta_j \end{bmatrix} \tag{20}$$

and after further simplification (20) can be rewritten as

$$e_j = \begin{bmatrix} e_{j1} \\ e_{j2} \\ e_{j3} \end{bmatrix} = \begin{bmatrix} L_{ijd}\cos(\Psi_{ijd}+e_{j3}) - L_{ij}\cos(\Psi_{ij}+e_{j3}) \\ L_{ijd}\sin(\Psi_{ijd}+e_{j3}) - L_{ij}\sin(\Psi_{ij}+e_{j3}) \\ \theta_i - \theta_j \end{bmatrix} \tag{21}$$

The transformed error system now acts as a formation tracking controller which not only seeks to remain at a fixed desired distance L_{ijd} with a desired angle ψ_{ijd} relative to the lead robot *i*, but also achieves the same orientation as the lead robot which is desirable when $\omega_i = 0$.

In order to calculate the dynamics of the error system (21), it is necessary to calculate the derivatives of L_{ij} and ψ_{ij}, where their desired values L_{ijd} and ψ_{ijd} are considered as constants. Consider the two robot formation depicted in Figure 3. The x and y components of L_{ij} can be defined as

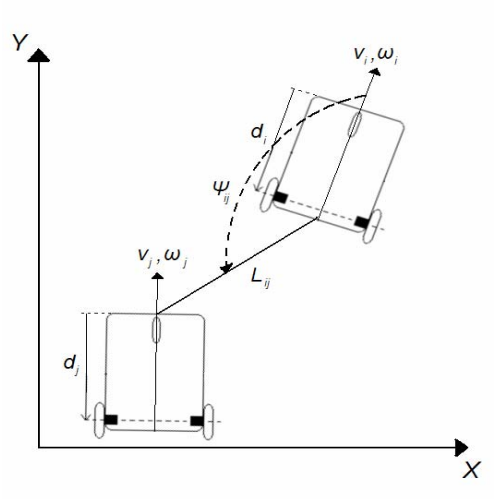

Figure 3: Leader-Follower Formation Control

$$\begin{aligned} L_{ijx} &= x_{i_{rear}} - x_{j_{front}} = x_i - d_i \cos\theta_i - x_j \\ L_{ijy} &= y_{i_{rear}} - y_{j_{rear}} = y_i - d_i \sin\theta_i - y_j \end{aligned} \tag{22}$$

and the derivative of the x and y components of L_{ij} can be found to be

$$\begin{aligned} \dot{L}_{ijx} &= v_i \cos\theta_i - v_j \cos\theta_j + d_j \omega_j \sin\theta_j \\ \dot{L}_{ijy} &= v_i \sin\theta_i - v_j \sin\theta_j - d_j \omega_j \cos\theta_j \end{aligned} \tag{23}$$

Noting that $L_{ij}^2 = L_{ijx}^2 + L_{ijy}^2$ and $\Psi_{ij} = \arctan\left(\frac{L_{ijy}}{L_{ijx}}\right) - \theta_i + \pi$, it can be shown that derivatives of the separation and bearing are consistent with [12] and [18] even when using the kinematics described in (8) such that

$$\begin{aligned}\dot{L}_{ij} &= v_j \cos\gamma_j - v_i \cos\Psi_{ij} + d_j w_j \sin\gamma_j \\ \dot{\Psi}_{ij} &= \frac{1}{L_{ij}}(v_i \sin\Psi_{ij} - v_j \sin\gamma_j + d_j w_j \cos\gamma_j - L_{ij} w_i)\end{aligned} \tag{24}$$

where $\gamma_j = \Psi_{ij} + e_{j3}$.

Now, using the derivative of (21), equation (24) and applying simple trigonometric identities, the error dynamics can be expressed as

$$\begin{bmatrix}\dot{e}_{j1} \\ \dot{e}_{j2} \\ \dot{e}_{j3}\end{bmatrix} = \begin{bmatrix}-v_j + v_i \cos e_{j3} + \omega_j e_{j2} - \omega_i L_{ijd} \sin(\Psi_{ijd} + e_{j3}) \\ -\omega_j e_{j1} + v_i \sin e_{j3} - d_j \omega_j + \omega_i L_{ijd} \cos(\Psi_{ijd} + e_{j3}) \\ \omega_i - \omega_j\end{bmatrix}. \tag{25}$$

Examining (25) and the error dynamics of a tracking controller for a single robot in [1], one can see that dynamics of a single follower with a leader is similar to [1], except additional terms are introduced as a result of (8) and (24).

To stabilize the kinematic system, we propose the following velocity control inputs for follower robot *j* to achieve the desired position and orientation with respect to leader *i* as

$$v_{jc} = \begin{bmatrix}v_{jc} \\ \omega_{jc}\end{bmatrix} = \begin{bmatrix}v_i \cos e_{j3} + k_1 e_{j1} \\ \omega_i + (v_i + k_v) k_2 e_{j2} + (v_i + k_v) k_3 \sin e_{j3}\end{bmatrix} + \begin{bmatrix}\gamma_{vjc} \\ \gamma_{wjc}\end{bmatrix} \tag{26}$$

where

$$\gamma_{vjc} = -\omega_i L_{ijd} \sin(\Psi_{ijd} + e_{j3}) \tag{27}$$

and

$$\gamma_{\omega jc} = -\frac{\left|e_{j2}\right|\left(\omega_i (d_j + L_{ijd}) + (v_i + k_v) k_3 d_j + k_v\right)}{1/k_2 + \left|e_{j2}\right| d_j} \tag{28}$$

Comparing this velocity control with the tracking controller designed for a single robot in [1], one can see that the two are similar except for the novel auxiliary terms

which ensure stability for the formation of two robots using kinematics alone. Additionally, the design parameter k_v was added to ensure that asymptotic stability holds even when $v_i = 0$.

Before we proceed, the following assumptions are needed.

Assumption 1. Complete knowledge of dynamics of follower *j* and leader *i* are known.

Assumption 2. Each follower has full knowledge of its leader's dynamics.

Assumption 3. Follower *j* is equipped with sensors capable of measuring the separation distance L_{ij} and bearing ψ_{ij} and both leader and follower are equipped with instrumentation to measure their linear and angular velocities as well as their orientations θ_i and θ_j.

Assumption 4. Wireless communication is available between follower *j* and leader *i* with communication delays being zero.

Assumption 5. Leader *i* communicates its linear and angular velocities v_i, ω_i as well as its orientation θ_i and control torque τ_i to its followers at each sampling instant.

Assumption 6. For the nonholonomic system of (8) and (10) with n generalized coordinates q, m independent constraints, and r actuators, the number of actuators is equal to the number of degrees of freedom ($r = n - m$).

Assumption 7. The reference linear and angular velocities measured from the leader *i* are bounded and $v_{jr}(t) \geq 0$ for all *t*.

Assumption 8. $K = [k_1 \quad k_2 \quad k_3]^T$ is a vector of positive constants.

Assumption 9. Let perfect velocity tracking hold such that $v_j = v_{jc}$ and $\dot{v}_j = \dot{v}_{jc}$ (this assumption is relaxed later).

Remark: These assumptions are standard in the formation control literature.

Theorem 1: Given the nonholonomic system of (8) and (10) with *n* generalized coordinates *q, m* independent constraints, and *r* actuators, along with the leader follower criterion of (7), let *Assumption 1-9* hold. Let a smooth velocity control input v_{jc} for the follower *j* given by (26), (27), and (28). Then the origin $e_j = 0$ consisting of the position and orientation error for the follower is asymptotically stable.

Proof: Consider the following Lyapunov function candidate

$$V_j = \frac{1}{2}(e_{j1}^2 + e_{j2}^2) + \frac{1-\cos e_{j3}}{k_2} \tag{29}$$

Clearly, $V_j > 0$ and $V_j = 0$ only when $e_j = 0$. Differentiating (29) and substitution of (25) yields

$$\begin{aligned}\dot{V}_j = {} & e_{j1}\left(-v_j + v_i \cos e_{j3} - \omega_i L_{ijd}\sin(\Psi_{ijd} + e_{j3})\right) + e_{j2}\left(v_i \sin e_{j3} - d_j\omega_j + \omega_i L_{ijd}\cos(\Psi_{ijd} + e_{j3})\right) \\ & + \frac{\sin e_{j3}}{k_2}(\omega_i - \omega_j)\end{aligned} \tag{30}$$

Substitution of (26) and (27) renders

$$\begin{aligned}\dot{V}_j = {} & -k_1 e_{j1}^2 - d_j(v_i + k_v)k_2 e_{j2}^2 - (v_i + k_v)\frac{k_3}{k_2}\sin^2 e_{j3} \\ & - e_{j2} d_j\left(\omega_i + (v_i + k_v)k_3 \sin e_{j3} + \omega_i L_{ijd}\cos(\Psi_{ijd} + e_{j3}) + \frac{k_v \sin e_{j3}}{d_j}\right) - \gamma_{\omega jc}\left(\frac{\sin e_{j3}}{k_2} + e_{j2} d_j\right)\end{aligned} \tag{31}$$

Equation (31) can be rewritten as

$$\begin{aligned}\dot{V}_j \le {} & -k_1 e_{j1}^2 - d_j(v_i + k_v)k_2 e_{j2}^2 - \frac{k_3}{k_2}(v_i + k_v)\sin^2 e_{j3} \\ & + \left|e_{j2}\right|\left(\omega_i d_j(1 + L_{ijd}) + (v_i + k_v)k_3 d_j + k_v\right) + \gamma_{\omega jc}\left(\frac{1}{k_2} + \left|e_{j2}\right| d_j\right)\end{aligned} \tag{32}$$

Clearly, the first three terms in (32) are strictly less than zero for $e_j \neq 0$. Now consider the last two terms of (32) in the inequality

$$\left|e_{j2}\right|\left(\omega_i(1+L_{ijd})d_j+(v_i+k_v)k_3d_j+k_v\right)+\gamma_{\omega jc}\left(\frac{1}{k_2}+\left|e_{j2}\right|d_j\right)\leq 0 \tag{33}$$

Substitution of (28) into (33) reveals

$$\dot{V}_j \leq -k_1e_{j1}^2-d_j(v_i+k_v)k_2e_{j2}^2-\frac{k_3}{k_2}(v_i+k_v)\sin^2 e_{j3} \tag{34}$$

Clearly $\dot{V}_j < 0$ for all $v_i \geq 0$, and the velocity control (26), (27) and (28) provides asymptotic stability for the error system (21) and (25) and $e_j \to 0$ as $t \to \infty$.

Remark: The asymptotic stability of the error system (21) and (25) is proven without the use of Barbalat's Lemma which is normally required in [1].

C. Dynamic Controller

Now assume that the perfect velocity tracking assumption does not hold making *Assumption 9* invalid. Define the velocity tracking error as

$$e_{jc} = v_{jc} - v_j \tag{35}$$

Adding and subtracting $\overline{M}_j(q_j)\dot{v}_{jc}$ and $\overline{V}_{mj}(q_j)v_{jc}$ to (10) as well as substituting (35) and its derivative into (10) allows the mobile robot dynamics to be written in terms of the velocity tracking error and its derivative as

$$\overline{M}_j(q_j)\dot{e}_{jc} = -\overline{V}_{mj}(q_j,\dot{q}_j)e_{jc} - \overline{\tau}_j + f_j(x) + \overline{\tau}_{dj} \tag{36}$$

where

$$f_j(x_j) = \overline{M}_j(q_j)\dot{v}_{jc} + \overline{V}_{mj}(q_j,\dot{q}_j)v_{jc} + \overline{F}_j(v_j) \tag{37}$$

with $x_j = [\dot{v}_i, \dot{\omega}_i, v_i, \omega_i, q_j^T, v_j, w_j, e_j^T, \dot{e}_j^T]^T$. The function $f_j(x_j)$ in (37) will be used to bring in the dynamics of leader *i* through $\dot{v}_{jc}$ by observing that

$$\dot{v}_{jc} = f_{vcj}(\dot{v}_i, \dot{\omega}_i, v_i, \omega_i, e_j, \dot{e}_j). \tag{38}$$

The leader *i*'s dynamics (16) can be rewritten as

$$\dot{v}_i = \bar{M}_i^{-1}(q_i)(\bar{B}_i(q_i)\tau_i - \bar{V}_{m_i}(q_i, \dot{q}_i)v_i - \bar{F}_i(v_i) - \bar{\tau}_{d_i}) \tag{39}$$

Substituting (39) into (38) results in the dynamics for leader *i* to become apart of $\dot{v}_{jc}$ as

$$\dot{v}_{jc} = f_{vcj}(v_i, \omega_i, \theta_i, \tau_i, e_j, \dot{e}_j) \tag{40}$$

Under *Assumptions 1-5*, follower *j* is able to construct $\dot{v}_{jc}$. Defining the auxiliary control input u_j from (12) to be [1]

$$u_j = \dot{v}_{jc} + K_4 e_{jc}, \tag{41}$$

the control torque for the j^{th} follower robot can be written in the form

$$\tau_j = \bar{B}_j^{-1}(\bar{M}_j K_4 e_{jc} + f_j(x_j)) \tag{42}$$

where K_4 is a positive definite matrix defined by

$$K_4 = k_4 I \tag{43}$$

Substituting (42) into the dynamics of follower robot *j* (10) produces the closed loop error dynamics shown below.

$$\bar{M}_j \dot{e}_{jc} = -(\bar{M}_j K_4 + \bar{V}_{mj}) e_{jc} + \bar{\tau}_{dj} \tag{44}$$

Remark: In [1], the reference velocity is considered to be constant, therefore the dynamics of the reference cart are never considered. That assumption is not being made here since the reference cart has been replaced by a physical robot *i*. Thus, the dynamics

of leader robot *i* must be considered and become an important term in follower *j*'s torque command.

Theorem 2: Let *Assumptions 1-8* hold, and let k_4 in (43) be a sufficiently large positive constant. Let a smooth velocity control input $v_{jc}(t)$ for the j^{th} follower be defined by (26), (27) and (28). Let the torque control (42) be applied for the j^{th} follower robot system (10). Then the origin $e_j = 0$ and $e_{jc} = 0$ which are the position, orientation and velocity tracking errors for follower *j* are asymptotically stable.

Proof : Consider the following Lyapunov candidate:

$$V_j' = V_j + \frac{1}{2} e_{jc}^T \overline{M}_j e_{jc} \tag{45}$$

where V_j is defined as (29). Differentiating (45) yields

$$\dot{V}_j' = \dot{V}_j + e_{jc}^T \overline{M}_j \dot{e}_{jc} + \frac{1}{2} e_{jc}^T \dot{\overline{M}}_j e_{jc} \tag{46}$$

In *Theorem 1,* it was proved that $\dot{V}_j < 0$. Assuming an ideal case such that the disturbance $\overline{\tau}_{dj} = 0$ and substituting (44) into (46), gives

$$\dot{V}_j' = \dot{V}_j - e_{jc}^T (\overline{M}_j K_4) e_{jc} + \frac{1}{2} e_{jc}^T (\dot{\overline{M}}_j - 2\overline{V}_{mj}) e_{jc} \tag{47}$$

After applying the *skew symmetric property,* (47) can be rewritten as

$$\dot{V}_j' = \dot{V}_j - e_{jc}^T (\overline{M}_j K_4) e_{jc} \tag{48}$$

Examining (48), it is clear that $\dot{V}_j' < 0$ and the position tracking error system $e_j = 0$ and velocity tracking error system $e_{jc} = 0$ are asymptotically stable.

D. Leader Control Structure

In every formation, we assume there is a leader *i* such that the following assumptions hold:

Assumption 10. The formation leader follows no physical robots, but follows the virtual leader described in [1].

Assumption 11. The formation leader is capable of measuring its absolute position via instrumentation like GPS so that tracking the virtual robot is possible.

The kinematics and dynamics of the formation leader *i* are defined by (15) and (16), respectively. From [1], the leader tracks a virtual reference robot with the kinematic constraints of (14), and the tracking error for the leader and its derivative are found to be

$$e_i = \begin{bmatrix} e_{i1} \\ e_{i2} \\ e_{i3} \end{bmatrix} = \begin{bmatrix} \cos\theta_i & \sin\theta_i & 0 \\ -\sin\theta_i & \cos\theta_i & 0 \\ 0 & 0 & 1 \end{bmatrix} \begin{bmatrix} x_r - x_i \\ y_r - y_i \\ \theta_r - \theta_i \end{bmatrix} \tag{49}$$

and

$$\dot{e}_i = \begin{bmatrix} \dot{e}_{i1} \\ \dot{e}_{i2} \\ \dot{e}_{i3} \end{bmatrix} = \begin{bmatrix} -v_i + v_{ir}\cos e_{i3} + \omega_i e_{i2} \\ -\omega_i e_{i1} + v_{ir}\sin e_{i3} \\ \omega_{ir} - \omega_i \end{bmatrix} \tag{50}$$

The control velocity $v_{ic}(t)$ can be defined as [1]

$$v_{ic} = \begin{bmatrix} v_{ir}\cos e_{i3} + k_{i1}e_{i1} \\ \omega_{ir} + k_{i2}v_{ir}e_{i2} + k_{i3}v_{ir}\sin e_{i3} \end{bmatrix} \tag{51}$$

Using similar steps and justification to form (36) and (37), the leader's error system can be formed similarly to follower *j's* and the leader's torque $\bar{\tau}_i$ is defined as [1]

$$\tau_i = \bar{B}_i^{-1}(\bar{M}_i(K_{i4}e_{ic} + \dot{v}_{ic}) + \bar{V}_{mi}v_i + \bar{F}_i(x_i)) \tag{52}$$

where e_{ic} and K_{i4} are defined similarly to (35) and (43). Substitution of (52) into the leader's error system in the form of (36), the closed loop error system can be written as

$$\overline{M}_i \dot{e}_{ic} = -(\overline{M}_i K_{i4} + \overline{V}_{ij}) e_{ic} + \overline{\tau}_{di} \tag{53}$$

The following additional mild assumptions are needed before proceeding.

Assumption 12. The reference linear velocity v_{ir} is greater than zero and bounded and the reference angular velocity ω_{ir} is bounded for all *t*.

Assumption 13. $K_i = [k_{i1} \quad k_{i2} \quad k_{i3}]^T$ is a vector of positive constants.

Theorem 3 [1]: Given the kinematic system of (15) and dynamic system of (16) for leader *i* with *n* generalized coordinates q_i, *m* independent constraints, and *r* actuators, let *Assumptions 1-6* and *Assumptions 10-13* hold. Let k_{i4} be a sufficiently large positive constant. Let there be a smooth velocity control input $v_{ic}(t)$ for the leader *i* given by (51). Let the torque control (52) for the lead robot *i* (16) be applied. Then the origin consisting of $e_i = 0$ and $e_{ic} = 0$, which denote the position, orientation and velocity tracking errors for leader *i* are asymptotically stable.

Next the stability of the formation is introduced.

E. Formation Stability

The stability of the formation can be demonstrated by using the individual Lyapunov functions as given in the following theorem.

Theorem 4: Consider a formation of *N+1* robots consisting a leader *i* and *N* followers. Let *Assumptions 1-8* and *10-13* hold. Let k_4 and k_{i4} be sufficiently large positive constants. Let there be a smooth velocity control input $v_{ic}(t)$ for the leader *i* given by (51), and let the torque control from (52) for the lead robot *i* (16) be applied. Let there be a smooth velocity control input $v_{jc}(t)$ given by (26), (27), and (28) for the j^{th}

follower and torque control given by (42) for the j^{th} follower robot (10) be applied and assume no disturbances. Then the origin $e_{ij} = [e_i^T \quad e_{ic}^T \quad e_j^T \quad e_{jc}^T]^T = 0$ where $e_{ij} \in \Re^{(n+r)(1+N)x1}$ represents the augmented position, orientation and velocity tracking error systems for the leader *i* and *N* followers, respectively is asymptotically stable.

Proof: Consider the following Lyapunov candidate

$$V_{ij} = \sum_{1}^{N} V_j' + V_i \tag{54}$$

where V_j' is defined by (45) and

$$V_i = \frac{1}{2}(e_{i1}^2 + e_{i2}^2) + \frac{1}{k_{i2}}(1 - \cos e_{i3}) + \frac{1}{2} e_{ic}^T \overline{M}_i e_{ic}. \tag{55}$$

Examining (45) and (55) it can be concluded that (54) is positive for $e_{ij} \neq 0$. Taking the derivative of (54) yields

$$\dot{V}_{ij} = \sum_{1}^{N} \dot{V}_j' + \dot{V}_i. \tag{56}$$

It was shown in *Theorem 2* that $\dot{V}_j' < 0$ for all *j* in *N*, so clearly

$$\sum_{1}^{N} \dot{V}_j' < 0 \tag{57}$$

Assuming $\overline{\tau}_{di} = 0$ and substituting the leader's position error dynamics (50), control velocities (51), and velocity tracking error dynamics (53) into the derivative of V_i gives

$$\dot{V}_i = -k_{i1}^2 e_{i1}^2 - \frac{k_{i3}}{k_{i2}} v_{ir} \sin^2 e_{i3} - e_{ic}^T (\overline{M}_i K_{i4}) e_{ic} + \frac{1}{2} e_{ic}^T (\dot{\overline{M}}_i - 2\overline{V}_{mi}) e_{ic} \tag{58}$$

After applying the *skew symmetric property*, (58) can be rewritten as

$$\dot{V}_i = -k_{i1}^2 e_{i1}^2 - \frac{k_{i3}}{k_{i2}} v_{ir} \sin^2 e_{i3} - e_{ic}^T (\overline{M}_i K_{i4}) e_{ic} \tag{59}$$

From (59), it can only be concluded that $\dot{V}_{ij}$ is negative semi-definite and therefore e_{ij} is bounded. Examining the error systems, control velocities and torques for the leader *i* and its followers, it can be deduced that $\|e_{ij}\|$ and $\|\dot{e}_{ij}\|$ are bounded. Furthermore, it is not difficult to show that $\|\ddot{V}_{ij}\| < \infty$ and therefore $\dot{V}_{ij}$ is uniformly continuous. Therefore, by Barbalat's Lemma [19], $\dot{V}_{ij} \to 0$ and thus $e_j \to 0$, $e_{jc} \to 0$, and $e_{ic} \to 0$ as $t \to \infty$. Then from (59)

$$k_{i1}^2 e_{i1}^2 + \frac{k_{i3}}{k_{i2}} v_{ir} \sin^2 e_{i3} = 0 \tag{60}$$

which implies $e_{i1} \to 0$ and $e_{i3} \to 0$ as $t \to \infty$. Examining (51) and the definition of e_{ic}, it is then straight forward to verify that $e_{i2} \to 0$ as $t \to \infty$. Therefore, the entire formation is asymptotically stable.

*Remark: T*he asymptotic stability of a formation for the case when follower *j* becomes a leader to follower *j+1* follows directly from *Theorem 2* and the Lyapunov candidate

$$V_j'' = \sum_j^{j+1} V_j' \tag{61}$$

where V_j' is defined in (35).

IV. Leader-Follower Obstacle Avoidance

In the previous section, a tracking controller for leader-follower based formation control was developed that sought to drive follower *j* to a reference location and desired

orientation with respect to leader *i*. However, with the introduction of obstacle avoidance schemes, the orientation of the follower *j* will vary from its leader's as a result of avoiding an obstacle that was in the path of follower *j* but not its leader. Therefore, when an obstacle is encountered, it is logical for follower *j* to track a reference point, but no specific orientation with respect to its leader so that it can avoid the obstacle.

The proposed obstacle avoidance scheme is designed to take advantage of the tracking ability of the follower robots. When an obstacle is encountered, the desired separation and bearing is redefined so that the follower robot is guided around the obstacle. To accomplish this, the desired separation and bearing are no longer considered to be constants but are considered to be time varying.

Remark: In this section, the time varying desired separation and bearing will be denoted as $L_{ijd}(t)$ and $\psi_{ijd}(t)$ while the constant desired separation and bearing will be written as L_{ijd} and ψ_{ijd}.

Consider the formation tracking control error system presented in (21), but rewritten as

$$e_{jo} = \begin{bmatrix} e_{jo1} \\ e_{jo2} \end{bmatrix} = \begin{bmatrix} L_{ijd}(t)\cos(\Psi_{ijd}(t) + \bar{\theta}_j) - L_{ij}\cos(\Psi_{ij} + \bar{\theta}_j) \\ L_{ijd}(t)\sin(\Psi_{ijd}(t) + \bar{\theta}_j) - L_{ij}\sin(\Psi_{ij} + \bar{\theta}_j) \end{bmatrix} \tag{62}$$

where $\bar{\theta}_j = \theta_i - \theta_j$ and only the normal and tangential components of the separation and bearing errors are considered. The dynamics of (62) can be found in a similar manner used to derive (25), and written as

$$\begin{bmatrix} \dot{e}_{jo1} \\ \dot{e}_{jo2} \end{bmatrix} = \begin{bmatrix} \dot{\bar{e}}_{jo1} - v_j + v_i\cos\bar{\theta}_j + \omega_j e_{jo2} - \omega_i L_{ijd}(t)\sin(\Psi_{ijd} + \bar{\theta}_j) \\ \dot{\bar{e}}_{jo2} - \omega_j e_{jo1} + v_i\sin\bar{\theta}_j - d_j\omega_j + \omega_i L_{ijd}(t)\cos(\Psi_{ijd} + \bar{\theta}_j) \end{bmatrix} \tag{63}$$

where

$$\dot{\bar{e}}_{jo1} = \dot{L}_{ijd}(t)\cos(\Psi_{ijd}(t) + \bar{\theta}_j) - \dot{\Psi}_{ijd}(t)L_{ijd}(t)\sin(\Psi_{ijd}(t) + \bar{\theta}_j) \tag{64}$$

and

$$\dot{\bar{e}}_{jo2} = \dot{L}_{ijd}(t)\sin(\Psi_{ijd}(t) + \bar{\theta}_j) + \dot{\Psi}_{ijd}(t)L_{ijd}(t)\cos(\Psi_{ijd}(t) + \bar{\theta}_j) \tag{65}$$

Comparing (63) with (25), one can see that they are identical except for the terms added as a result of the time varying desired separation and bearing.

A. Obstacle Avoidance

Consider the configuration shown in Figure 4. It is desired that follower robot *j* maintains a distance s_d from all obstacles; therefore, to navigate around the obstacle, the following simple approach is proposed.

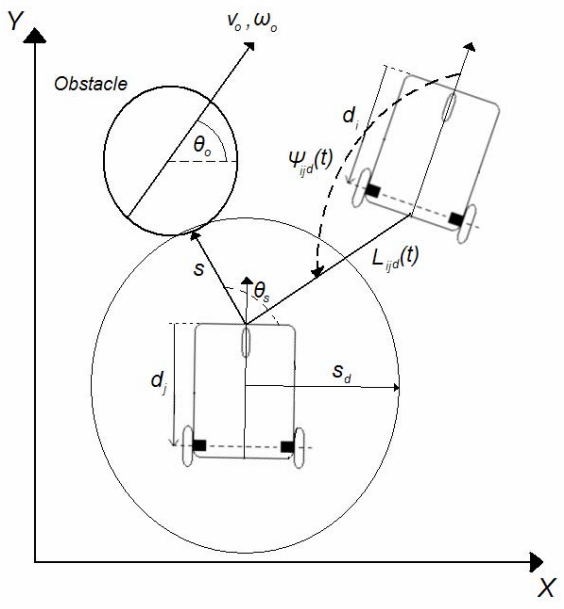

Figure 4: Obstacle Encounter

When the nearest edge of an obstacle is detected at an angle θ_s and distance *s* relative to follower *j* such that $s < s_d$, the desired separation and bearing, $L_{ijd}(t)$ and $\psi_{ijd}(t)$, are modified such that the follower is steered away from the obstacle by

$$L_{ijd}(t) = L_{ijd} - \frac{1}{2}K_L\left(\frac{1}{s} - \frac{1}{s_d}\right)^2$$
$$\Psi_{ijd}(t) = \Psi_{ijd} + \frac{1}{2}K_\Psi\left(\frac{1}{s} - \frac{1}{s_d}\right)^2 \operatorname{sgn}(\Psi_{ijd}) \tag{66}$$

where *sgn* is the signum function and K_L and K_ψ are positive design constants. Examining (66), one can see that the shifts introduced to the desired separation and bearing are similar to repulsive potential functions commonly used in robotic path planning [20]. Here we use the potential like function to push the desired set point of the follower robot *j* away from the encountered obstacle thus steering the robot around the obstruction.

In order to calculate the expressions in (64) and (65), derivatives of the desired separation and bearing are necessary. The measured distance *s* and angle θ_s can be written in terms of the *x* and *y* components *s* as

$$s^2 = s_x^2 + s_y^2$$
$$\theta_s = \arctan\left(\frac{s_y}{s_x}\right) \tag{67}$$

where
$$s_x = x_j - x_o$$
$$s_y = y_j - y_o \tag{68}$$

and x_o and y_o are the coordinates of the obstacle. Note that the obstacle is not necessarily stationary, and assume that the obstacle can be defined by the kinematic model

$$\dot{x}_o = v_o \cos\theta_o$$
$$\dot{y}_o = v_o \sin\theta_o \tag{69}$$

Differentiating (67) and (68), and substitution of (8) and (69) reveals

$$\begin{aligned}\dot{s} &= v_j \cos(\theta_j - \theta_s) - d_j w_j \sin(\theta_j - \theta_s) - v_o \cos(\theta_o - \theta_s) \\ \dot{\theta}_s &= \frac{1}{s}(v_j \sin(\theta_j - \theta_s) + d_j w_j \cos(\theta_j - \theta_s) - v_o \sin(\theta_o - \theta_s))\end{aligned} \tag{70}$$

Before continuing, the following assumptions are required.

Assumption 14. Follower *j* and the leader *i* are equipped with instrumentation capable of measuring the distance *s* and relative angle of the obstacle θ_s.

Assumption 15. The velocity v_o and orientation θ_o of the obstacle are not available to follower *j* and leader *i.*

Since the velocity v_o and orientation θ_o of the obstacle are not available to follower *j,* the derivatives in (70) must be estimated. Assuming that $\dot{s}$ and $\dot{\theta}_s$ are smooth functions, define the estimates of $\dot{s}$ and $\dot{\theta}_s$ using standard backwards difference equations as

$$\begin{aligned}\dot{\hat{s}} &= s(t) - s(t - \Delta t) \\ \dot{\hat{\theta}}_s &= \theta_s(t) - \theta_s(t - \Delta t)\end{aligned} \tag{71}$$

where Δt is an arbitrarily small sampling period.

Now we can define the derivative of (66) as

$$\begin{aligned}\dot{L}_{ijd}(t) &= K_L\left(\frac{1}{s} - \frac{1}{s_d}\right)\frac{1}{s^2}\dot{\hat{s}} \\ \dot{\Psi}_{ijd}(t) &= -\operatorname{sgn}(\Psi_{ijd})K_\psi\left(\frac{1}{s} - \frac{1}{s_d}\right)\frac{1}{s^2}\dot{\hat{s}}\end{aligned} \tag{72}$$

Substitution of (72) into the error dynamics defined in (64) and (65) yields

$$\dot{\hat{e}}_{jo1} = K_L\left(\frac{1}{s} - \frac{1}{s_d}\right)\frac{1}{s^2}\dot{\hat{s}}\cos(\Psi_{ijd}(t) + \bar{\theta}_j) + \operatorname{sgn}(\Psi_{ijd})K_\psi\left(\frac{1}{s} - \frac{1}{s_d}\right)\frac{1}{s^2}\dot{\hat{s}}L_{ijd}(t)\sin(\Psi_{ijd}(t) + \bar{\theta}_j) \tag{73}$$

$$\dot{\hat{e}}_{jo2} = K_L\left(\frac{1}{s} - \frac{1}{s_d}\right)\frac{1}{s^2}\dot{\hat{s}}\sin(\Psi_{ijd}(t) + \bar{\theta}_j) - \operatorname{sgn}(\Psi_{ijd})K_\psi\left(\frac{1}{s} - \frac{1}{s_d}\right)\frac{1}{s^2}\dot{\hat{s}}L_{ijd}(t)\cos(\Psi_{ijd}(t) + \bar{\theta}_j) \tag{74}$$

To stabilize the error dynamics in the presence of an obstacle, the following velocity control inputs for follower robot *j* is proposed to achieve the desired position and orientation with respect to leader *i* as

$$v_{jco} = \begin{bmatrix} v_{jco} \\ \omega_{jco} \end{bmatrix} = \begin{bmatrix} v_i \cos\bar{\theta}_j + k_1 e_{j1} - \omega_i L_{ijd} \sin(\Psi_{12d} + \bar{\theta}_j) \\ \frac{1}{d_j}(\omega_i L_{ijd} \cos(\Psi_{ijd} + \bar{\theta}_j) + k_2 e_{j2} + v_i \sin\bar{\theta}_j) \end{bmatrix} + \begin{bmatrix} \dot{\hat{e}}_{j1} \\ \frac{\dot{\hat{e}}_{j2}}{d_j} \end{bmatrix} \tag{75}$$

Theorem 5: Given the kinematic model of nonholonomic mobile robot in (8), along with the leader follower criterion of (7), let *Assumptions 1-7* and *Assumption 9* hold. Let k_1, k_2, K_L and K_ψ be positive constants, and let the smooth velocity control input $v_{jco}(t)$ for the j^{th} follower be given by (75). Then the origin $e_{jo} = 0$ consisting of the position error for the follower is stable in the sense of Lyapunov.

Proof: Consider the following Lyapunov candidate

$$V_{jo} = \frac{1}{2}(e_{jo1}^2 + e_{jo2}^2) \tag{76}$$

Clearly, $V_{jo} > 0$ and $V_{jo} = 0$ only when $e_{jo} = 0$. Taking the time derivate of (76) and substitution of the error dynamics (63) reveals

$$\begin{aligned} \dot{V}_{jo} = e_{jo1}(\dot{\bar{e}}_{jo1} - v_j + v_i \cos\bar{\theta}_j - \omega_i L_{ijd}(t) \sin(\Psi_{ijd} + \bar{\theta}_j)) \\ + e_{jo2}(\dot{\bar{e}}_{jo2} + v_i \sin\bar{\theta}_j - d_j \omega_j + \omega_i L_{ijd}(t) \cos(\Psi_{ijd} + \bar{\theta}_j)) \end{aligned} \tag{77}$$

Substitution of (75) into (77) reveals

$$\dot{V}_{jo} = -k_1 e_{jo1}^2 - k_2 e_{jo2}^2 + e_{jo1}\dot{\tilde{e}}_{sj1} + e_{jo2}\dot{\tilde{e}}_{sj2} \tag{78}$$

where $\dot{\tilde{e}}_{sj1} = \dot{\bar{e}}_{jo1} - \dot{\hat{e}}_{jo1}$ and $\dot{\tilde{e}}_{sj2} = \dot{\bar{e}}_{jo2} - \dot{\hat{e}}_{jo2}$. Equation (78) can then be rewritten as

$$\dot{V}_{jo} \le -\bar{k}\left\|e_{jo}\right\|^2 + \varepsilon_j \left\|e_{jo}\right\| \tag{79}$$

where $\bar{k} = \min(k_1, k_2)$ and $\varepsilon_j = \left|\dot{\tilde{e}}_{sj1}\right| + \left|\dot{\tilde{e}}_{sj2}\right|$. Completing the square with respect to $\left\|e_{jo}\right\|$ yields

$$\dot{V}_{jo} \leq -\frac{\bar{k}}{2}\left\|e_{jo}\right\|^2 - \frac{\bar{k}}{2}\left(\left\|e_{jo}\right\| - \frac{\varepsilon_j}{\bar{k}}\right)^2 + \frac{\varepsilon_j^2}{2\bar{k}} \tag{80}$$

and it can be concluded that the formation errors are bounded during an obstacle avoidance maneuver. Note that the bounds on the formation error system can be made arbitrary small by increasing $\bar{k}$.

Remark: In order to remove the perfect velocity tracking assumption of *Assumption 9,* the dynamic control presented in *Theorem 2* can be applied by replacing the velocity control input (26) with (75) when in the presence of an obstacle. Also, since leader robot *i* does not track a physical robot, any existing obstacle avoidance method can be utilized by the leader. When the leader robot performs an obstacle avoidance maneuver, the entire formation will continue to track the leader, and once the leader has steered around the obstacle, the followers can navigate the obstruction on an individual bases. That is, the obstacle avoidance method selected for the leader does not affect the stability of the entire formation in the presence of obstacles.

B. Formation Stability in the Presence of Obstacles

Before proving the stability of the entire formation in the presence of obstacles, an additional assumption is required.

Assumption 16. Leader *i* utilizes a path planning algorithm such that by tracking the virtual reference cart described in [1], the lead robot *i* navigates around any encountered obstacles.

Under *Assumption 16*, the lead robot *i* navigates around the obstacles by tracking its virtual reference cart. Therefore, the controller described in *Theorem 3* is used to control the leader in both the absence and presence of obstacles. The path planning algorithm for the leader *i* is beyond the scope of this paper and therefore is not included here.

Theorem 6. Consider a formation of *N+1* robots consisting of a leader *i* and *N* followers in the presence of obstacles. Let *Assumptions 1-7* and *10-16* hold. Let k_1, k_2, K_L, K_ψ, k_4 and k_{i4} be sufficiently large positive constants. Let there be a smooth velocity control input $v_{ic}(t)$ for the leader *i* given by (51), and let the torque control for the lead robot *i* from (52) be applied to the mobile robot system (16). Let there be a smooth velocity control input $v_{jco}(t)$ for the j^{th} follower given by (75) and torque control for the j^{th} follower robot given by (42) be applied to the mobile robot system (10). Then the origin $e_{ijo} = [e_i^T \quad e_{ic}^T \quad e_{jo}^T \quad e_{jc}^T]^T = 0$ where $e_{ijo} \in \Re^{(r(1+N)+n+(n-1)N)x1}$ is the augmented position, orientation and velocity tracking error systems for the leader *i* and the position and velocity tracking error systems for *N* followers, respectively is stable in the sense of Lyapunov.

Proof: Consider the following Lyapunov candidate

$$V_{ijo} = \sum_{1}^{N} V'_{jo} + V_i \tag{81}$$

where V_i is defined in (55) and

$$V'_{jo} = \frac{1}{2}(e_{jo1}^2 + e_{jo2}^2) + \frac{1}{2} e_{jc}^T \overline{M}_j e_{jc} \tag{82}$$

Differentiating (81) yields

$$\dot{V}_{ijo} = \sum_{1}^{N} \dot{V}'_{jo} + \dot{V}_i \tag{83}$$

and it was shown in *Theorem 3* that the derivative of (55) can be written as

$$\dot{V}_i = -k_{i1}^2 e_{i1}^2 - \frac{k_{i3}}{k_{i2}} v_{ir} \sin^2 e_{i3} - e_{ic}^T (\overline{M}_i K_{i4}) e_{ic} \tag{84}$$

after substitution of the error dynamics and control inputs (50), (51), and (52), respectively. Substitution of the error dynamics and control inputs (63), (75), and (42), respectively, into $\dot{V}'_{jo}$ reveals

$$\sum_{1}^{N} \dot{V}'_{jo} = \sum_{1}^{N} \left(- k_1 e_{jo1}^2 - k_2 e_{jo2}^2 + e_{jo1} \dot{\tilde{e}}_{sj1} + e_{jo2} \dot{\tilde{e}}_{sj2} \right) - \sum_{1}^{N} \left(e_{jc}^T (\overline{M}_j K_4) e_{jc} \right) \tag{85}$$

where $\dot{\tilde{e}}_{sj1} = \dot{\bar{e}}_{jo1} - \dot{\hat{\bar{e}}}_{jo1}$ and $\dot{\tilde{e}}_{sj2} = \dot{\bar{e}}_{jo2} - \dot{\hat{\bar{e}}}_{jo2}$. Noting the similarities of the first summation with *Theorem 5* allows (85) to be written as

$$\sum_{1}^{N} \dot{V}'_{jo} \le \sum_{1}^{N} \left(- \bar{k} \left\| e_{jo} \right\|^2 + \varepsilon_j \left\| e_{jo} \right\| \right) - \sum_{1}^{N} \left(e_{jc}^T (\overline{M}_j K_4) e_{jc} \right) \tag{86}$$

where $\bar{k} = \min(k_1, k_2)$ and $\varepsilon_j = \left| \dot{\tilde{e}}_{sj1} \right| + \left| \dot{\tilde{e}}_{sj2} \right|$. Completing the square with respect to each $\left\| e_{jo} \right\|$ yields

$$\sum_{1}^{N} \dot{V}'_{jo} \le \sum_{1}^{N} \left(-\frac{\bar{k}}{2} \left\| e_{jo} \right\|^2 - \frac{\bar{k}}{2} \left(\left\| e_{jo} \right\| - \frac{\varepsilon_j}{\bar{k}} \right)^2 + \frac{\varepsilon_j^2}{2\bar{k}} \right) - \sum_{1}^{N} \left(e_{jc}^T (\overline{M}_j K_4) e_{jc} \right) \tag{87}$$

and (87) can be rewritten as

$$\sum_{1}^{N} \dot{V}'_{jo} \le - \sum_{1}^{N} \left(\frac{\bar{k}}{2} \left\| e_{jo} \right\|^2 + \frac{\bar{k}}{2} \left(\left\| e_{jo} \right\| - \frac{\varepsilon_j}{\bar{k}} \right)^2 \right) - \sum_{1}^{N} \left(e_{jc}^T (\overline{M}_j K_4) e_{jc} \right) + \sum_{1}^{N} \frac{\varepsilon_j^2}{2\bar{k}} \tag{88}$$

Note that the first two summations in (88) are always less than or equal to zero, and the last summation can be made arbitrarily small by increasing $\bar{k}$. Therefore, combining (84)

and (88) reveals that the entire formation is stable in the sense of Lyapunov in the presence of obstacles.

Remark: The stability of the formation for the case when follower *j* becomes a leader to follower *j+1* follows directly from the Lyapunov candidate

$$\overline{V}_{jo} = \sum_{j}^{j+1}\left(\frac{1}{2}(e_{jo1}^2 + e_{jo2}^2) + \frac{1}{2}e_{jc}^T \overline{M}_j e_{jc}\right) \tag{89}$$

and noting equation (88).

V. Simulation Results

A wedge formation of five identical nonholonomic mobile robots is considered where the leader's trajectory is the desired formation trajectory, and simulations are carried out in MATLAB under two scenarios: with and without obstacles. First, in the absence of obstacles, only the kinematic steering system (8) under perfect velocity tracking such that $v_j = v_{jc}$ and $\dot{v}_j = \dot{v}_{jc}$ is considered for the leader and its followers in the absence of all dynamics. Then, the full dynamics as well as the kinematics of all the robots are considered. Under both cases, the leader's reference linear velocity is 5 m/s while the reference linear velocity is allowed to vary. Results for the leader's tracking ability are presented in [1] and are therefore not shown here. In the second scenario, obstacles are added in the path of the follower robots and the obstacle avoidance scheme of *Theorem 5* is demonstrated, and both a static and dynamic obstacle environment is considered.

A simple wedge formation is considered such that follower *j* should track its leader at separation of $L_{ijd} = 2$ meters and a bearing of $\psi_{ijd} = \pm 120°$ depending on the follower's location, and the formation leader is located at the apex of the wedge. The wedge

formation that will be considered is shown in Figure 5. In the figure, followers 1 and 3 track the leader and followers 2 and 4 track followers 1 and 3, respectively.

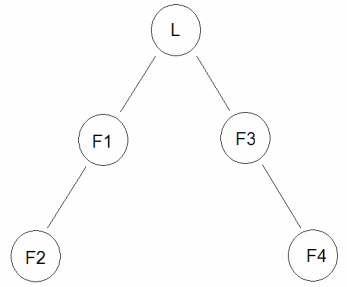

Figure 5: Formation Structure

Remark: In the proceeding analysis, $L, F1, F2, F3,$ and $F4$ will be used to denote the *leader, follower 1*, *follower 2, follower 3,* and *follower 4,* respectively.

The gains shown in Table I are utilized for the controllers.

Table I: Controller Gains

Leader	$K_{i4} = diag\{40\}$	$k_{i1} = 10$	$k_{i2} = 5$	$k_{i3} = 4$	
Follower j ($j = 1,2,3,4$)	$K_4 = diag\{40\}$	$k_1 = 7$	$k_2 = 20$	$k_3 = .01$	$k_v = 1$

The following robotic parameters are considered for the leader and its followers: $m = 5\,kg$, $I = 3\,kg^2$, $R = .175\,m$, $r = 0.08\,m$, and $d = 0.45\,m$. Friction is added to both the leader's and its followers' dynamics and modeled as

$$F = \begin{bmatrix} .5sign(v) + .25v \\ .75sign(\omega) + .3\omega \end{bmatrix}$$

A. Scenario I: Obstacle Free Environment

Figure 6 shows the resulting trajectories for two cases: when only the kinematics are considered and when both the kinematics and dynamics are considered. In both cases,

the robots start in the bottom left corner of Figure 6 and travel toward the top right corner of the figure, and a steering command in the form of angular acceleration is given to the formation at $x = 2$. From Figure 6, it is apparent that the wedge formation can be achieved under both cases. However, when the steering command is issued, the dynamics of the robots become an apparent influence, and the two trajectories deviate from each other. During the steering command, dynamics like the centripetal/coriolis become an influence on the robots when the dynamics are considered, and the path the robots take when the dynamics are modeled is slightly different than the path the robots take when the dynamics are ignored. This is an important result that displays the importance of incorporating the dynamics of the robots into the control law. In an obstacle ridden environment, it is important that the formation follows a specific trajectory to ensure safe passage. Ignoring the dynamics of the robots, one cannot guarantee the trajectory the formation follows is the desired trajectory.

Figures 7 and 8 display the bearing and separation errors for the proposed dynamical controller. It is evident that both the bearing errors and separation errors converge to zero very quickly and remain there so that the wedge formation is maintained.

B. Scenario II: Obstacle Ridden Environment

Now, the wedge formation of five robots is considered in an environment with stationary and moving obstacles, and the controller gains outlined in Table I along with the gains shown in Table II were utilized.

Table II: Obstacle Avoidance Gains

$K_L = 5$	$K_\psi = 1.5$

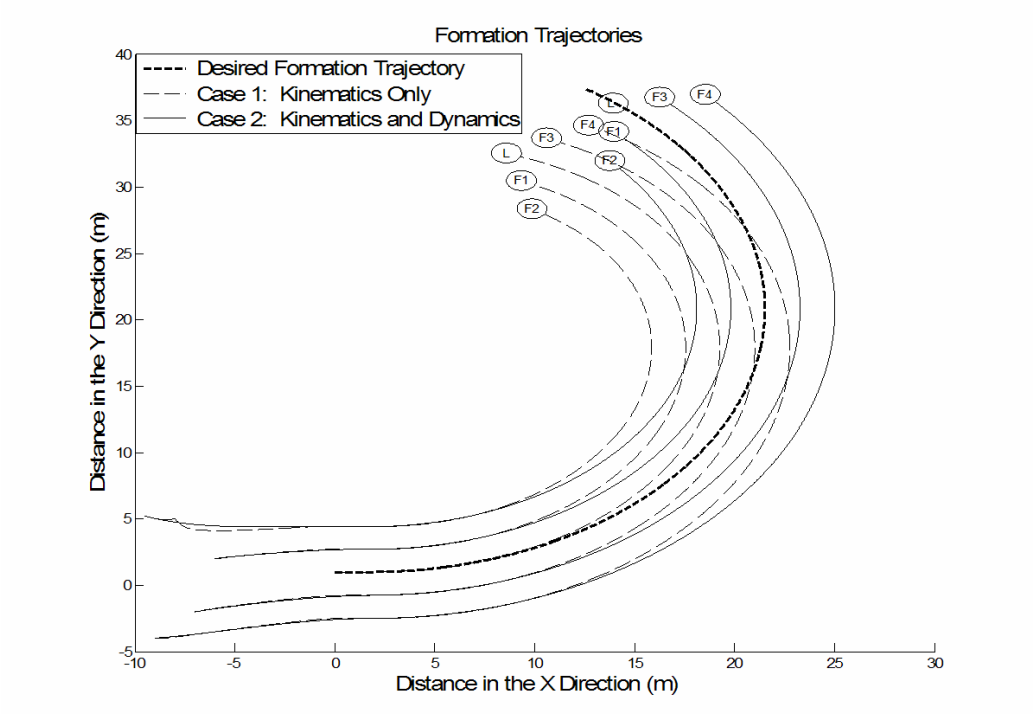

Figure 6: Trajectory when Dynamics are Included and when Only Kinematics are Considered

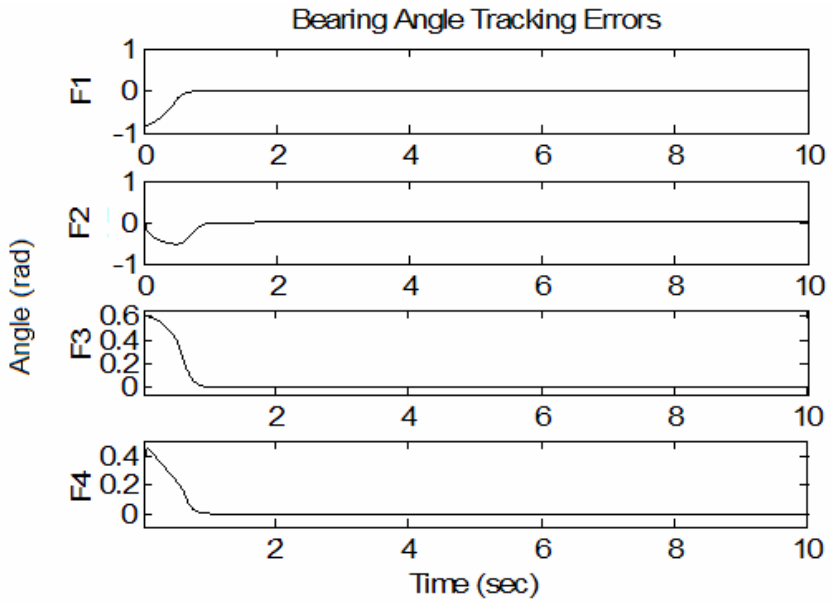

Figure 7: Bearing Errors for Dynamical Controller

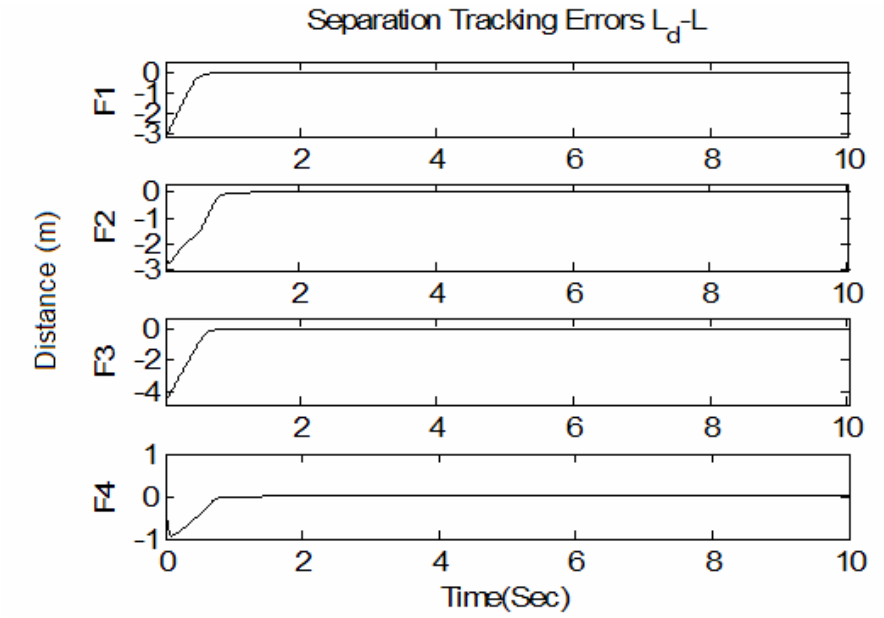

Figure 8: Separation Errors for Dynamical Controller

Figures 9 and 10 depict the formation trajectories in the presence of stationary obstacles. Examining the zoomed formation trajectories shown in Figure 10, it is evident that the robots are able to maneuver around the encountered obstacle while simultaneously tracking their leaders. Because the followers on the outside of the formation track the robots in the inner formation, the movements of the robots in the interior of the formation propagate to followers on the exterior of the formation. Thus, when a robot on the interior of the formation performs an obstacle avoidance maneuver, their movements are mimicked by their followers, which is evident in Figures 9 and 10. Figures 11 and 12 illustrate the desired separation and bearing, respectively, for follower robot 2. Examining the plots, the constant set points become time varying when an obstacle is encountered and return to constant values once the obstruction is navigated. Figures 13 and 14 display the formation tracking errors for all followers. Examining the plots, one can see that the separation and bearing tracking errors are small and bounded

when in the presence of an encountered obstacle which supports the theoretical conjecture.

Next, the formation is tested in the presence of a dynamic obstacle environment. When the obstacle is encountered in this scenario, the obstacle begins to move with a constant velocity until the robot has completely navigated around the obstacle to avoid it. Figures 15 and 16 show the formation trajectories. The dotted lines represent the path of moving obstacles, and the connected circles denote the obstacles' final positions. Figures 17 and 18 display the desired separation and bearing time history of follower 2 in the dynamic environment. Again, the influence of the obstacle on follower 2 can be observed when the desired separation and bearing become time varying. Figures 19 and 20 present the formation tracking errors for all four followers. Examining the figures, it is clear that the separation and bearing tracking errors are small and bounded in the presence of moving obstacles.

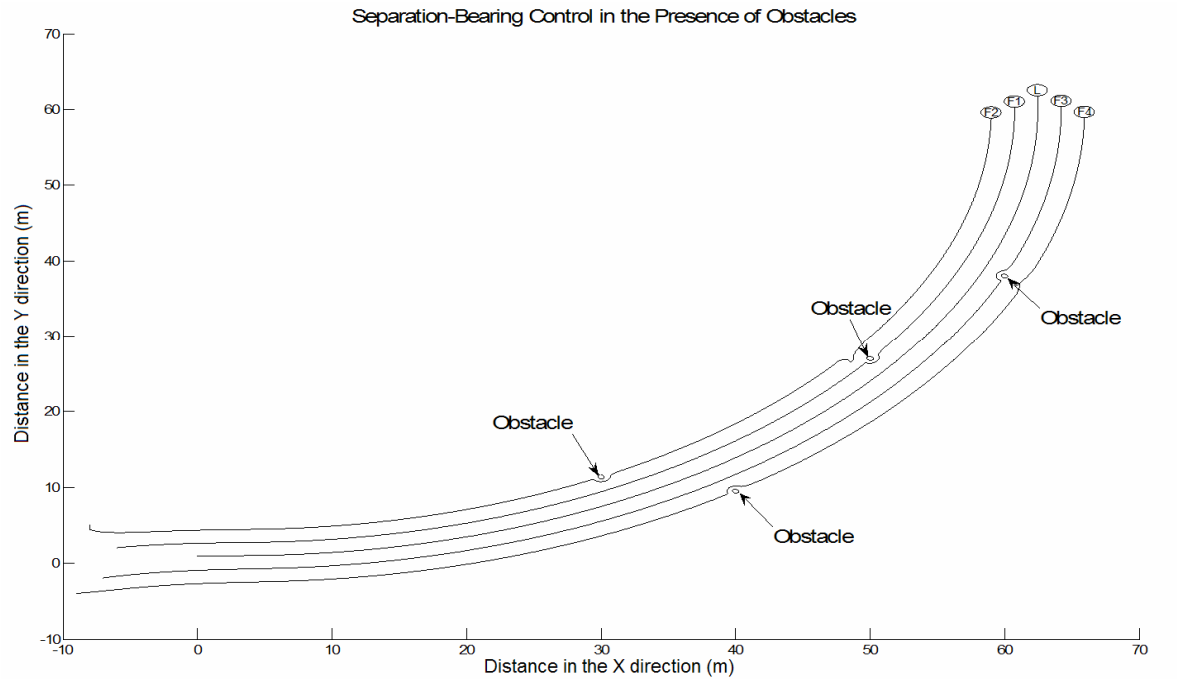

Figure 9: Formation Trajectories with Obstacles

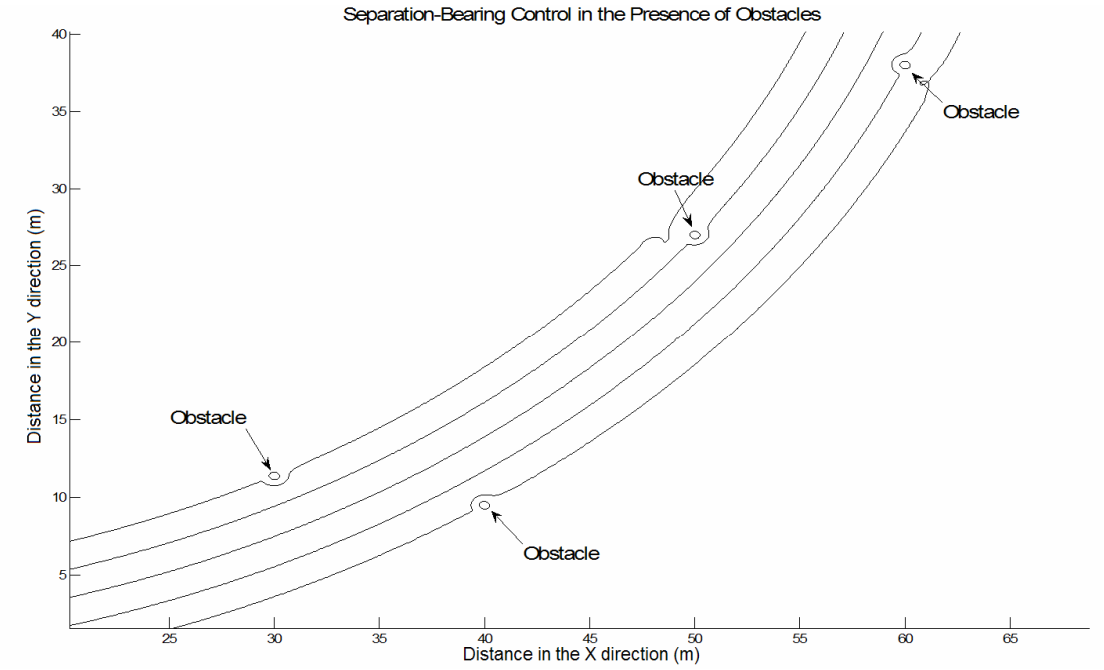

Figure 10: Zoomed Formation Trajectories with Obstacles

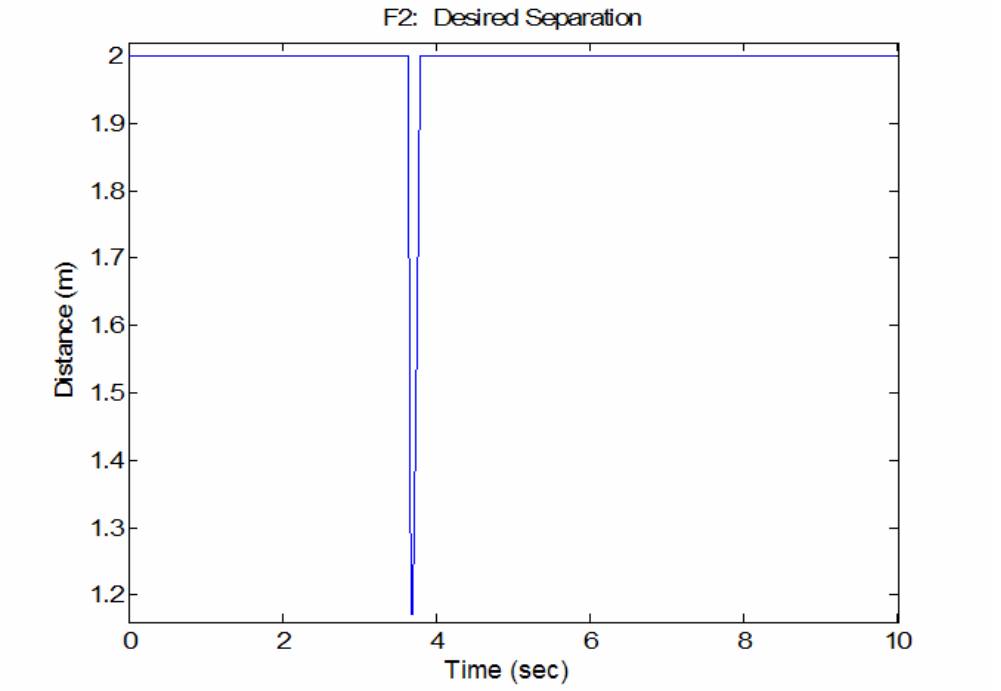

Figure 11: Desired Separation for Follower 2

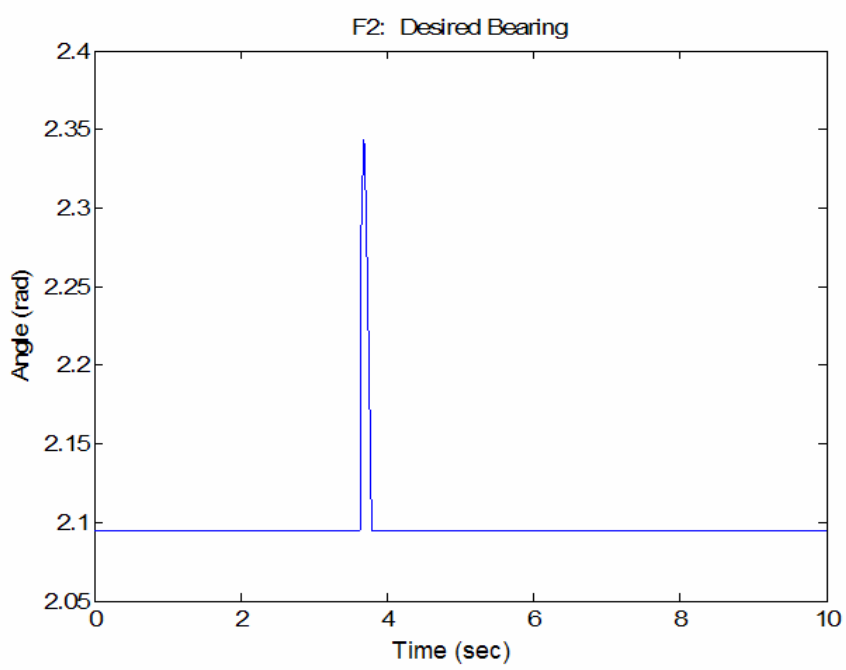

Figure 12: Desired Bearing for Follower 2

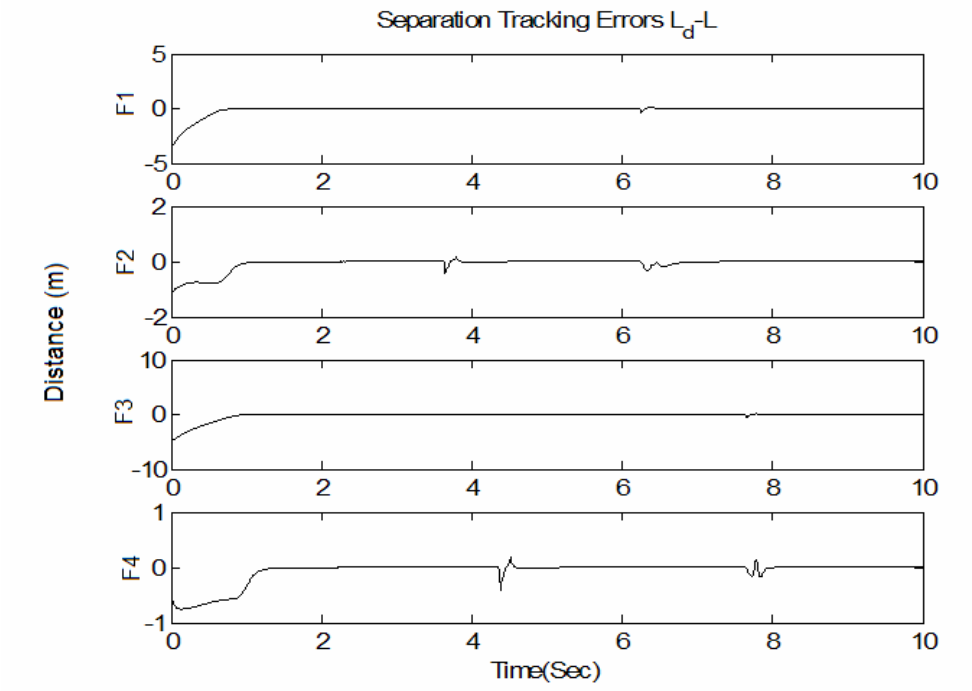

Figure 13: Separation Errors

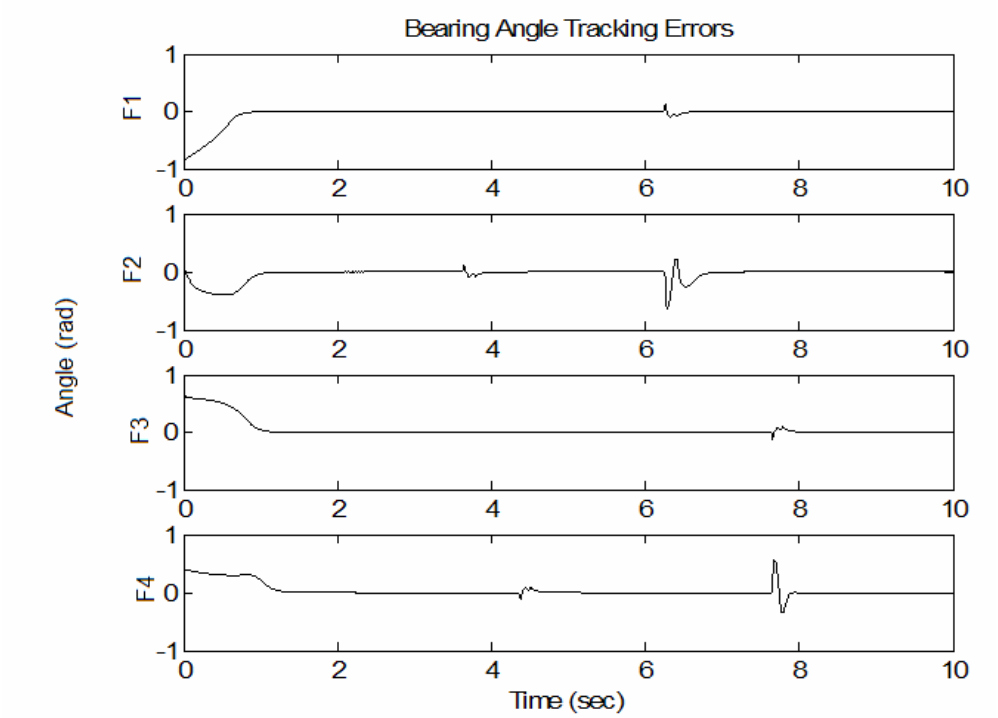

Figure 14: Bearing Errors

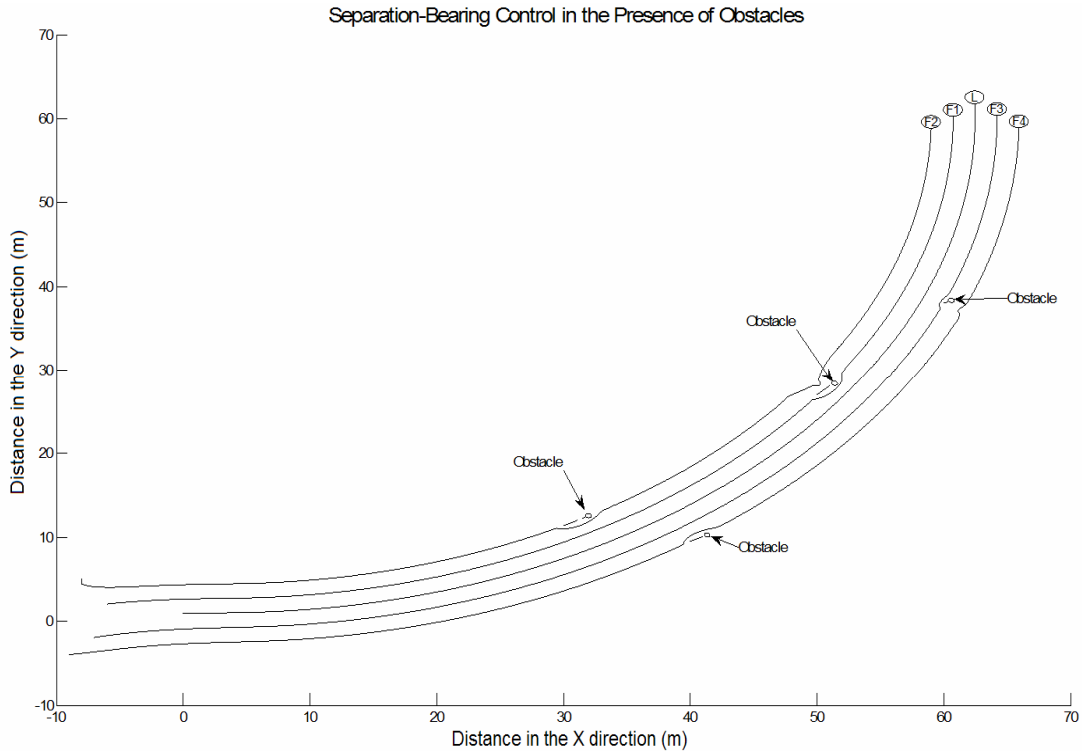

Figure 15: Formation Trajectories in a Dynamic Obstacle Environment

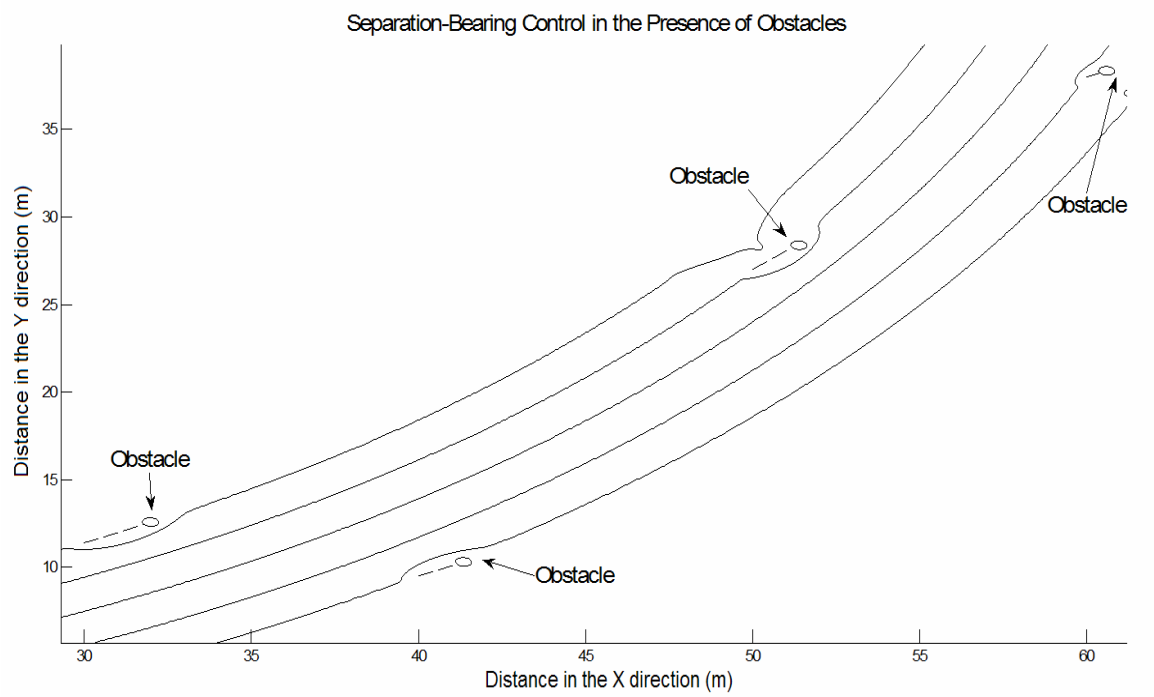

Figure 16: Zoomed Formation Trajectories in a Dynamic Obstacle Environment

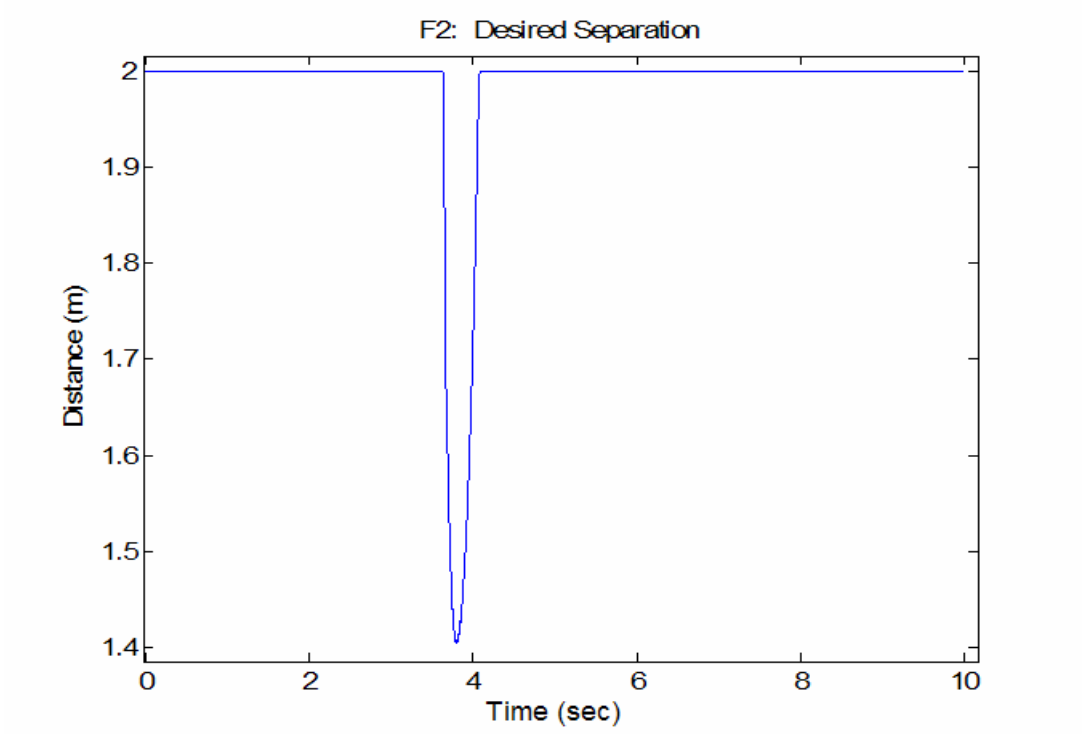

Figure 17: Desired Separation in Dynamic Obstacle Environment

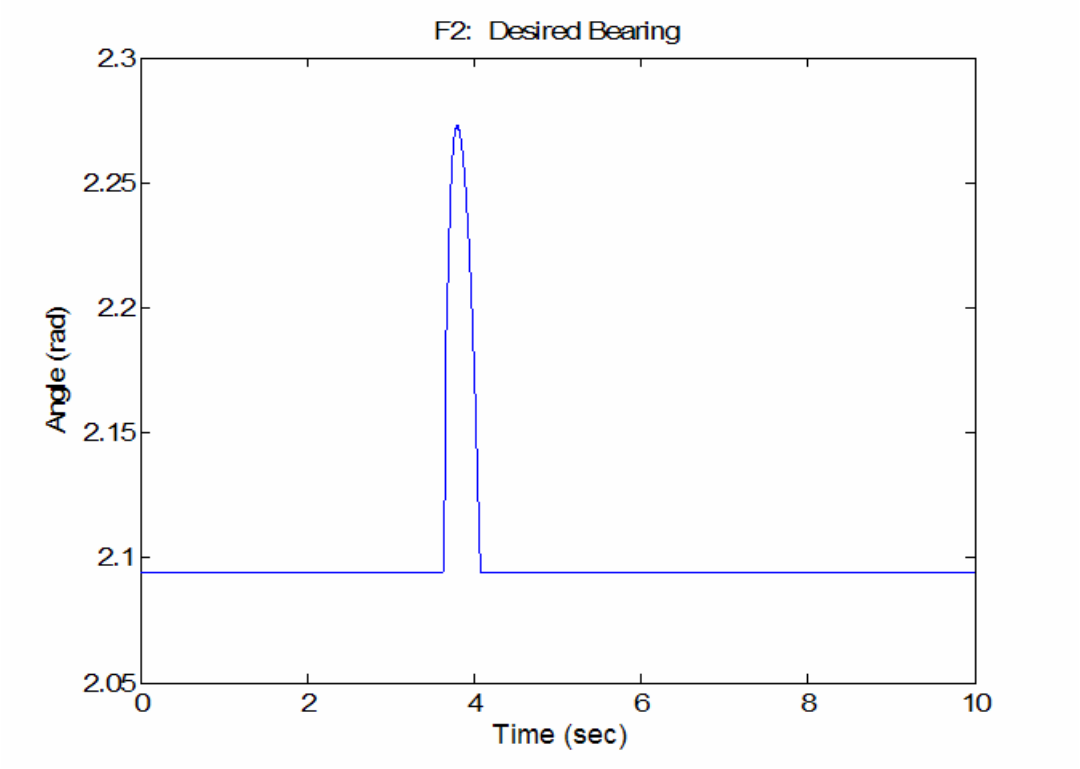

Figure 18: Desired Bearing in a Dynamic Obstacle Environment

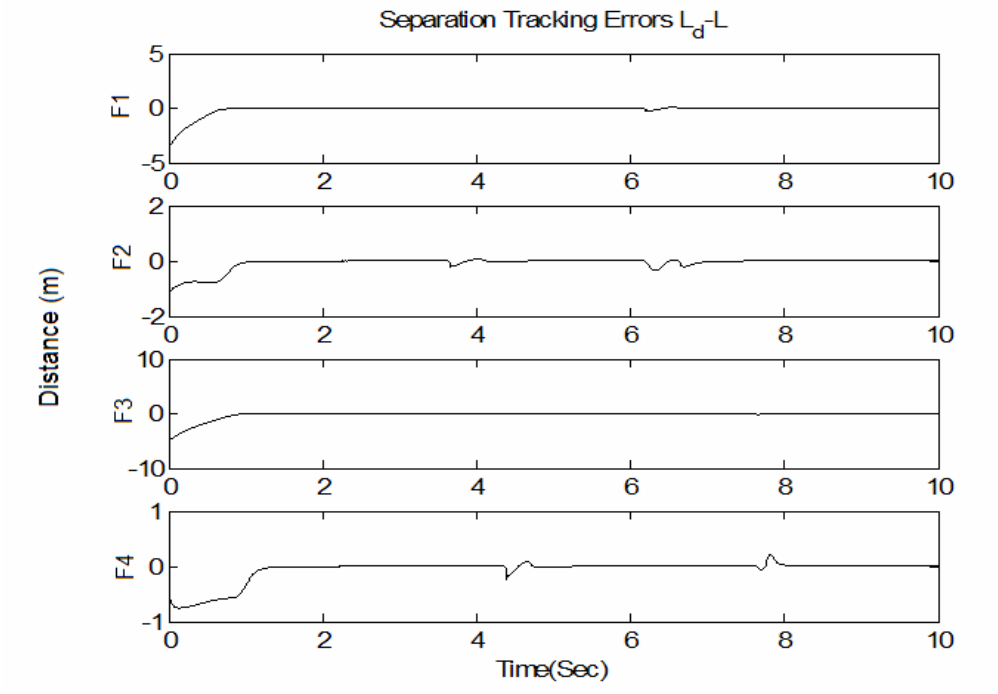

Figure 19: Separation Tracking Errors in a Dynamic Obstacle Environment

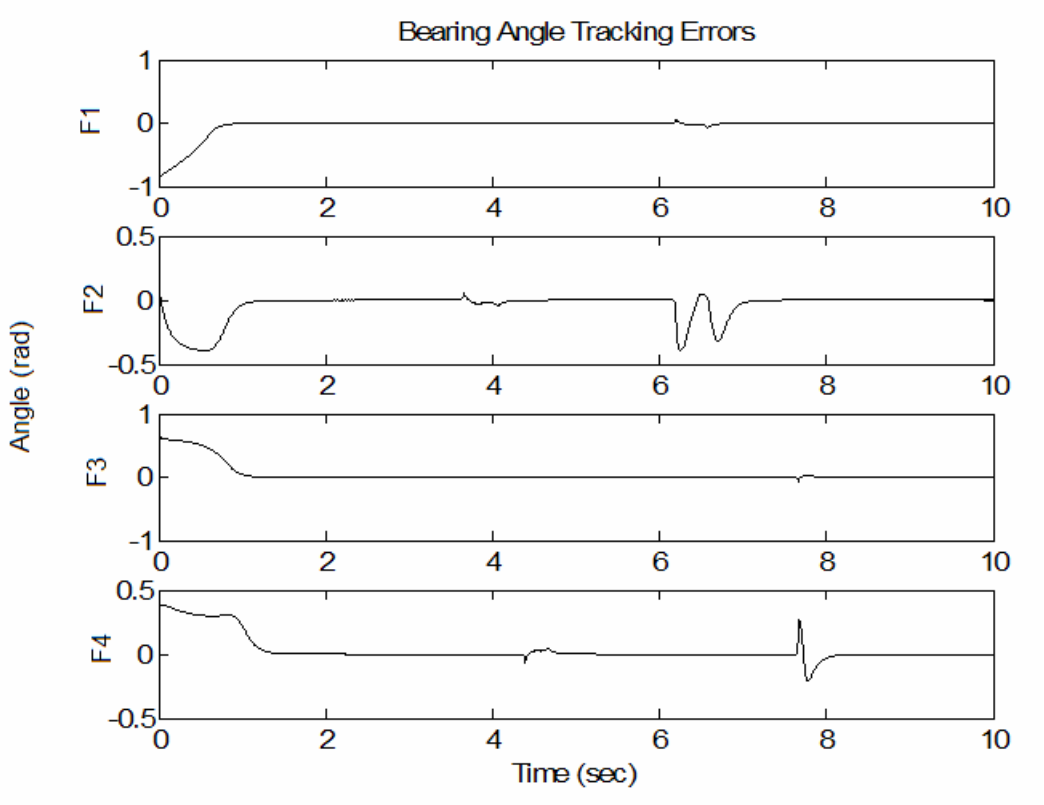

Figure 20: Bearing Errors in Dynamic Obstacle Environment

VI. Conclusions

In the absence of obstacles, an asymptotically stable tracking controller for leader-follower based formation control was presented that considers the dynamics of the leader and the follower using backstepping. The feedback control scheme is valid as long as the complete dynamics of the followers and their leader are known. Numerical results were presented and the stability of the system was verified. Simulation results verify the theoretical conjecture and expose the flaws in ignoring the dynamics of the mobile robots. In the presence of obstacles, a stable tracking controller was presented which allows each follower robot to navigate around obstacles while simultaneously tracking its leader. The control was shown to be effective in both a static and dynamic obstacle

environment, and numerical results were presented. The stability of the system was verified, and the simulation results verified the theoretical conjecture.

VII. REFERENCES

[1] R. Fierro and F.L. Lewis, "Control of a Nonholonomic Mobile Robot: Backstepping Kinematics Into Dynamics," *Proc. IEEE Conf. on Decision and Contr.*, Kobe, Japan, 1996, pp. 1722-1727.

[2] Y. Kanayama, Y. Kimura, F. Miyazaki, and T. Noguchi, "A Stable Tracking Control Method for an Autonomous Mobile Robot," *Proc. IEEE International Conference on Robotics and Automation*, vol. 1, pp384-389, May 1990.

[3] R. Fierro and F. L. Lewis, "Control of a Nonholonomic Mobile Robot Using Neural Networks," *IEEE Transactions on Neural Networks*, vol. 8, pp589-600, July 1998.

[4] M. Egerstedt, X. Hu, and A. Stotsky, "Control of Mobile Platforms Using a Virtual Vehicle Approach," *IEEE Transactions on Automatic Control*, vol. 46, pp 1777-1782, November 2001.

[5] T. Fukao, H. Nakagawa, and N. Adachi, "Adaptive Tracking Control of a Nonholonomic Mobile Robot," *IEEE Transactions on Robotics and Automation*, vol. 16, pp 609-615, October 2000.

[6] J. Lawton, R. Bear, and B. Young, "A Decentralized Approach to Formation Maneuvers," *IEEE Transactions on Robotics and Automation*, vol. 19, pp 933-941, December 2003.

[7] T. Balch and R. Arkin, "Behavior-Based Formation Control for Multirobot Teams," *IEEE Transaction on Robotics and Automation*, vol. 15, pp 926-939, December 1998.

[8] J. Fredslund and M. Mataric, "A General Algorithm for Robot Formations Using Local Sensing and Minimal Communication," *IEEE Transactions on Robotics and Automation*, vol. 18, pp 837-846, October 2002.

[9] Stephen Spry and J. Karl Hedrick, "Formation Control Using Generalized Coordinates," in *Proceedings of IEEE International Conference on Decision and Control*, Atlantis, Paradise Island, Bahamas, pp. 2441 – 2446, December 2004.

[10] P. Ogren, M. Egerstedt, and X. Hu, "A Control Lyapunov Function Approach to Multiagent Coordination," *IEEE Transactions on Robotics and Automation*, vol. 18, pp 847-851, October 2002.

[11] Kar-Han Tan and M. A. Lewis, "Virtual Structures for High-Precision Cooperative Mobile Robotic Control," *Proceedings of the 1996 IEEE/RSJ International Conference Intelligent Robots and Systems*, vol. 1, pp. 132–139, November 1996.

[12] G. L. Mariottini, G. Pappas, D. Prattichizzo, and K. Daniilidis, "Vision-based Localization of Leader-Follower Formations," *Proc. IEEE European Control Conference on Decision and Control*, pp 635-640, December 2005.

[13] X. Li, J. Xiao, and Z. Cai, "Backstepping Based Multiple Mobile Robots Formation Control," *Proc. IEEE International Conference on Intelligent Robots and Systems*, pp 887-892, August 2005.

[14] A. Das, R. Fierro, V. Kumar, J. Ostrowski, and J. Spletzer, C. Taylor, "A Vision-Based Formation Control Framework," *IEEE Transactions on Robotics and Automation*, vol. 18, pp 813-825, October 2002.

[15] H. Hsu and A. Liu, "Multi-Agent Based Formation Control Using a Simple Representation," *Proc. IEEE International Conference on Networking, Sensing & Control*, Taipei, Taiwan, pp 276-282, March 2004.

[16] J. Shao, G. Xie, J. Yu, and L. Wang, "A Tracking Controller for Motion Coordination of Multiple Mobile Robots," *Proc. IEEE International Conference on Intelligent Robots and Systems*, pp 783-788, August 2005.

[17] Y. Li and X. Chen, " Dynamic Control of Multi-robot Formation," P*roc. IEEE International Conference on Mechatronics*, Taipei, Taiwan, pp 352-357, July 2005.

[18] Jaydev P. Desai, Jim Ostrowski, and Vijay Kumar, "Controlling Formations of Multiple Mobile Robots," *Proc. IEEE International Conference on Robotics and Automation*, pp. 2864-2869, Leuven, Belgium, May 1998.

[19] F.L. Lewis, S. Jagannathan, and A. Yesilderek, "*Neural Network Control of Robot Manipulators and Nonlinear Systems*," Taylor and Francis, London, UK, 1999.

[20] O. Khatib, "Real-time obstacle avoidance for manipulators and mobile robots," *Intl. Journal of Robotics Research*, vol. 5, no. 1, pp. 90–98, 1986.

PAPER 2

Neural Network Control of Nonholonomic Mobile Robot Formations[1]

Travis Dierks* and S. Jagannathan

***Abstract*—*In this paper the control of formations of multiple nonholonomic mobile robots is attempted by integrating a kinematic controller with a neural network (NN) computed-torque controller. A combined kinematic/torque control law is developed for leader-follower based formation control using backstepping in order to accommodate the dynamics of the robots and the formation in contrast with kinematic-based formation controllers. It is found that the dynamical controller torque control inputs for the follower robots include the dynamics of the follower robot as well as the dynamics of its leader. The NN is introduced to approximate the dynamics of the follower as well as its leader using online weight tuning. It is shown using Lyapunov theory that the errors for the entire formation are uniformly ultimately bounded, and numerical results are provided. Additionally, a novel obstacle avoidance scheme for leader-follower based formation control is introduced which allows each follower robot to navigate around obstacles while simultaneously tracking its leader. The stability of the follower robots as well as the entire formation during an obstacle avoidance maneuver is demonstrated using Lyapunov methods and numerical results are provided.*

Keywords: Nonholonomic Mobile Robot Formation, Backstepping Control, Neural Networks, Lyapunov Stability, Obstacle Avoidance

I. INTRODUCTION

Over the past decade, the attention has shifted from the control of a single mobile robot [1-5] to the control of multiple mobile robots because of the advantages a team of robots offer such as increased efficiency and more systematic approaches to tasks like search and rescue operations, mapping unknown or hazardous environments, and security and bomb sniffing.

[1] Research Supported in part by GAANN Program through the Department of Education and Intelligent Systems Center. Authors are with the Department of Electrical and Computer Engineering, University of Missouri-Rolla, 1870 Miner Circle, Rolla, MO 65409. Contact author Email: tad5x4@umr.edu.

There are several methodologies [6-18] to robotic formation control which include behavior-based [6][7][8], generalized coordinates [9], virtual structures [10][11], and leader-follower [12][13] to name a few. Perhaps the most popular and intuitive approach is the leader-follower method. In this method, a follower robot stays at a specified separation and bearing from a designated leader robot.

In [12] and [14], local sensory information and a vision based approach to leader-following is undertaken, respectively. In both approaches, the sensory information was used to calculate velocity control inputs. In [15], another kinematic controller is presented making use of a virtual operator multi-agent system (VOMAS) to assist formation control in joining robots into a team or removing robots from a team. A modified leader follower control is introduced in [13] where Cartesian coordinates are used rather than polar. A characteristic that is common in many formation control papers [7-16] is the design of a kinematic controller, thus requiring a perfect velocity tracking assumption.

In [16], it is acknowledged that the separation-bearing methodologies of leader-follower formation control closely resemble a tracking controller problem, and a reactive tracking control strategy that converts a relative pose control into a tracking problem by defining a virtual robot for each follower to track using separation-bearing techniques is presented. Drawbacks of this controller are the need for a virtual robot and the dynamics are not considered.

In this paper, we examine framework developed for controlling single nonholonomic mobile robots and seek to expand them to be used in leader-follower formation control. We seek to bring in the dynamics of the robots themselves thus incorporating the

formation dynamics in the controller design. The dynamics of the leader become part of the follower robot's control torque input through the derivative follower's kinematic velocity control, which is a function of the leader's velocity. In [17], the dynamics of the follower robot are considered, but the effect the leader's dynamics has on the follower (formation dynamics) is not incorporated. The leader's dynamics become apart of the follower robot's control torque input through the derivative of the follower's kinematic velocity control, which is a function of the leader's velocity. In other words, the dynamical extension introduced in this paper provides a rigorous method of taking into account the specific vehicle dynamics to convert a steering system command into control inputs via backstepping approach. The universal approximation property of a neural network (NN) is utilized to learn the dynamics of the follower robots well as their leaders' online so that a torque command for the follower robots can be calculated. Both feedback velocity control inputs and velocity following control law are presented to prove the formation is uniformly ultimately bounded in the presence of bounded disturbances and numerical results are provided.

Furthermore, a simple but effective obstacle avoidance scheme is proposed that allows each follower robot to navigate around obstacles while simultaneously tracking its leader. The obstacle avoidance method is designed to utilize the ability of each follower robot to maintain a desired location with respect to its leader. When an obstacle is encountered, the desired location of the follower robot with respect to its leader is modified so that the follower navigates around the obstacle. In [16], the desired location of a follower with respect to its leader is modified by using separation-bearing [18] based formation control wherein the desired bearing is modified while steering the follower

robot around an obstacle. The drawback of only varying the desired bearing is that the new reference point for the follower to track may lie behind the follower robot's current position which is the case when the magnitude of the new desired bearing is greater than the magnitude of the current one making it undesirable.

By contrast in our approach, both the desired separation and desired bearing are altered to ensure the above scenario does not occur. Our proposed obstacle avoidance scheme is shown to achieve stability in the sense of Lyapunov for each follower as well as the entire formation during an obstacle avoidance maneuver. Simulation results are provided illustrating the effectiveness of the approach in both a static and dynamic environment.

II. Leader-Follower Formation Control

The two popular techniques in leader-follower formation control include separation-separation and separation-bearing [12][18]. The goal of separation-bearing formation control is to find a velocity control input such that

$$\lim_{t\to\infty}(L_{ijd} - L_{ij}) = 0 \text{ and } \lim_{t\to\infty}(\Psi_{ijd} - \Psi_{ij}) = 0 \tag{1}$$

where L_{ij} and ψ_{ij} are the measured separation and bearing of the follower robot with L_{ijd} and ψ_{ijd} represent desired distance and angles, respectively [12][18]. Only separation-bearing techniques are considered in this paper, but our approach can be extended to separation-separation control.

To avoid collisions, separation distances are measured from the back of the leader to the front of the follower. The kinematic equations for the front of the j^{th} follower robot can be written as

$$\dot{q}_j = \begin{bmatrix} \dot{x}_j \\ \dot{y}_j \\ \dot{\theta}_j \end{bmatrix} = \begin{bmatrix} \cos\theta_j & -d_j \sin\theta_j \\ \sin\theta_j & d_j \cos\theta_j \\ 0 & 1 \end{bmatrix} \begin{bmatrix} v_j \\ \omega_j \end{bmatrix} = S_j(q_j) v_j \tag{2}$$

where d_j is the distance from the rear axle to the to front of the robot, x_j, y_j, and θ_j are actual Cartesian position and orientation of the physical robot, and v_j, and ω_j are linear and angular velocities, respectively. Many robotic systems can be characterized as a robotic system having an *n*-dimensional configuration space $\mathcal{C}$ with generalized coordinates $(q_1,...q_n)$ subject to m constraints [1] where after applying the transformation in [1], the dynamics are given by

$$\overline{M}_j(q_j)\dot{v}_j + \overline{V}_{mj}(q_j,\dot{q}_j)v_j + \overline{F}_j(v_j) + \overline{\tau}_{d_j} = \overline{B}_j(q_j)\tau_j. \tag{3}$$

where $\overline{M}_j \in \Re^{rxr}$ is a symmetric positive definite inertia matrix, $\overline{V}_{mj} \in \Re^{rxr}$ is the bounded centripetal and coriolis matrix, $\overline{F}_j \in \Re^{rx1}$ is the friction vector, $\overline{\tau}_{dj}$ represents unknown bounded disturbances, and $\overline{\tau}_j = \overline{B}_j \tau \in \Re^{rx1}$ is the input vector. Robotic systems satisfy [1]:

1. *Boundedness:* $\overline{M}_j$, the norm of $\overline{V}_{mj}$, and τ_{dj} are all bounded.
2. *Skew Symmetric:* The matrix $\dot{\overline{M}}_j - 2\overline{V}_{mj}$ is skew symmetric such that $\dot{\overline{M}}_j - 2\overline{V}_{mj} = 0$.

A. Backstepping Controller Design

The complete description of the behavior of a mobile robot is given by (2) and (3). Standard approaches to leader follower formation control deal only with (2) and assume that perfect velocity tracking holds. This paper seeks to remove that assumption by defining the nonlinear feedback control input

$$\tau_j = \overline{B}_j^{-1}(\overline{M}_j u_j + \overline{V}_{mj} v_j + \overline{F}_j(v_j) + \overline{\tau}_{dj}) \tag{4}$$

where u_j is an auxiliary input. Applying this control law to (3) allows one to convert the dynamic control problem into the kinematic control problem [1] such that

$$\begin{aligned} \dot{q}_j &= S_j(q_j)v_j \\ \dot{v}_j &= u_j. \end{aligned} \tag{5}$$

Tracking controller frameworks have been derived for controlling single mobile robots, and there are many ways [1-5] to choose velocity control inputs $v_{jc}(t)$ for steering system (2). To incorporate the dynamics of the mobile platform, it is desirable to convert $v_{jc}(t)$ into a control torque, $\tau_j(t)$ for the physical robot. Contributions in single robot frameworks are now considered and expanded upon in the development a kinematic controller for the separation-bearing formation control technique. Our aim to design a conventional computed torque controller such that (2) and (3) exhibit the desired behavior for a given control $v_{jc}(t)$ thus removing perfect velocity tracking assumptions.

Consider the tracking error system [1] used to control a single robot as

$$\begin{bmatrix} e_{j1} \\ e_{j2} \\ e_{j3} \end{bmatrix} = T_{ej}(q_{jr} - q_j) = \begin{bmatrix} \cos\theta_j & \sin\theta_j & 0 \\ -\sin\theta_j & \cos\theta_j & 0 \\ 0 & 0 & 1 \end{bmatrix} \begin{bmatrix} x_{jr} - x_j \\ y_{jr} - y_j \\ \theta_{jr} - \theta_j \end{bmatrix} \tag{6}$$

$$\dot{x}_{jr} = v_{jr}\sin\theta_{jr},\ \ \dot{y}_{jr} = v_{jr}\sin\theta_{jr},\ \ \dot{\theta}_{jr} = \omega_{jr},\ \dot{q}_{jr} = \begin{bmatrix} \dot{x}_{jr} & \dot{y}_{jr} & \dot{\theta}_{jr} \end{bmatrix}^T \tag{7}$$

where x_{jr}, y_{jr}, and θ_{jr} are the positions and orientation of a virtual reference robot j seeks to follow [1].

In a single robot control, a steering control input $v_{jc}(t)$ is designed to solve three basic problems: path following, point stabilization, and trajectory following such that $\lim_{t\to\infty}(q_{jr} - q_j) = 0$ and $\lim_{t\to\infty}(v_{jc} - v_j) = 0$ [1]. If the mobile robot controller can

successfully track a class of smooth velocity control inputs, then all three problems can be solved with the same controller [1].

The three basic tracking control problems can be extended to leader-follower based formation control as follows. The virtual reference cart is replaced with a physical mobile robot acting as the leader i, and x_{jr} and y_{jr} are defined as points at a distance L_{ijd} and a desired angle ψ_{ijd} from the lead robot. Now the three basic navigation problems can be introduced for leader-follower formation control as follows.

Tracking: Let there be a leader i for follower j such that

$$\dot{q}_i = \begin{bmatrix} \dot{x}_i \\ \dot{y}_i \\ \dot{\theta}_i \end{bmatrix} = \begin{bmatrix} \cos\theta_i & -d_i \sin\theta_i \\ \sin\theta_i & d_i \cos\theta_i \\ 0 & 1 \end{bmatrix} \begin{bmatrix} v_i \\ \omega_i \end{bmatrix} \tag{8}$$

$$\overline{M}_i(q_i)\dot{v}_i + \overline{V}_{mi}(q_i,\dot{q}_i)v_j + \overline{F}_i(v_i) + \overline{\tau}_{d_i} = \overline{B}_i(q_i)\tau_i \tag{9}$$

$$\begin{aligned} x_{jr} &= x_i - d_i\cos\theta_i + L_{ijd}\cos(\Psi_{ijd} + \theta_i) \\ y_{jr} &= y_i - d_i\sin\theta_i + L_{ijd}\sin(\Psi_{ijd} + \theta_i) \\ \theta_{jr} &= \theta_i \end{aligned} \tag{10}$$

$$v_{jr} = [|v_i| \quad |\omega_i|]^T \tag{11}$$

where v_{jr} is the time varying linear and angular speeds of the leader such that $v_{jr} \geq 0$ for all time. Then define the actual position and orientation of follower j as

$$\begin{aligned} x_j &= x_i - d_i\cos\theta_i + L_{ij}\cos(\Psi_{ij} + \theta_i) \\ y_j &= y_i - d_i\sin\theta_i + L_{ij}\sin(\Psi_{ij} + \theta_i) \\ \theta_j &= \theta_j \end{aligned} \tag{12}$$

where L_{ij} and ψ_{ij} are the actual separation and bearing of follower j. In order to solve the formation tracking problem with one follower, find a smooth velocity

input $v_{jc} = f(e_{jp}, v_{jr}, K)$ such that $\lim_{t\to\infty}(q_{jr} - q_j) = 0$, where e_{jp}, v_{jr}, and K are the tracking position errors, reference velocity for follower j robot, and gain vector, respectively. Then compute the torque $\tau_j(t)$ for the dynamic system of (3) so that $\lim_{t\to\infty}(v_{jc} - v_j) = 0$. Achieving this for every leader i and follower $j = 1,2,...N$ ensures that the entire formation tracks the formation trajectory.

B. Leader-Follower Tracking Control

Many solutions [12-16] to the leader-follower formation control problem of (1) and the kinematic model (2) have been suggested and smooth velocity control inputs for the follower have been derived. Unfortunately, dynamical models are rarely studied, and the effect of the dynamics of mobile robot leader *i* on follower *j* has not been well understood in the process of incorporating the dynamics of the formation. This paper will now address these issues.

The contribution in this paper lies in incorporating a NN into the dynamic controller using online weight tuning to approximate the dynamics of the robot and the formation. The NN controller is introduced so that the specific torque $\tau_j(t)$ may be calculated so that the alternative control velocity v_{jc} derived in [22] can be tracked without knowing the complete dynamics of the formation. It is common in the literature to assume perfect velocity tracking which does not hold in real applications. To remove this assumption, integrator backstepping is applied. A general control structure for mobile robot follower *j* is presented in Figure 1.

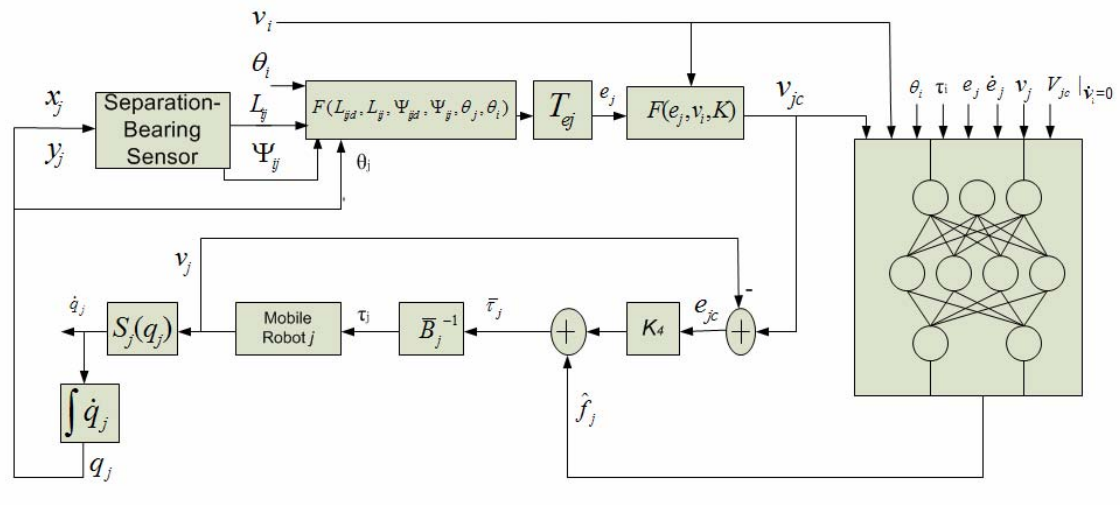

Figure 1: Follower *j* Controller Structure

Using (10), (12) and simple trigonometric identities, the error system (6) can be rewritten as

$$\begin{bmatrix} e_{j1} \\ e_{j2} \\ e_{j3} \end{bmatrix} = \begin{bmatrix} \cos\theta_j & \sin\theta_j & 0 \\ -\sin\theta_j & \cos\theta_j & 0 \\ 0 & 0 & 1 \end{bmatrix} \begin{bmatrix} L_{ijd}\cos(\Psi_{ijd}+\theta_i) - L_{ij}\cos(\Psi_{ij}+\theta_i) \\ L_{ijd}\sin(\Psi_{ijd}+\theta_i) - L_{ij}\sin(\Psi_{ij}+\theta_i) \\ \theta_i - \theta_j \end{bmatrix} \tag{13}$$

After further simplification, (13) can be rewritten as

$$e_j = \begin{bmatrix} e_{j1} \\ e_{j2} \\ e_{j3} \end{bmatrix} = \begin{bmatrix} L_{ijd}\cos(\Psi_{ijd}+e_{j3}) - L_{ij}\cos(\Psi_{ij}+e_{j3}) \\ L_{ijd}\sin(\Psi_{ijd}+e_{j3}) - L_{ij}\sin(\Psi_{ij}+e_{j3}) \\ \theta_i - \theta_j \end{bmatrix} \tag{14}$$

The transformed error system now acts as a formation tracking controller which not only seeks to remain at a fixed desired distance L_{ijd} with a desired angle ψ_{ijd} relative to the lead robot *i*, but also achieves the same orientation as the lead robot which is desirable when $\omega_i = 0$.

In order to calculate the dynamics of the error system (14), it is necessary to calculate the derivatives of L_{ij} and ψ_{ij}, where their desired values L_{ijd} and ψ_{ijd} are considered as constants. Consider the two robot formation depicted in Figure 2. The *x* and *y* components of L_{ij} can be defined as

$$\begin{aligned} L_{ijx} &= x_{i_{rear}} - x_{j_{front}} = x_i - d_i \cos\theta_i - x_j \\ L_{ijy} &= y_{i_{rear}} - y_{j_{rear}} = y_i - d_i \sin\theta_i - y_j \end{aligned} \tag{15}$$

and the derivative of the *x* and *y* components of L_{ij} can be found to be

$$\begin{aligned} \dot{L}_{ijx} &= v_i \cos\theta_i - v_j \cos\theta_j + d_j \omega_j \sin\theta_j \\ \dot{L}_{ijy} &= v_i \sin\theta_i - v_j \sin\theta_j - d_j \omega_j \cos\theta_j \end{aligned} \tag{16}$$

Noting that $L_{ij}^2 = L_{ijx}^2 + L_{ijy}^2$ and $\Psi_{ij} = \arctan\left(\frac{L_{ijy}}{L_{ijx}}\right) - \theta_i + \pi$, it can be shown that derivatives of the separation and bearing are consistent with [12] and [18] even when using the kinematics described in (2) such that

$$\begin{aligned} \dot{L}_{ij} &= v_j \cos\gamma_j - v_i \cos\Psi_{ij} + d_j w_j \sin\gamma_j \\ \dot{\Psi}_{ij} &= \frac{1}{L_{ij}}(v_i \sin\Psi_{ij} - v_j \sin\gamma_j + d_j w_j \cos\gamma_j - L_{ij} w_i) \end{aligned} \tag{17}$$

where $\gamma_j = \Psi_{ij} + e_{j3}$.

Now, using the derivative of (14), equation (17) and applying simple trigonometric identities, the error dynamics can be expressed as

$$\begin{bmatrix} \dot{e}_{j1} \\ \dot{e}_{j2} \\ \dot{e}_{j3} \end{bmatrix} = \begin{bmatrix} -v_j + v_i \cos e_{j3} + \omega_j e_{j2} - \omega_i L_{ijd} \sin(\Psi_{ijd} + e_{j3}) \\ -\omega_j e_{j1} + v_i \sin e_{j3} - d_j \omega_j + \omega_i L_{ijd} \cos(\Psi_{ijd} + e_{j3}) \\ \omega_i - \omega_j \end{bmatrix}. \tag{18}$$

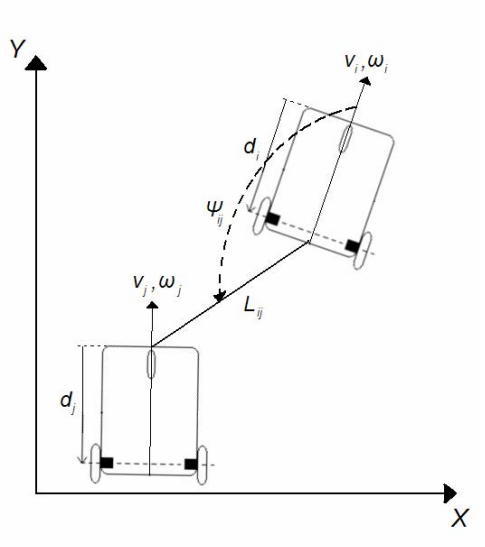

Figure 2: Leader-Follower Formation Control

Examining (18) and the error dynamics of a tracking controller for a single robot in [1], one can see that dynamics of a single follower with a leader is similar to [1], except additional terms are introduced as a result of (2) and (17).

To stabilize the kinematic system, we propose the following velocity control inputs for follower robot *j* to achieve the desired position and orientation with respect to leader *i* as

$$v_{jc} = \begin{bmatrix} v_{jc} \\ \omega_{jc} \end{bmatrix} = \begin{bmatrix} v_i \cos e_{j3} + k_1 e_{j1} \\ \omega_i + (v_i + k_v) k_2 e_{j2} + (v_i + k_v) k_3 \sin e_{j3} \end{bmatrix} + \begin{bmatrix} \gamma_{vjc} \\ \gamma_{wjc} \end{bmatrix} \tag{19}$$

where

$$\gamma_{vjc} = -\omega_i L_{ijd} \sin(\Psi_{ijd} + e_{j3}) \tag{20}$$

and

$$\gamma_{\omega jc} = -\frac{\left|e_{j2}\right|\left(\omega_i (d_j + L_{ijd}) + (v_i + k_v) k_3 d_j + k_v\right)}{1/k_2 + \left|e_{j2}\right| d_j} \tag{21}$$

Comparing this velocity control with the tracking controller designed for a single robot in [1], one can see that the two are similar except for the novel auxiliary terms which ensure stability for the formation of two robots using kinematics alone. Additionally, the design parameter k_v was added to ensure that asymptotic stability holds even when $v_i = 0$.

Before we proceed, the following assumptions are needed.

Assumption 1. Follower j is equipped with sensors capable of measuring the separation distance L_{ij} and bearing ψ_{ij} and both leader and follower are equipped with instrumentation to measure their linear and angular velocities as well as their orientations θ_i and θ_j.

Assumption 2. Wireless communication is available between follower j and leader i with communication delays being zero.

Assumption 3. Leader i communicates its linear and angular velocities v_i, ω_i as well as its orientation θ_i and control torque τ_i to its followers at each sampling instant.

Assumption 4. For the nonholonomic system of (2) and (3) with n generalized coordinates q, m independent constraints, and r actuators, the number of actuators is equal to the number of degrees of freedom ($r = n - m$).

Assumption 5. The reference linear and angular velocities measured from the leader i are bounded and $v_{jr}(t) \geq 0$ for all t.

Assumption 6. $K = [k_1 \quad k_2 \quad k_3]^T$ is a vector of positive constants.

Assumption 7. Let perfect velocity tracking hold such that $v_j = v_{jc}$ and $\dot{v}_j = \dot{v}_{jc}$ (this assumption is relaxed later).

Remark: These assumptions are standard in the formation control literature.

Theorem 1 [22]*:* Given the nonholonomic system of (2) and (3) with *n* generalized coordinates *q, m* independent constraints, and *r* actuators, along with the leader follower criterion of (1), let *Assumption 1-7* hold. Let a smooth velocity control input v_{jc} for the follower *j* given by (19), (20), and (21). Then the origin $e_j = 0$ consisting of the position and orientation error for the follower is asymptotically stable.

Proof: Consider the following Lyapunov function candidate

$$V_j = \frac{1}{2}(e_{j1}^2 + e_{j2}^2) + \frac{1-\cos e_{j3}}{k_2} \tag{22}$$

Clearly, $V_j > 0$ and $V_j = 0$ only when $e_j = 0$. In [22], it is shown that the derivative of (22) is

$$\dot{V}_j \le -k_1 e_{j1}^2 - d_j(v_i + k_v)k_2 e_{j2}^2 - \frac{k_3}{k_2}(v_i + k_v)\sin^2 e_{j3} \tag{23}$$

Clearly $\dot{V}_j < 0$ for all $v_i \ge 0$, and the velocity control (19), (20) and (21) provides asymptotic stability for the error system (14) and (18) and $e_j \to 0$ as $t \to \infty$.

Remark: The asymptotic stability of the error system (14) and (18) is proven without the use of Barbalat's Lemma which is required in [1].

C. Dynamic Controller

Now assume that the perfect velocity tracking assumption does not hold making *Assumption 7* invalid. A two-layer NN is considered here consisting of one layer of randomly assigned constant weights $V \in \Re^{axL}$ in the first layer and one layer of tunable weights $W \in \Re^{Lxb}$ in the second with *a* inputs, *b* outputs, and *L* hidden neurons. The *universal approximation property* for NN's [19] states that for any smooth function $f(x)$,

there exists a NN such that $f(x) = W^T \sigma(V^T x) + \varepsilon$ where ε is the NN functional approximation error and $\sigma(\cdot) : \Re^a \to \Re^L$ is the activation function in the hidden layers. The sigmoid activation function is considered here. For complete details of the NN and its properties, see [19].

Remark: $\|\cdot\|$ and $\|\cdot\|_F$ will be used interchangeably as the Frobenius vector and matrix norms [19].

Define the velocity tracking error as

$$e_{jc} = v_{jc} - v_j \tag{24}$$

Differentiating (24) and adding and subtracting $\overline{M}_j(q_j)\dot{v}_{jc}$ and $\overline{V}_{mj}(q_j)v_{jc}$ to (3) allows the mobile robot dynamics to be written in terms of the velocity tracking error and its derivative as

$$\overline{M}_j(q_j)\dot{e}_{jc} = -\overline{V}_{mj}(q_j, \dot{q}_j)\dot{e}_{j_c} + f_j(x_j) + \overline{\tau}_{dj} \tag{25}$$

where

$$f_j(x_j) = \overline{M}_j(q_j)\dot{v}_{jc} + \overline{V}_{mj}(q_j, \dot{q}_j)v_{jc} + \overline{F}_j(v_j) \tag{26}$$

Define $x_j = [\dot{v}_i, \dot{\omega}_i, v_i, \omega_i, q_j^T, v_j, w_j, e_j^T, \dot{e}_j^T]^T$. The function $f_j(x_j)$ in (26) will be used to bring in the dynamics of leader *i* through $\dot{v}_{jc}$ by observing that

$$\dot{v}_{jc} = f_{vcj}(\dot{v}_i, \dot{\omega}_i, v_i, \omega_i, e_j, \dot{e}_j). \tag{27}$$

The leader *i*'s dynamics (9) can be rewritten as

$$\dot{v}_i = \overline{M}_i^{-1}(q_i)\left(\overline{B}_i(q_i)\tau_i - \overline{V}_{mi}(q_i, \dot{q}_i)v_j - \overline{F}_i(v_i) - \overline{\tau}_{d_i}\right) \tag{28}$$

Substituting (28) into (27) results in the dynamics of the i^{th} leader robot to become apart of $\dot{v}_{jc}$ as

$$\dot{v}_{jc} = f_{vcj}(v_i, \omega_i, \theta_i, \tau_i, e_j, \dot{e}_j) \tag{29}$$

A conventional computed torque controller with velocity tracking could be defined as [21] and [22]

$$\tau_j = \overline{B}_j^{-1}(\overline{M}_j K_4 e_{jc} + f_j(x_j)) \tag{30}$$

where $f_j(x_j)$ is defined by (26) and K_4 is a positive gain matrix. However, the j^{th} follower is not able to construct $\dot{v}_{jc}$ since knowledge of the dynamics of leader *i* is required, making (30) unavailable.

Remark: In [1] and [2], the reference velocity is taken as a constant by ignoring the dynamics of the reference cart. That assumption is not valid here since the reference cart has been replaced by a physical robot *i* which appears to be the leader. Thus, the dynamics of leader robot *i* must be considered in follower *j*'s torque command.

Therefore, the NN is introduced to approximate the dynamics of the mobile robots—both leader and followers. Define a control torque for follower *j* to be as

$$\bar{\tau}_j = \hat{W}_j^{\ T}\sigma(\bar{x}_j) + K_4 e_{jc}, = \hat{f}_j + K_4 e_{jc} \tag{31}$$

where

$$\bar{x}_j = V^T[v_{jr}^T \quad \theta_i \quad \tau_i^T \quad e_j^T \quad \dot{e}_j^T \quad v_j^T \quad v_{jc}^T \quad \dot{v}_{jc}^T\big|_{\dot{v}_i=0}]^T \tag{32}$$

and K_4 is a positive definite matrix defined by $K_4 = k_4 I$ and $\hat{f}_j$ is the NN estimate of (26). The last element of the NN input vector (32) is a preprocessed derivative of control velocity (19), (20) and (21) assuming the leader's acceleration is zero (i.e. $\dot{v}_{jr} = 0$). Since

the leader's acceleration is not always zero, the first four terms of (32) are introduced to accommodate the dynamics of the leader and the omitted terms of $\dot{v}_{jc}^{T}$. Substituting the torque control (31) into the mobile robot error system (25), the closed loop equations become

$$\overline{M}_j \dot{e}_{jc} = -(K_4 + \overline{V}_{mj}) e_{jc} + \widetilde{f}_j + \overline{\tau}_d + \varepsilon_j \tag{33}$$

where the velocity tracking error e_{jc}, is driven by the NN functional estimation error

$$\widetilde{f}_j = f_j - \hat{f}_j \tag{34}$$

According to [19] and [2], applying control (31) does not guarantee that the $\overline{\tau}_j$ will make the velocity tracking error (24) small. In order to guarantee that (24) is small, it is required to specify a method of selecting K_4 and $\hat{f}_j$ such that the velocity tracking error is bounded. The weight estimation errors for follower *j* can be defined similarly to (34), such that

$$\widetilde{W}_j = W_j - \hat{W}_j \tag{35}$$

Before proceeding, the following are required.

Definition 1: An equilibrium point x_e is said to be *uniformly ultimately bounded (UUB)* if there exists a compact set $S \subset \Re^n$ so that for all $x_0 \in S$ there exists a bound B and a time $T(B, x_o)$ such that $\|x(t) - x_e\| \leq B$ for all $t \geq t_0 + T$ [19].

Assumption 8. On any compact subset of $\Re^n$, the ideal NN weights are bounded by known positive values for all followers $j = 1,2,...N$ such that $\|W_j\|_F \leq W_M$ [19].

Assumption 9. The NN reconstruction error for all followers *j* is bounded such that $\|\varepsilon_j\| < \varepsilon_N$, and the disturbances are bounded such that $\|\overline{\tau}_{dj}\| \leq d_M$ [2].

Assumption 10. Let the NN approximation property hold for the function $f_j(x_j)$ (26) with accuracy ε_N for all followers j for all $x_j \quad j = 1,2,...N$ in the compact set S [19].

Theorem 2: Let *Assumptions 1-6* and *8-10* hold and let k_4 be a sufficiently large positive constant. Let a smooth velocity control input $v_{jc}(t)$ be defined by (19), (20) and (21) for the j^{th} follower. Let the torque control (31) for the j^{th} follower robot (3) be applied and let the weight tuning law be given as

$$\dot{\hat{W}}_j = F\sigma_j e_{jc}^T - \kappa F \left\| e_{jc} \right\| \hat{W}_j \tag{36}$$

where $F = F^T > 0$ and $\kappa > 0$ a small design parameter. Then e_j, e_{jc} and $\tilde{W}_j$ which are the position, orientation , and velocity tracking errors as well as the NN weight estimates, respectively, for follower j are UUB. Furthermore, the velocity tracking errors can be made as small as desired by increasing the gain matrix K_4.

Proof: Consider the following Lyapunov candidate:

$$V_j' = V_j + V_{jNN} \tag{37}$$

where V_j is the Lyapunov candidate from *Theorem 1* and defined in (22). V_{jNN} is defined as

$$V_{jNN} = \frac{1}{2} e_{jc}^T \overline{M}_j e_{jc} + \frac{1}{2} tr\{\tilde{W}_j^T F^{-1} \tilde{W}_j\}. \tag{38}$$

Differentiating (37) yields $\dot{V}_j' = \dot{V}_j + \dot{V}_{jNN}$, and in *Theorem 1,* it was stated and proved that $\dot{V}_j < 0$, therefore, we will focus on $\dot{V}_{jNN}$ which is

$$\dot{V}_{jNN} = e_{jc}^T \overline{M}_j \dot{e}_{jc} + \frac{1}{2} e_{jc}^T \dot{\overline{M}}_j e_{jc} + tr\{\tilde{W}_j^T F^{-1} \dot{\tilde{W}}_j\} \tag{39}$$

Substitution of the closed loop error dynamics of follower j (33) and the weight tuning law (36) into (39) and application of the *skew symmetric property* produces

$$\dot{V}_{jNN} = -e_{jc}^T K_4 e_{jc} + \kappa \left\| e_{jc} \right\| tr\{\tilde{W}_j^T (W_j - \tilde{W}_j)\} + e_{jc}^T (\varepsilon_j + \bar{\tau}_{dj}) \tag{40}$$

after simplifications. Applying *Assumptions 8* and *9* and noting that [19]

$$tr\{\tilde{W}_j^T (W_j - \tilde{W}_j)\} = \left\langle \tilde{W}_j, W_j \right\rangle_F - \left\| \tilde{W}_j \right\|_F^2 \le \left\| \tilde{W}_j \right\|_F \left\| W_j \right\|_F - \left\| \tilde{W}_j \right\|_F^2$$

allows (40) to be written as

$$\dot{V}_{jNN} \le -\left\| e_{jc} \right\| [K_4 \left\| e_{jc} \right\| + \kappa \left\| \tilde{W}_j \right\|_F (\left\| \tilde{W}_j \right\|_F - W_M) - (\varepsilon_N + d_M)] \tag{41}$$

Completing the square with respect to $\left\| \tilde{W}_j \right\|_F$ produces

$$\dot{V}_{jNN} \le -\left\| e_{jc} \right\| [K_{4\min} \left\| e_{jc} \right\| + \kappa \left(\left\| \tilde{W}_j \right\|_F - \frac{W_M}{2} \right)^2 - \kappa \frac{W_M^2}{4} - (\varepsilon_N + d_M)] \tag{42}$$

where $K_{4\min}$ is the minimum singular value of K_4. Equation (42) is less than zero if the terms in the braces are greater than zero. The term in the braces is guaranteed to be positive if

$$\left\| e_{jc} \right\| > \frac{\kappa \frac{W_M^2}{4} + \varepsilon_N + d_M}{K_{4\min}} \equiv b_{ecj} \tag{43}$$

or

$$\left\| \tilde{W}_j \right\|_F > \frac{W_M}{2} + \sqrt{\kappa \frac{W_M^2}{4} + \frac{\varepsilon_N + d_M}{K_{4\min}}} \equiv b_{Wj} \tag{44}$$

Examining (43), it is evident that $\left\| e_{jc} \right\|$ can be made arbitrarily small by increasing the gain matrix K_4. Therefore, it can be concluded that $\dot{V}_{jNN}$ is negative outside of a compact set. Selecting the gain matrix K_4 such that (43) and (44) are satisfied ensures that the

compact set defined by $\|e_{jc}\| \le b_{ecj}$ is contained in S so that the approximation property holds [19]. Thus, the position, orientation, velocity tracking errors and NN weight estimates for follower j are UUB.

D. Leader Control Structure

In every formation, we assume there is leader i such that the following assumptions hold:

Assumption 11. The formation leader follows no physical robots, but follows the virtual leader described in [1].

Assumption 12. The formation leader is capable of measuring its absolute position via instrumentation like GPS so that tracking the virtual robot is possible.

The kinematics and dynamics of the formation leader i are defined by (8) and (9), respectively. From [1], the leader tracks a virtual reference robot with the kinematic constraints of (7), and the tracking error for the leader and its derivative are found to be

$$e_i = \begin{bmatrix} e_{i1} \\ e_{i2} \\ e_{i3} \end{bmatrix} = \begin{bmatrix} \cos\theta_i & \sin\theta_i & 0 \\ -\sin\theta_i & \cos\theta_i & 0 \\ 0 & 0 & 1 \end{bmatrix} \begin{bmatrix} x_r - x_i \\ y_r - y_i \\ \theta_r - \theta_i \end{bmatrix} \tag{45}$$

and

$$\dot{e}_i = \begin{bmatrix} \dot{e}_{i1} \\ \dot{e}_{i2} \\ \dot{e}_{i3} \end{bmatrix} = \begin{bmatrix} -v_i + v_{ir}\cos e_{i3} + \omega_i e_{i2} \\ -\omega_i e_{i1} + v_{ir}\sin e_{i3} \\ \omega_{ir} - \omega_i \end{bmatrix} \tag{46}$$

The control velocity $v_{ic}(t)$ can be defined as [1]

$$v_{ic} = \begin{bmatrix} v_{ir}\cos e_{i3} + k_{i1}e_{i1} \\ \omega_{ir} + k_{i2}v_{ir}e_{i2} + k_{i3}v_{ir}\sin e_{i3} \end{bmatrix} \tag{47}$$

Defining the error system for leader i using similar steps used to form (25) and (26) for follower j, the control torque for leader i can be defined similarly to follower j's as

$$\bar{\tau}_i = \hat{W}_i^T \phi(\bar{x}_i) + K_{i4} e_{ic}, = \hat{f}_i + K_{i4} e_{ic} \tag{48}$$

where $\bar{x}_j = V^T [v_i^T \quad v_{ic}^T \quad \dot{v}_{ic}^T]$, $K_{i4} = k_{i4} I$, and e_{ic} is defined similarly to (24). Let the NN weight updates for the leader *i* be given by

$$\dot{\hat{W}}_i = F \sigma_i e_{ic}^T - \kappa F \| e_{ic} \| \hat{W}_i \tag{49}$$

Remark: Since the formation leader tracks a virtual robot, it is able to calculate $\dot{v}_{ic}^T$ since the virtual robot does not have dynamics.

Assumption 13. The leader's reference linear velocity v_{ir} is greater than zero and bounded and the reference angular velocity ω_{ir} is bounded for all *t*.

Assumption 14. $K_i = [k_{i1} \quad k_{i2} \quad k_{i3}]^T$ is a vector of positive constants.

Theorem 3: Given the kinematic system of (8) and dynamic system (9) for leader *i* with *n* generalized coordinates q_i, *m* independent constraints, and *r* actuators, let *Assumption 4* and *Assumptions 8-14* hold for leader *i.* Let k_{i4} be a sufficiently large positive constant. Let there be a smooth velocity control input $v_{ic}(t)$ for the leader *i* given by (47), and let the torque control for the lead robot *i* (48) be applied to the mobile robot system (9). Then leader's position, orientation, and velocity tracking errors as well as the NN weight estimates error are UUB.

Proof : Consider the following Lyapunov candidate $V_i' = V_i + V_{iNN}$

where $$V_i = \frac{1}{2}(e_{i1}^2 + e_{i2}^2) + \frac{1 - \cos e_{i3}}{k_{i2}} \tag{50}$$

and $$V_{iNN} = \frac{1}{2} e_{ic}^T \overline{M}_i e_{ic} + \frac{1}{2} tr\{\tilde{W}_i^T F^{-1} \tilde{W}_i)\} \tag{51}$$

Taking the derivative of (50) and substitution of the error dynamics and control velocity (46) and (47), respectively, reveals the following after simplification

$$\dot{V}_i = -k_{i1} e_{i1}^2 - \frac{k_{i3}}{k_{i2}} v_{ir} \sin^2 e_{i3} \leq 0 \tag{52}$$

Examining (51) and comparing it with follower *j's* Lyapunov function (38), one can see that they are identical in structure. Define the error dynamics for the leader *i* using the same methods used to find the follower's error dynamics (25) and (26). Then it is straight forward to conclude using the same steps and justifications used to derive equations (39)-(44) that the leader's position, orientation, and tracking velocity errors as well as its NN weight estimation errors are all UUB. Next the stability of the formation is introduced.

E. Formation Stability

The stability of the formation can be demonstrated by using the individual Lyapunov functions as given in the following theorem.

Theorem 4: Consider a formation of *N+1* robots consisting a leader *i* and *N* followers. Let *Assumptions 1-6* and *8-14* hold. Let k_4 and k_{i4} be sufficiently large positive constants. Let there be a smooth velocity control input $v_{ic}(t)$ given by (47) for the leader *i*, and let the torque control from (48) for the lead robot *i* (9) be applied. Let there be a smooth velocity control input $v_{jc}(t)$ given by (19), (20), and (21) for the j^{th} follower and torque control given by (31) for the j^{th} follower robot (3) be applied. Then the origin $e_{ij} = [e_i^T \quad e_{ic}^T \quad e_j^T \quad e_{jc}^T]^T = 0$ where $e_{ij} \in \Re^{(n+r)(1+N)x1}$ is the augmented position, orientation and velocity tracking error systems and $\tilde{Z}_{ij}^{\ T} = [\tilde{W}_i \quad \tilde{W}_j] = 0$

where $\widetilde{Z}_{ij}^{\ T} \in \Re^{rxL(N+1)}$ is the augmented NN weight estimation error matrix for the leader *i* and *N* followers, respectively, is UUB.

Let the augmented NN weight update be given by

$$\dot{\hat{Z}} = \overline{F}\sigma_{ij}e_c^T - \kappa\overline{F}\left\|e_c\right\|\hat{Z} \tag{53}$$

where $e_c^T = [e_{ic}^T \quad e_{jc}^T] \in \Re^{1xr(N+1)}$, $\sigma_{ij} = [\sigma_i(\bar{x}_i)^T \quad \sigma_j(\bar{x}_j)^T]^T \in \Re^{L(N+1)x1}$ and $\overline{F} = diag(F) \in \Re^{L(N+1)xL(N+1)}$ for $j = 1,2,...N$.

Proof: Consider the following Lyapunov candidate

$$V_{ij} = \sum_1^N V_j + V_i + V_{NN} \tag{54}$$

where V_j is defined by (22), V_i is defined by (50), and V_{NN} is defined as

$$V_{NN} = \frac{1}{2}e_c^T\overline{M}\ e_c + \frac{1}{2}tr\{\widetilde{Z}_{ij}^T\overline{F}^{-1}\widetilde{Z}_{ij}) \tag{55}$$

where $\overline{M} = diag(\overline{M}_i, \overline{M}_j) \in \Re^{r(N+1)xr(N+1)}$ for $j = 1,2,...N$. Examining (22), (50) and (55) it can be concluded that (54) is positive definite for $e_{ij} \neq 0$ and $\widetilde{Z}_{ij} \neq 0$. Taking the derivative of (54) yields

$$\dot{V}_{ij} = \sum_1^N \dot{V}_j + \dot{V}_i + \dot{V}_{NN} \tag{56}$$

It was shown in *Theorem 1* that $\dot{V}_j < 0$ for all *j* in *N*, so clearly

$$\sum_1^N \dot{V}_j < 0 \tag{57}$$

In *Theorem 3* it was shown that $\dot{V}_i \leq 0$, so consider now

$$\dot{V}_{NN} = e_c^T\overline{M}\ \dot{e}_c + \frac{1}{2}e_c^T\dot{\overline{M}}\ e_c + tr\{\widetilde{Z}_{ij}^T\overline{F}^{-1}\dot{\widetilde{Z}}_{ij}\} \tag{58}$$

Examining (58) and comparing it with follower *j's* Lyapunov function (39), one can see that they are identical in structure. Define the augmented error dynamics system to include leader *i* as well as followers $j = 1,2,...N$ such that $\overline{M} = diag(\overline{M}_i, \overline{M}_j) \in \Re^{r(N+1)xr(N+1)}$ and $e_c^T = [e_{ic}^T \quad e_{jc}^T] \in \Re^{1xr(N+1)}$ are valid using the same methods used to find the follower's error dynamics (25) and (26). Then it is straight forward to conclude using the same steps and justifications used to derive equations (39)-(44), that the position, orientation, velocity tracking, and the NN weight estimations errors for the entire formation are UUB.

Remark: The position, orientation, velocity tracking, and the NN weight estimations errors for the entire formation are UUB for the case when follower *j* becomes a leader to follower *j+1*. Proof of this claim follows directly from *Theorem 2* and the Lyapunov candidate

$$V_j'' = \sum_{j}^{j+1} V_j' \tag{59}$$

where V_j' is defined in (37).

III. Leader-Follower Obstacle Avoidance

In the previous section, a tracking controller for leader-follower based formation control was developed that sought to drive follower *j* to a reference location and desired orientation with respect to leader *i*. However, with the introduction of obstacle avoidance schemes, the orientation of the follower *j* will vary from its leader's as a result of avoiding an obstacle that was in the path of follower *j* but not its leader. Therefore, when an obstacle is encountered, it is logical for follower *j* to track a reference point, but no specific orientation with respect to its leader so that it can avoid the obstacle.

The proposed obstacle avoidance scheme is designed to take advantage of the tracking ability of the follower robots. When an obstacle is encountered, the desired separation and bearing is redefined so that the follower robot is guided around the obstacle. To accomplish this, the desired separation and bearing are no longer considered to be constants but are considered to be time varying.

Remark: In this section, the time varying desired separation and bearing will be denoted as $L_{ijd}(t)$ and $\psi_{ijd}(t)$ while the constant desired separation and bearing will be written as L_{ijd} and ψ_{ijd}.

Consider the formation tracking control error system presented in (14), but rewritten as

$$e_{jo} = \begin{bmatrix} e_{jo1} \\ e_{jo2} \end{bmatrix} = \begin{bmatrix} L_{ijd}(t)\cos(\Psi_{ijd}(t) + \bar{\theta}_j) - L_{ij}\cos(\Psi_{ij} + \bar{\theta}_j) \\ L_{ijd}(t)\sin(\Psi_{ijd}(t) + \bar{\theta}_j) - L_{ij}\sin(\Psi_{ij} + \bar{\theta}_j) \end{bmatrix} \tag{60}$$

where $\bar{\theta}_j = \theta_i - \theta_j$ and only the normal and tangential components of the separation and bearing errors are considered. The dynamics of (60) can be found in a similar manner used to derive (18), and written as

$$\begin{bmatrix} \dot{e}_{jo1} \\ \dot{e}_{jo2} \end{bmatrix} = \begin{bmatrix} \dot{\bar{e}}_{jo1} - v_j + v_i\cos\bar{\theta}_j + \omega_j e_{jo2} - \omega_i L_{ijd}(t)\sin(\Psi_{ijd} + \bar{\theta}_j) \\ \dot{\bar{e}}_{jo2} - \omega_j e_{jo1} + v_i\sin\bar{\theta}_j - d_j\omega_j + \omega_i L_{ijd}(t)\cos(\Psi_{ijd} + \bar{\theta}_j) \end{bmatrix} \tag{61}$$

where

$$\dot{\bar{e}}_{jo1} = \dot{L}_{ijd}(t)\cos(\Psi_{ijd}(t) + \bar{\theta}_j) - \dot{\Psi}_{ijd}(t)L_{ijd}(t)\sin(\Psi_{ijd}(t) + \bar{\theta}_j) \tag{62}$$

and

$$\dot{\bar{e}}_{jo2} = \dot{L}_{ijd}(t)\sin(\Psi_{ijd}(t) + \bar{\theta}_j) + \dot{\Psi}_{ijd}(t)L_{ijd}(t)\cos(\Psi_{ijd}(t) + \bar{\theta}_j) \tag{63}$$

Comparing (61) with (18), one can see that they are identical except for the terms added as a result of the time varying desired separation and bearing

A. Obstacle Avoidance

Consider the configuration shown in Figure 3. It is desired that follower robot *j* maintains a distance s_d from all obstacles; therefore, to navigate around the obstacle, the following simple approach is proposed.

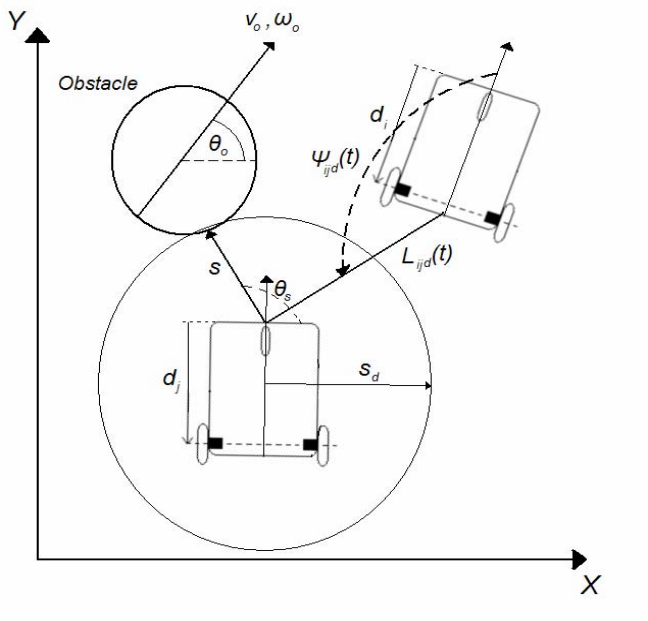

Figure 3: Obstacle Encounter

When the nearest edge of an obstacle is detected at an angle θ_s and distance *s* relative to follower *j* such that $s < s_d$, the desired separation and bearing, $L_{ijd}(t)$ and $\psi_{ijd}(t)$, are modified such that the follower is steered away from the obstacle by

$$\begin{aligned} L_{ijd}(t) &= L_{ijd} - \frac{1}{2}K_L\left(\frac{1}{s} - \frac{1}{s_d}\right)^2 \\ \Psi_{ijd}(t) &= \Psi_{ijd} + \frac{1}{2}K_\Psi\left(\frac{1}{s} - \frac{1}{s_d}\right)^2 \operatorname{sgn}(\Psi_{ijd}) \end{aligned} \tag{64}$$

where *sgn* is the signum function and K_L and K_ψ are positive design constants. Examining (64), one can see that the shifts introduced to the desired separation and bearing are similar to repulsive potential functions commonly used in robotic path

planning [20]. Here we use the potential like function to push the desired set point of the follower robot *j* away from the encountered obstacle thus steering the robot around the obstruction.

In order to calculate the expressions in (62) and (63), derivatives of the desired separation and bearing are necessary. The measured distance *s* and angle θ_s can be written in terms of the *x* and *y* components *s* as

$$\begin{aligned} s^2 &= s_x^2 + s_y^2 \\ \theta_s &= \arctan\left(\frac{s_y}{s_x}\right) \end{aligned} \tag{65}$$

where

$$\begin{aligned} s_x &= x_j - x_o \\ s_y &= y_j - y_o \end{aligned} \tag{66}$$

and x_o and y_o are the coordinates of the obstacle. Note that the obstacle is not necessarily stationary, and assume that the obstacle can be defined by the kinematic model

$$\begin{aligned} \dot{x}_o &= v_o \cos\theta_o \\ \dot{y}_o &= v_o \sin\theta_o \end{aligned}. \tag{67}$$

Differentiating (65) and (66), and substitution of (2) and (67) reveals

$$\begin{aligned} \dot{s} &= v_j \cos(\theta_j - \theta_s) - d_j w_j \sin(\theta_j - \theta_s) - v_o \cos(\theta_o - \theta_s) \\ \dot{\theta}_s &= \frac{1}{s}(v_j \sin(\theta_j - \theta_s) + d_j w_j \cos(\theta_j - \theta_s) - v_o \sin(\theta_o - \theta_s)) \end{aligned} \tag{68}$$

Before continuing, the following assumptions are required.

Assumption 15. Follower *j* and the leader *i* are equipped with instrumentation capable of measuring the distance *s* and relative angle of the obstacle θ_s.

Assumption 16. The velocity v_o and orientation θ_o of the obstacle are not available to follower *j* and leader *i*.

Since the velocity v_o and orientation θ_o of the obstacle are not available to follower *j,* the derivatives in (68) must be estimated. Assuming that $\dot{s}$ and $\dot{\theta}_s$ are smooth functions, define the estimates of $\dot{s}$ and $\dot{\theta}_s$ using standard backwards difference equations as

$$\begin{aligned} \dot{\hat{s}} &= s(t) - s(t - \Delta t) \\ \dot{\hat{\theta}}_s &= \theta_s(t) - \theta_s(t - \Delta t) \end{aligned} \tag{69}$$

where Δt is an arbitrarily small sampling period.

Now we can define the derivative of (64) as

$$\begin{aligned} \dot{L}_{ijd}(t) &= K_L\left(\frac{1}{s} - \frac{1}{s_d}\right)\frac{1}{s^2}\dot{\hat{s}} \\ \dot{\Psi}_{ijd}(t) &= -\operatorname{sgn}(\Psi_{ijd})K_\psi\left(\frac{1}{s} - \frac{1}{s_d}\right)\frac{1}{s^2}\dot{\hat{s}} \end{aligned} \tag{70}$$

Substitution of (70) into the error dynamics defined in (62) and (63) yields

$$\dot{\bar{e}}_{jo1} = K_L\left(\frac{1}{s} - \frac{1}{s_d}\right)\frac{1}{s^2}\dot{\hat{s}}\cos(\Psi_{ijd}(t) + \bar{\theta}_j) + \operatorname{sgn}(\Psi_{ijd})K_\psi\left(\frac{1}{s} - \frac{1}{s_d}\right)\frac{1}{s^2}\dot{\hat{s}}L_{ijd}(t)\sin(\Psi_{ijd}(t) + \bar{\theta}_j) \tag{71}$$

$$\dot{\bar{e}}_{jo2} = K_L\left(\frac{1}{s} - \frac{1}{s_d}\right)\frac{1}{s^2}\dot{\hat{s}}\sin(\Psi_{ijd}(t) + \bar{\theta}_j) - \operatorname{sgn}(\Psi_{ijd})K_\psi\left(\frac{1}{s} - \frac{1}{s_d}\right)\frac{1}{s^2}\dot{\hat{s}}L_{ijd}(t)\cos(\Psi_{ijd}(t) + \bar{\theta}_j) \tag{72}$$

To stabilize the error dynamics in the presence of an obstacle, the following velocity control inputs for follower robot *j* is proposed to achieve the desired position and orientation with respect to leader *i* as

$$v_{jco} = \begin{bmatrix} v_{jco} \\ \omega_{jco} \end{bmatrix} = \begin{bmatrix} v_i\cos\bar{\theta}_j + k_1 e_{j1} - \omega_i L_{ijd}\sin(\Psi_{12d} + \bar{\theta}_j) \\ \dfrac{1}{d_j}(\omega_i L_{ijd}\cos(\Psi_{ijd} + \bar{\theta}_j) + k_2 e_{j2} + v_i\sin\bar{\theta}_j) \end{bmatrix} + \begin{bmatrix} \dot{\bar{e}}_{j1} \\ \dfrac{\dot{\bar{e}}_{j2}}{d_j} \end{bmatrix} \tag{73}$$

Theorem 5 [22]*:* Given the kinematic model of nonholonomic mobile robot in (2), along with the leader follower criterion of (1), let *Assumptions 1-5* and *Assumption 7* hold. Let k_1, k_2, K_L and K_ψ be positive constants, and let the smooth velocity control input $v_{jco}(t)$ for the j^{th} follower be given by (73). Then the origin $e_{jo} = 0$ consisting of the position error for the follower is stable in the sense of Lyapunov.

Proof: Consider the following Lyapunov candidate

$$V_{jo} = \frac{1}{2}(e_{jo1}^2 + e_{jo2}^2) \tag{74}$$

Clearly, $V_{jo} > 0$ and $V_{jo} = 0$ only when $e_{jo} = 0$. It is shown in [22] that taking the time derivate of (74) and substitution of the error dynamics (61) and control velocity (73) reveals

$$\dot{V}_{jo} \leq -\frac{\bar{k}}{2}\left\|e_{jo}\right\|^2 - \frac{\bar{k}}{2}\left(\left\|e_{jo}\right\| - \frac{\varepsilon_j}{\bar{k}}\right)^2 + \frac{\varepsilon_j^2}{2\bar{k}} \tag{75}$$

and it can be concluded that the formation errors are bounded during an obstacle avoidance maneuver. Moreover, these bounds can be made arbitrary small by increasing $\bar{k}$.

Remark: In order to remove the perfect velocity tracking assumption of *Assumption 7,* the dynamic control presented in *Theorem 2* can be applied by replacing the velocity control input (19) with (73) when in the presence of an obstacle. Also, since leader robot *i* does not track a physical robot, any existing obstacle avoidance method can be utilized by the leader. When the leader robot performs an obstacle avoidance maneuver, the entire formation will continue to track the leader, and once the leader has steered around the obstacle, the followers can navigate the obstruction on an individual bases. That is,

the obstacle avoidance method selected for the leader does not affect the stability of the entire formation in the presence of obstacles.

B. Formation Stability in the Presence of Obstacles

Before proving the stability of the entire formation in the presence of obstacles, an additional assumption is required.

Assumption 17. Leader *i* utilizes a path planning algorithm such that by tracking the virtual reference cart described in [1], the lead robot *i* navigates around any encountered obstacles.

Under *Assumption 17*, the lead robot *i* navigate around obstacles by tracking its virtual reference cart. Therefore, the controller described in *Theorem 3* is used to control the leader in both the absence and presence of obstacles. The path planning algorithm for the leader *i* is beyond the scope of this paper and therefore is not included here.

Theorem 6. Consider a formation of *N+1* robots consisting of a leader *i* and *N* followers in the presence of obstacles. Let *Assumptions 1-6* and *8-17* hold. Let Let $k_1, k_2, K_L, K_\psi,\ k_4$ and k_{i4} be sufficiently large positive constants. Let there be a smooth velocity control input $v_{ic}(t)$ for the leader *i* given by (47), and let the torque control for the lead robot *i* from (48) be applied to the mobile robot system (9). Let there be a smooth velocity control input $v_{jco}(t)$ for the j^{th} follower given by (73) and torque control for the j^{th} follower robot given by (31) be applied to the mobile robot system (3). Let the augmented NN weight update be given by (53). Then the origin $e_{ijo} = [e_i^T \quad e_{ic}^T \quad e_{jo}^T \quad e_{jc}^T]^T = 0$ where $e_{ijo} \in \Re^{(r(1+N)+n+(n-1)N)x1}$ is the augmented position, orientation and velocity tracking error systems and $\tilde{Z}_{ij}^{\ T} = [\tilde{W}_i \quad \tilde{W}_j] = 0$

where $\widetilde{Z}_{ij}^{\ T} \in \Re^{rxL(N+1)}$ is the augmented NN weight estimation error matrix for the leader *i* and *N* followers, respectively, is stable in the sense of Lyapunov.

Proof: Consider the following Lyapunov candidate

$$V_{ijo} = \sum_{1}^{N} V_{jo} + V_i + V_{NN} \tag{76}$$

where V_{jo} is defined in (74), V_i is defined in (50) and V_{NN} is defined in (55). Differentiating (76) yields

$$\dot{V}_{ijo} = \sum_{1}^{N} \dot{V}_{jo} + \dot{V}_i + \dot{V}_{NN} \tag{77}$$

and it was shown in equation (52) of *Theorem 3* that $\dot{V}_i \leq 0$ after substitution of the error dynamics and velocity control inputs (46) and (47), respectively. Substitution of the error dynamics and control inputs (61) and (73), respectively, into $\dot{V}_{jo}$ reveals

$$\sum_{1}^{N} \dot{V}'_{jo} = \sum_{1}^{N} \left(-k_1 e_{jo1}^2 - k_2 e_{jo2}^2 + e_{jo1} \dot{\tilde{e}}_{sj1} + e_{jo2} \dot{\tilde{e}}_{sj2} \right) \tag{78}$$

where $\dot{\tilde{e}}_{sj1} = \dot{\bar{e}}_{jo1} - \dot{\hat{\bar{e}}}_{jo1}$ and $\dot{\tilde{e}}_{sj2} = \dot{\bar{e}}_{jo2} - \dot{\hat{\bar{e}}}_{jo2}$. Noting the similarities of (78) with *Theorem 5* allows (78) to be written as

$$\sum_{1}^{N} \dot{V}'_{jo} \leq \sum_{1}^{N} \left(-\bar{k} \left\| e_{jo} \right\|^2 + \varepsilon_j \left\| e_{jo} \right\| \right) \tag{79}$$

where $\bar{k} = \min(k_1, k_2)$ and $\varepsilon_j = \left| \dot{\tilde{e}}_{sj1} \right| + \left| \dot{\tilde{e}}_{sj2} \right|$. Completing the square with respect to each $\left\| e_{jo} \right\|$ yields

$$\sum_{1}^{N} \dot{V}'_{jo} \leq \sum_{1}^{N} \left(-\frac{\bar{k}}{2} \left\| e_{jo} \right\|^2 - \frac{\bar{k}}{2} \left(\left\| e_{jo} \right\| - \frac{\varepsilon_j}{\bar{k}} \right)^2 + \frac{\varepsilon_j^2}{2\bar{k}} \right) \tag{80}$$

and (80) can be rewritten as

$$\sum_{1}^{N}\dot{V}_{jo} \le -\sum_{1}^{N}\left(\frac{\bar{k}}{2}\left\|e_{jo}\right\|^2 + \frac{\bar{k}}{2}\left(\left\|e_{jo}\right\| - \frac{\varepsilon_j}{\bar{k}}\right)^2\right) + \sum_{1}^{N}\frac{\varepsilon_j^2}{2\bar{k}} \tag{81}$$

Note that the first summation in (81) is always less than or equal to zero, and the last summation can be made arbitrarily small by increasing $\bar{k}$. Next, note that $\dot{V}_{NN}$ is as defined in (58). Examining (58) and comparing it with follower *j's* Lyapunov function (39), one can see that they are identical in structure. Define the augmented error dynamics system to include leader *i* as well as followers $j = 1,2,...N$ such that $\overline{M} = diag(\overline{M}_i, \overline{M}_j) \in \Re^{r(N+1)xr(N+1)}$ and $e_c^T = [e_{ic}^T \quad e_{jc}^T] \in \Re^{1xr(N+1)}$ are valid using the same methods used to find the follower's error dynamics (25) and (26). Then it is straight forward to conclude using the same steps and justifications used to derive equations (39)-(44) that $\dot{V}_{NN}$ is negative outside of a compact set *S.* Therefore, combining this result with the results of (52) and (81), it can be concluded that the entire formation is stable in the sense of Lyapunov when in the presence of obstacles.

Remark: The stability of the formation for the case when follower *j* becomes a leader to follower *j+1* follows directly from the Lyapunov candidate

$$\overline{V}_{jo} = \sum_{j}^{j+1}\left(V_{jo} + V_{jNN}\right) \tag{82}$$

and applying *Theorem 2* and *Theorem 5*.

IV. Simulation Results

A wedge formation of five identical nonholonomic mobile robots is considered where the leader's trajectory is the desired formation trajectory and simulations are carried out in

MATLAB under two scenarios: with and without obstacles. In the first scenario, two cases are considered. First, perfect velocity tracking in the presence of dynamics examined. In this case, the mass, coriolis, and input transformation matrices are assumed to be known by both the leader and its followers so that the control torque $\tau = \overline{B}^{-1}(\overline{M}(q)\dot{v}_c + \overline{V}_m(q,\dot{q})v_c)$ can be calculated. In the second case, only the input transformation matrix is assumed to be known, perfect velocity tracking is not assumed, and the control torques (31) and (48) are applied. In both cases, unmodeled dynamics are introduced in the form of friction as

$$\overline{F}_j = \begin{bmatrix} \mu_{j1} sign(v_j) + \mu_{j2} v_j \\ \mu_{j3} sign(\omega_j) + \mu_{j4} \omega_j \end{bmatrix}$$

where μ_{ji} varied between 0 and 1 for each robot. The leader's reference linear velocity is 5 m/s while the reference angular velocity is allowed to vary.

In the second scenario, obstacles are added in the path of the follower robots and the obstacle avoidance scheme of *Theorem 5* is demonstrated, and both a static and dynamic obstacle environment is considered.

A simple wedge formation is considered such that follower *j* should track its leader at separation of $L_{ijd} = 2$ meters and a bearing of $\psi_{ijd} = \pm 120°$ depending on the follower's location, and the formation leader is located at the apex of the wedge. The wedge formation that will be considered is shown in Figure 4. In the figure, followers 1 and 3 track the leader and followers 2 and 4 track followers 1 and 3, respectively.

Remark: In the proceeding analysis, $L, F1, F2, F3,$ and $F4$ will be used to denote the *leader, follower 1*, *follower 2, follower 3,* and *follower 4,* respectively.

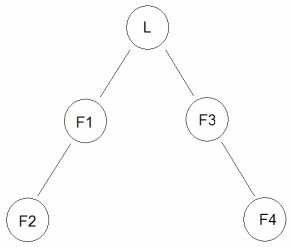

Figure 4: Formation Structure

The controller gains are shown in Table I.

Table I: Controller Gains

Leader	$K_{i4} = diag\{40\}$	$k_{i1} = 10$	$k_{i2} = 5$	$k_{i3} = 4$	
Follower j ($j = 1,2,3,4$)	$K_4 = diag\{40\}$	$k_1 = 7$	$k_2 = 20$	$k_3 = .01$	$k_v = 1$

For the NN controllers, $F = diag\{40\}$, $\kappa = 0.1$ are used for both leader and follower controllers. The following robotic parameters are considered for the leader and its followers: $m = 5kg$, $I = 3kg^2$, $R = .175m$, $r = 0.08m$, and $d = 0.45m$.

A. Scenario I: Obstacle Free Environment

Figure 5 shows the resulting trajectories for both cases described above. In both cases, the robots start in the bottom left corner of Figure 5 and travel towards the top right corner of the figure. A steering command in the form of angular acceleration is given to the formation at $x = 2$. Examining Figure 5, it is apparent that perfect velocity tracking does not hold in presence of dynamics as the formation not only forms incorrectly, but also does not follow its trajectory. Even if a velocity tracking loop is introduced, knowledge of the full dynamics is necessary for conventional torque controllers, and full information is very unlikely and impractical. In case 2, only the torque input transformation matrix is known. All other dynamics, including terms like friction, are

learned online. With the NN dynamical controllers, the wedge formation was achieved and maintained, and small, bounded errors are observed in Figures 6 and 7.

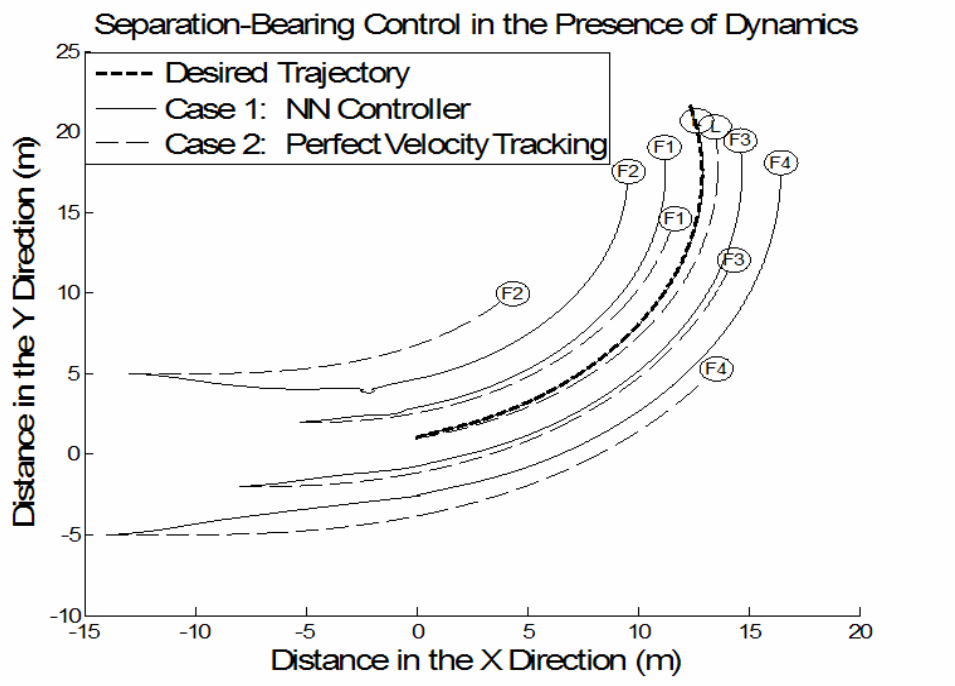

Figure 5: Formation Trajectories for Case 1 and Case 2

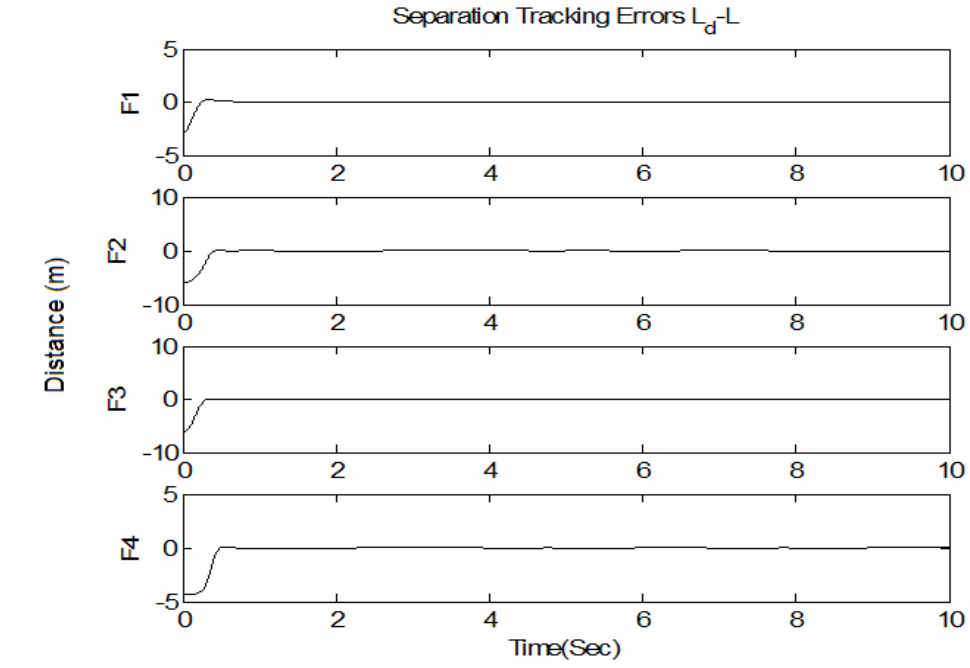

Figure 6: Separation tracking errors

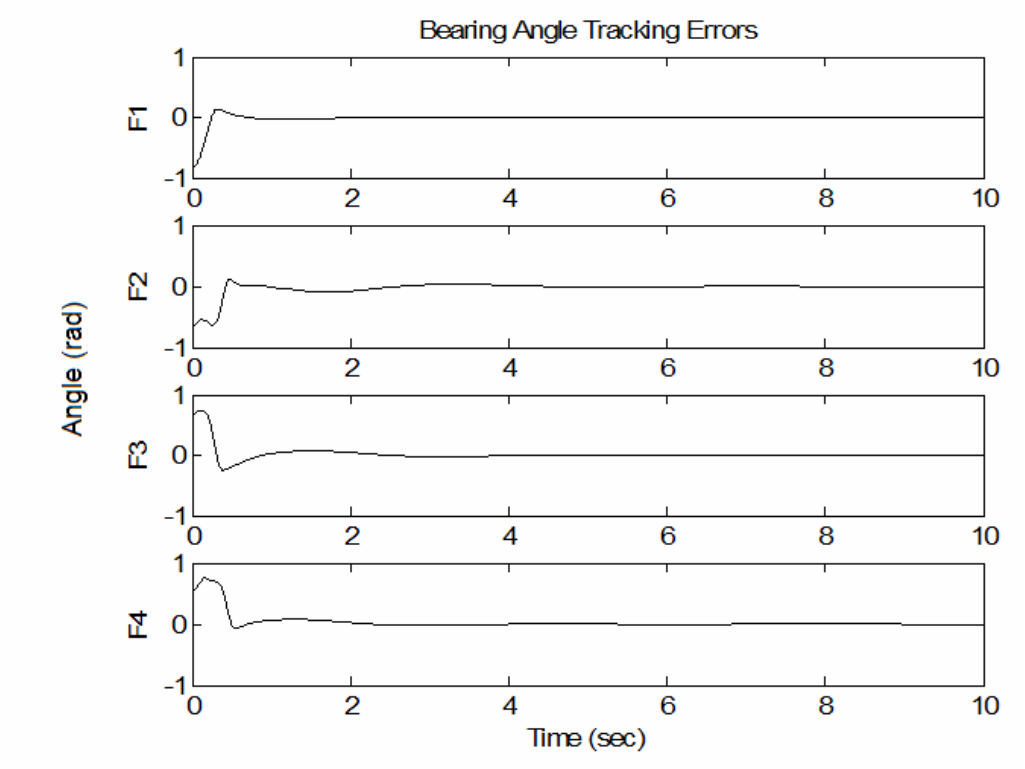

Figure 7: Bearing tracking errors

B. Scenario II: Obstacle Ridden Environment

Now, the wedge formation of five robots is considered in an environment with stationary and moving obstacles, and the controller gains outlined in Table I along with the gains shown in Table II were utilized.

Table II: Obstacle Avoidance Gains

$K_L = 5$	$K_\psi = 1.5$

Figures 8 and 9 depict the formation trajectories in the presence of stationary obstacles. Examining the zoomed formation trajectories shown in Figure 9, it is evident that the robots are able to maneuver around the encountered obstacle while simultaneously tracking their leaders. Because the followers on the outside of the formation track the robots in the inner formation, the movements of the robots in the

interior of the formation propagate to followers on the exterior of the formation. Thus, when a robot on the interior of the formation performs an obstacle avoidance maneuver, their movements are mimicked by their followers which is evident in Figures 8 and 9. Figures 10 and 11 illustrate the desired separation and bearing, respectively, for follower robot 2. Examining the plots, the constant set points become time varying when an obstacle is encountered and return to constant values once the obstruction is navigated. Figures 12 and 13 display the formation tracking errors for all followers. Examining the plots, one can see that the separation and bearing tracking errors are small and bounded when in the presence of an encountered obstacle which supports the theoretical conjecture.

Next, the formation is tested in the presence of a dynamic obstacle environment. When the obstacle is encountered in this scenario, the obstacle begins to move with a constant velocity until the robot has completely navigated around the obstacle to avoid it. Figures 14 and 15 show the formation trajectories. The dotted lines represent the path of moving obstacles, and the connected circles denote the obstacles' final positions. Figures 16 and 17 display the desired separation and bearing time history of follower 2 in the dynamic environment. Again, the influence of the obstacle on follower 2 can be observed when the desired separation and bearing become time varying. Figures 18 and 19 present the formation tracking errors for all four followers. Examining the figures, it is clear that the separation and bearing tracking errors are small and bounded in the presence of moving obstacles.

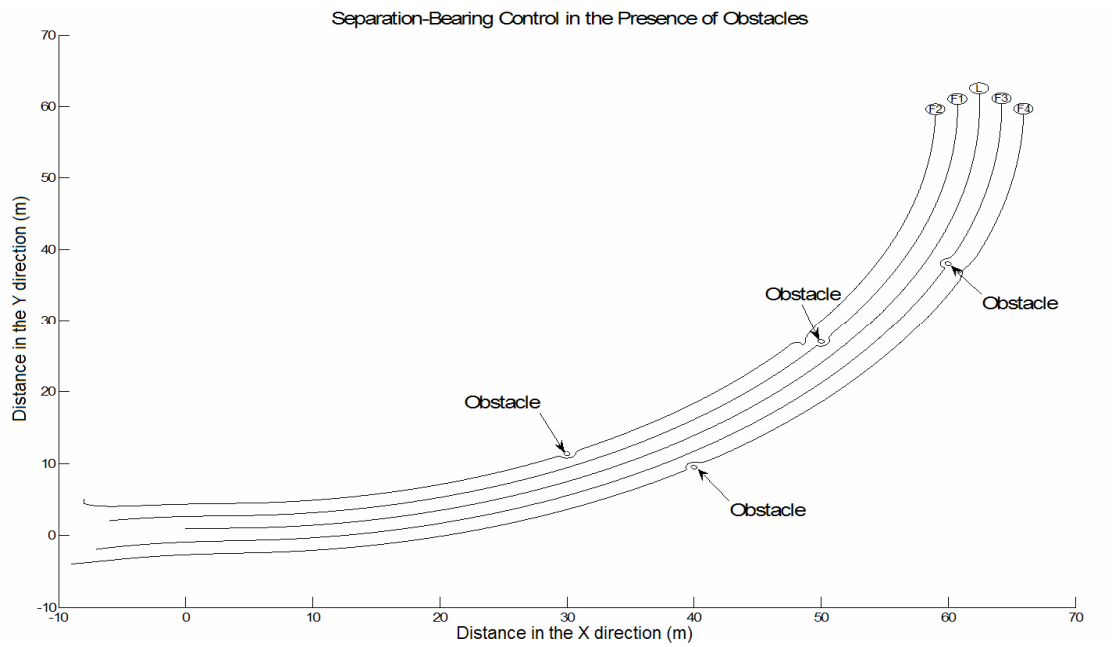

Figure 8: Formation Trajectories with Obstacles

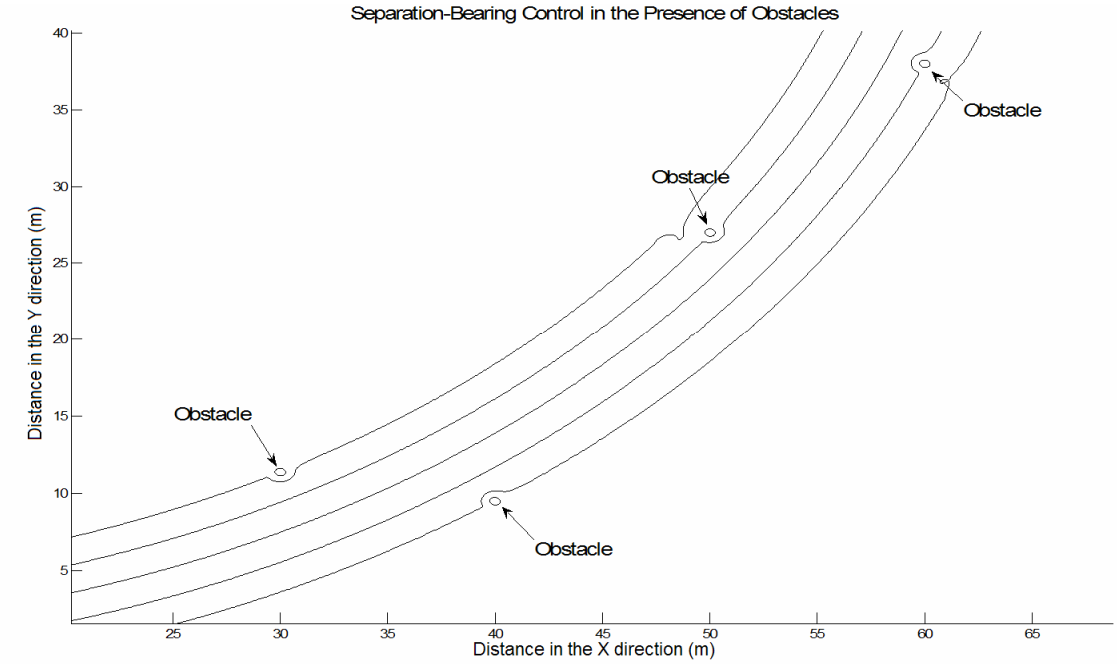

Figure 9: Zoomed Formation Trajectories with Obstacles

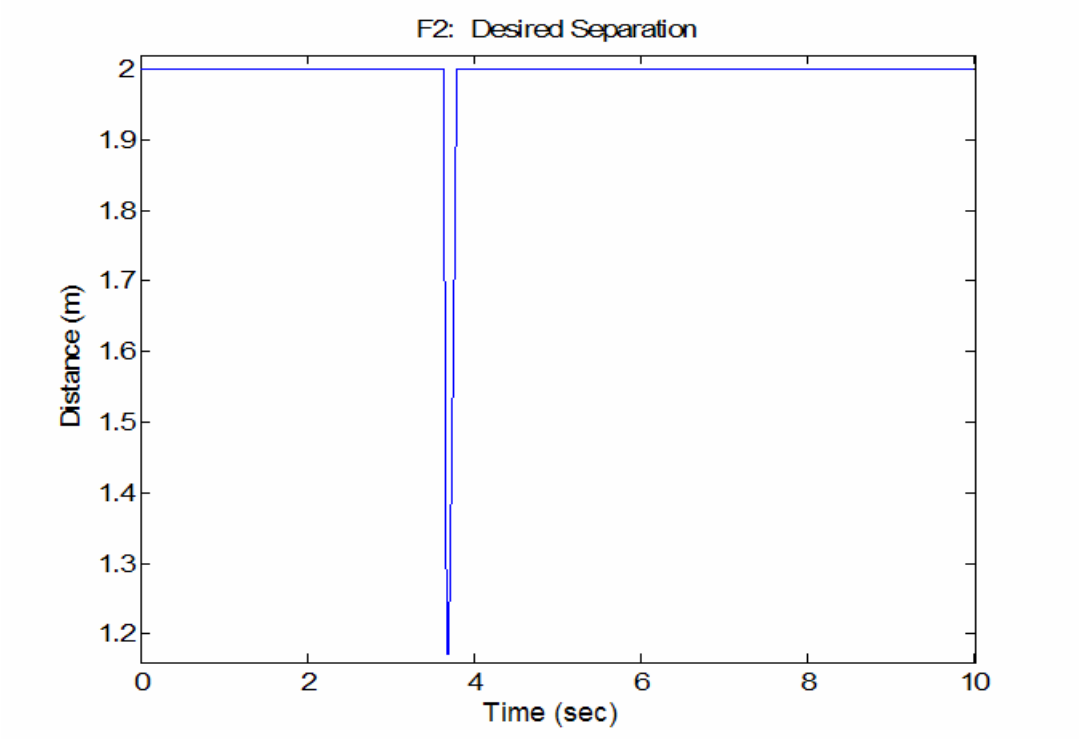

Figure 10: Desired Separation for Follower 2

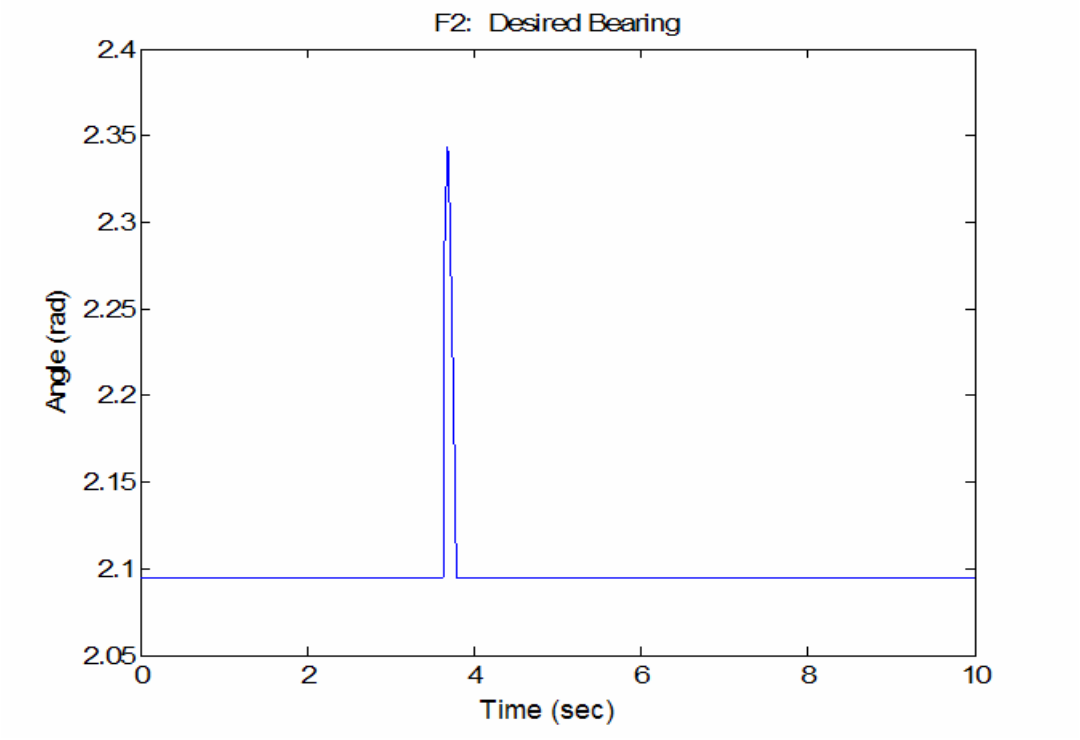

Figure 11: Desired Bearing for Follower 2

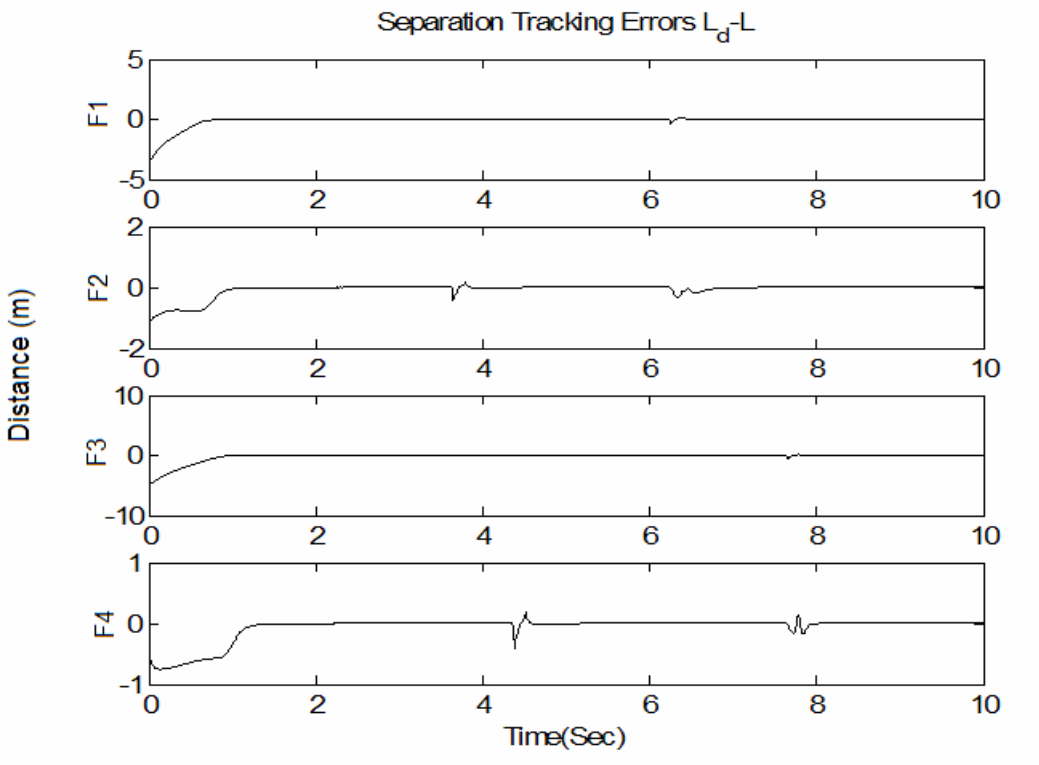

Figure 12: Separation Errors

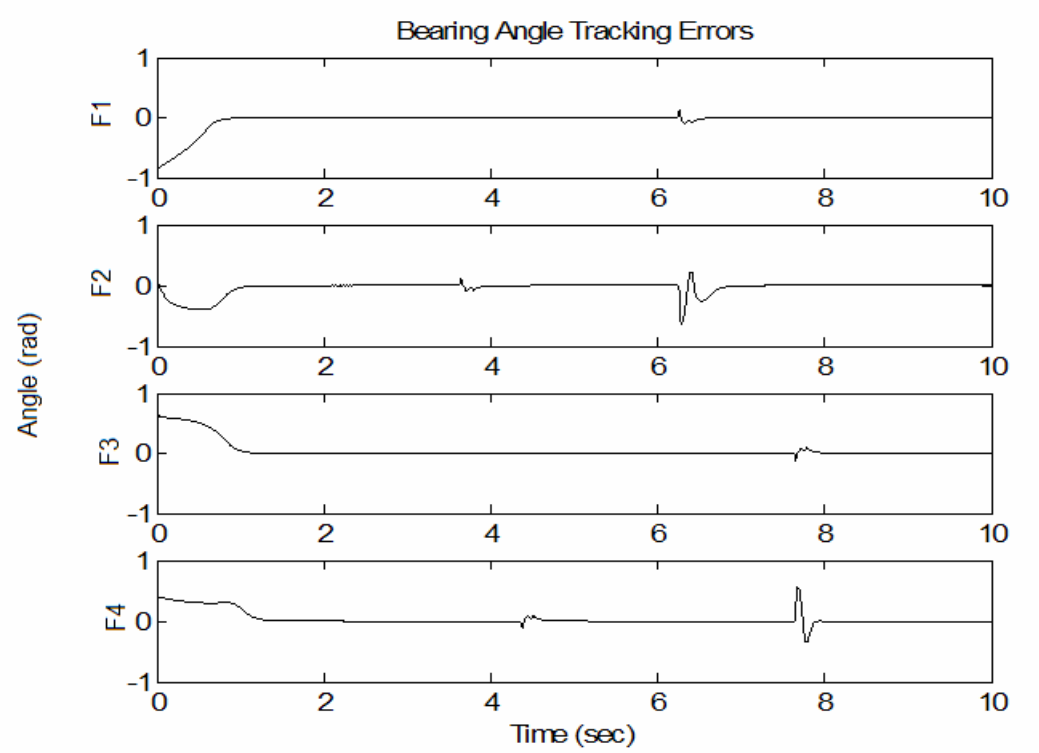

Figure 13: Bearing Errors

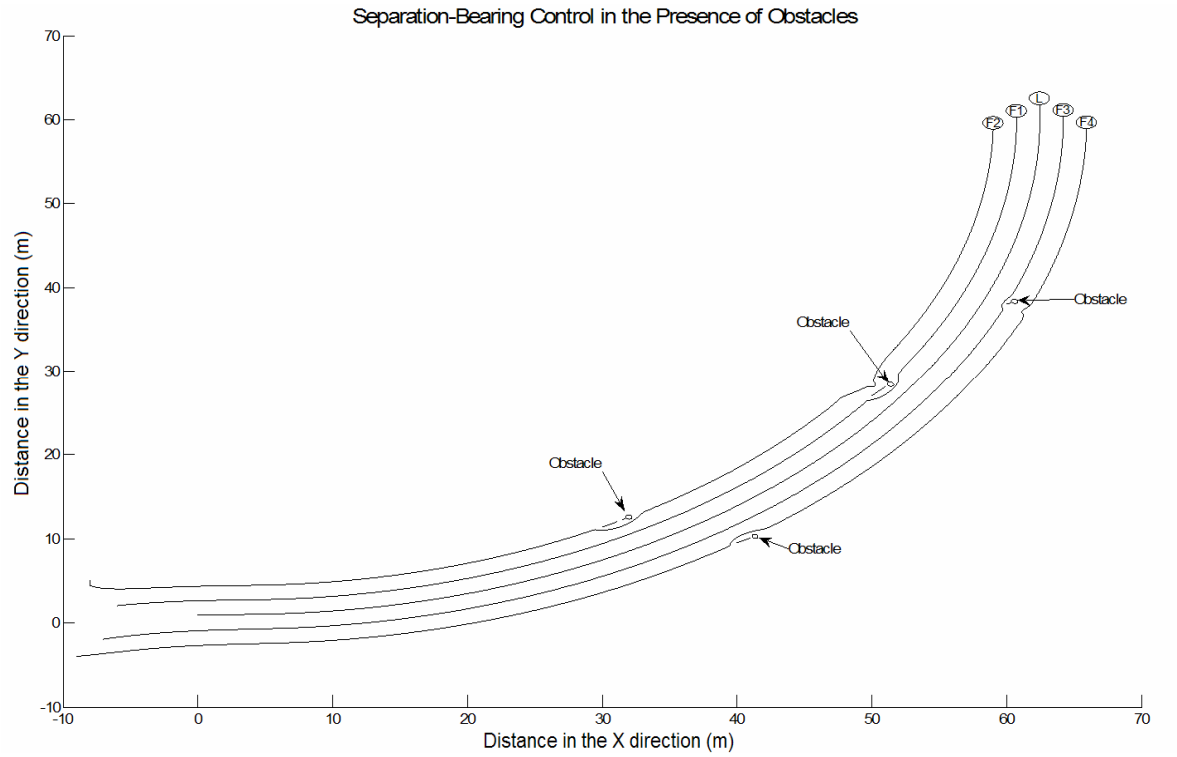

Figure 14: Formation Trajectories in a Dynamic Obstacle Environment

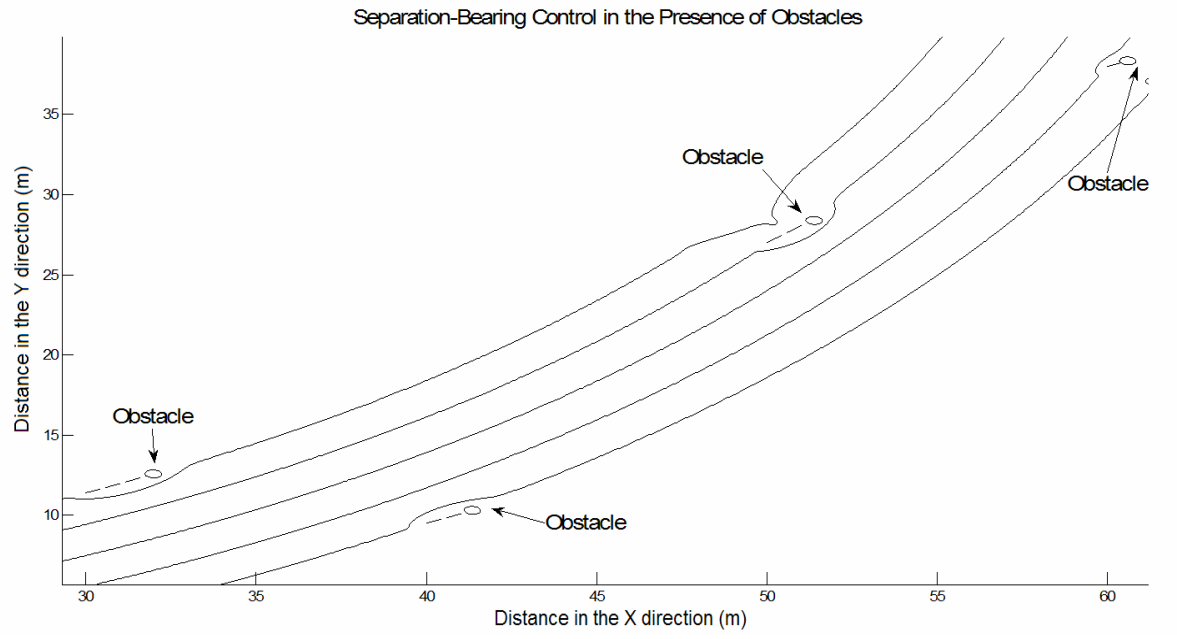

Figure 15: Zoomed Formation Trajectories in a Dynamic Obstacle Environment

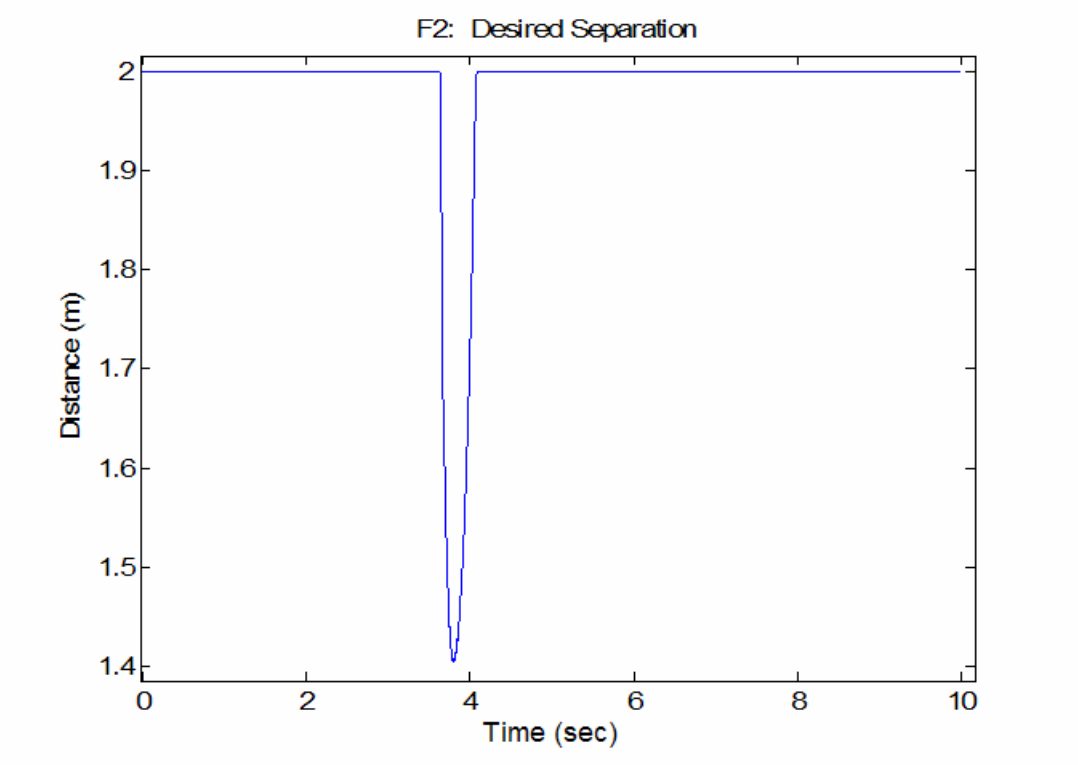

Figure 16: Desired Separation in a Dynamic Obstacle Environment

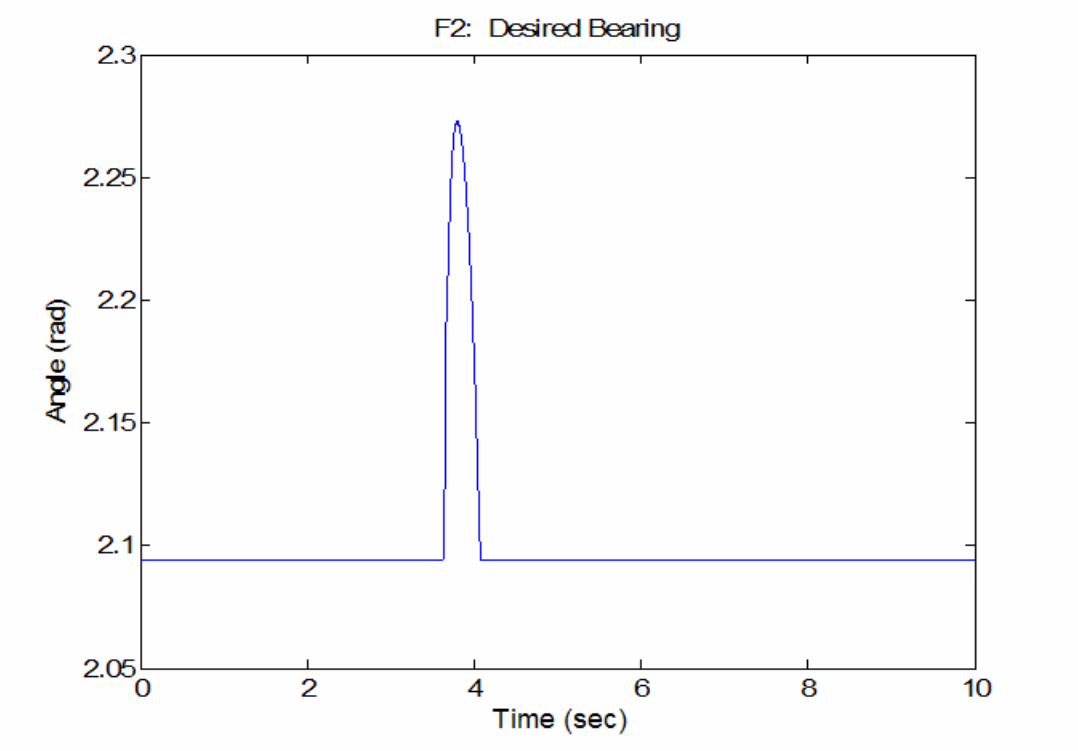

Figure 17: Desired Bearing in a Dynamic Obstacle Environment

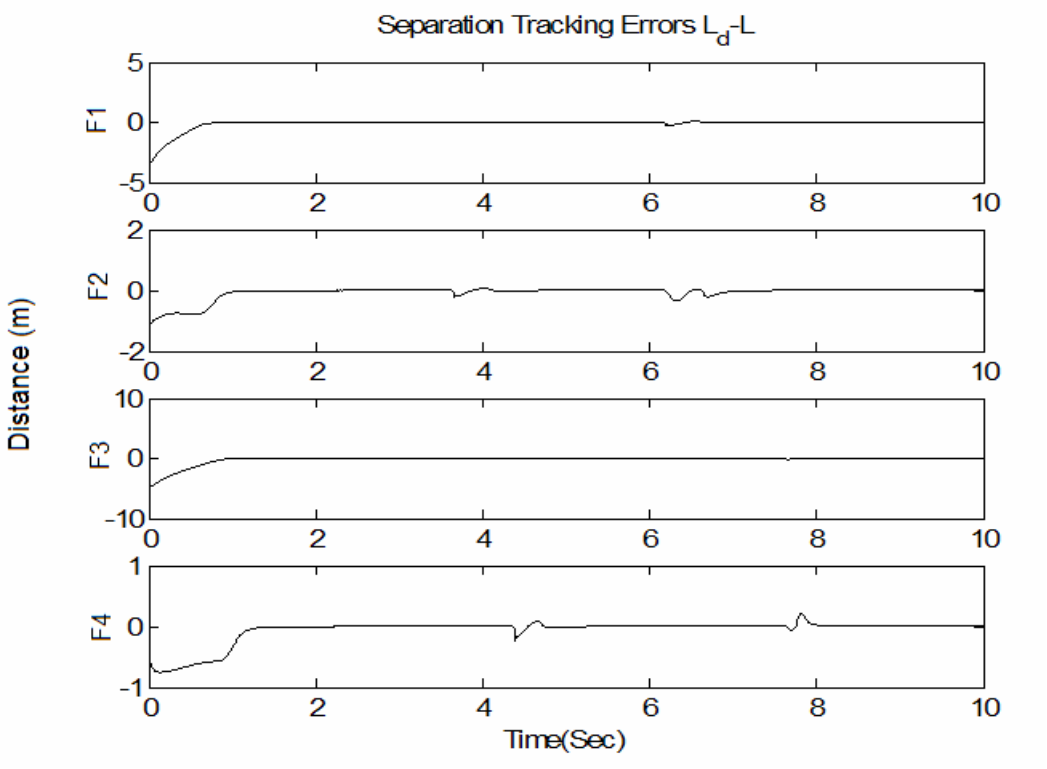

Figure 18: Separation Tracking Errors in a Dynamic Obstacle Environment

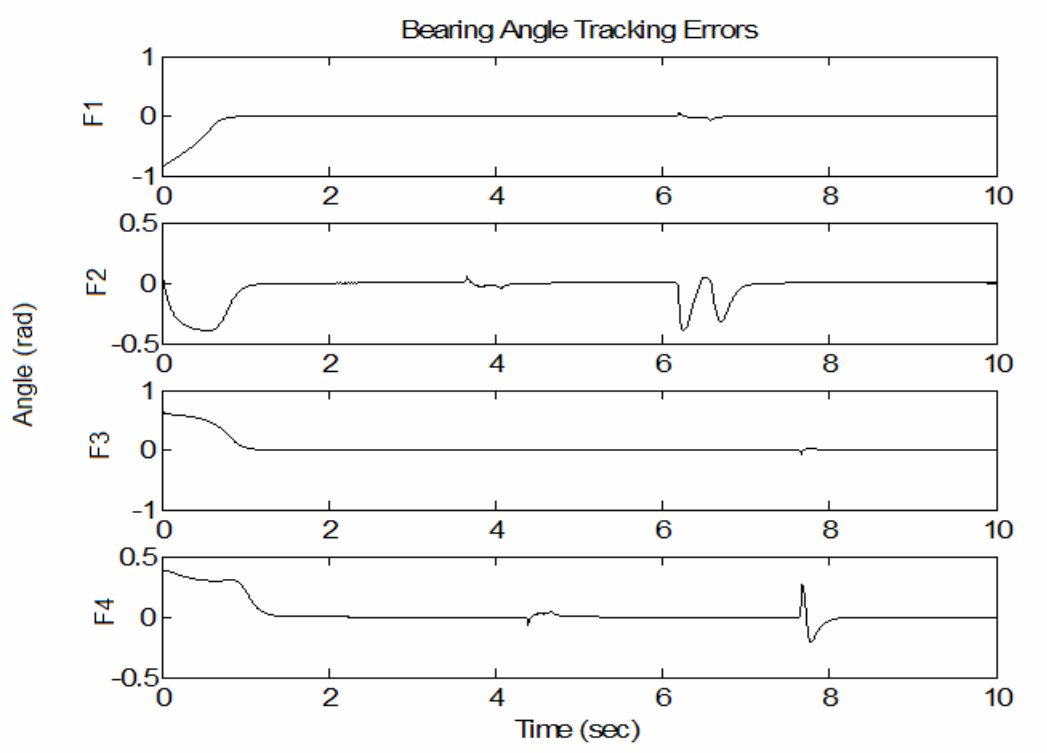

Figure 19: Bearing Errors in a Dynamic Obstacle Environment

V. Conclusions

In the absence of obstacles, a stable tracking controller for leader-follower based formation control was presented that considers the dynamics of the leader and the follower using backstepping. The feedback control scheme is valid even when the dynamics of the followers and their leader are unknown since the NN learns them all online. Numerical results were presented and the stability of the system was verified. Simulation results verify the theoretical conjecture and expose the flaws in ignoring the dynamics of the mobile robots as well as the effects unmodeled dynamics have on conventional computed torque controllers with perfect velocity tracking assumption. In the presence of obstacles, a stable tracking controller was presented which allows each follower robot to navigate around obstacles while simultaneously tracking its leader. The control was shown to be effective in both a static and dynamic obstacle environment, and numerical results were presented. The stability of the system was verified, and the simulation results verified the theoretical conjecture.

VI. References

[1] R. Fierro and F.L. Lewis, "Control of a Nonholonomic Mobile Robot: Backstepping Kinematics Into Dynamics," *Proc. IEEE Conf. on Decision and Contr.*, Kobe, Japan, 1996, pp. 1722-1727.

[2] Y. Kanayama, Y. Kimura, F. Miyazaki, and T. Noguchi, "A Stable Tracking Control Method for an Autonomous Mobile Robot," *Proc. IEEE International Conference on Robotics and Automation*, vol. 1, pp384-389, May 1990.

[3] R. Fierro and F. L. Lewis, "Control of a Nonholonomic Mobile Robot Using Neural Networks," *IEEE Transactions on Neural Networks*, vol. 8, pp589-600, July 1998.

[4] M. Egerstedt, X. Hu, and A. Stotsky, "Control of Mobile Platforms Using a Virtual Vehicle Approach," *IEEE Transactions on Automatic Control*, vol. 46, pp 1777-1782, November 2001.

[5] T. Fukao, H. Nakagawa, and N. Adachi, "Adaptive Tracking Control of a Nonholonomic Mobile Robot," *IEEE Transactions on Robotics and Automation*, vol. 16, pp 609-615, October 2000.

[6] J. Lawton, R. Bear, and B. Young, "A Decentralized Approach to Formation Maneuvers," *IEEE Transactions on Robotics and Automation*, vol. 19, pp 933-941, December 2003.

[7] T. Balch and R. Arkin, "Behavior-Based Formation Control for Multirobot Teams," *IEEE Transaction on Robotics and Automation*, vol. 15, pp 926-939, December 1998.

[8] J. Fredslund and M. Mataric, "A General Algorithm for Robot Formations Using Local Sensing and Minimal Communication," *IEEE Transactions on Robotics and Automation*, vol. 18, pp 837-846, October 2002.

[9] Stephen Spry and J. Karl Hedrick, "Formation Control Using Generalized Coordinates," in *Proceedings of IEEE International Conference on Decision and Control*, Atlantis, Paradise Island, Bahamas, pp. 2441 – 2446, December 2004.

[10] P. Ogren, M. Egerstedt, and X. Hu, " A Control Lyapunov Function Approach to Multiagent Coordination," *IEEE Transactions on Robotics and Automation*, vol. 18, pp 847-851, October 2002.

[11] Kar-Han Tan and M. A. Lewis, "Virtual Structures for High-Precision Cooperative Mobile Robotic Control," *Proceedings of the 1996 IEEE/RSJ International Conference Intelligent Robots and Systems*, vol. 1, pp. 132–139, November 1996.

[12] G. L. Mariottini, G. Pappas, D. Prattichizzo, and K. Daniilidis, "Vision-based Localization of Leader-Follower Formations," *Proc. IEEE European Control Conference on Decision and Control*, pp 635-640, December 2005.

[13] X. Li, J. Xiao, and Z. Cai, "Backstepping Based Multiple Mobile Robots Formation Control," *Proc. IEEE International Conference on Intelligent Robots and Systems*, pp 887-892, August 2005.

[14] A. Das, R. Fierro, V. Kumar, J. Ostrowski, and J. Spletzer, C. Taylor, "A Vision-Based Formation Control Framework," *IEEE Transactions on Robotics and Automation*, vol. 18, pp 813-825, October 2002.

[15] H. Hsu and A. Liu, "Multi-Agent Based Formation Control Using a Simple Representation," *Proc. IEEE International Conference on Networking, Sensing & Control*, Taipei, Taiwan, pp 276-282, March 2004.

[16] J. Shao, G. Xie, J. Yu, and L. Wang, "A Tracking Controller for Motion Coordination of Multiple Mobile Robots," *Proc. IEEE International Conference on Intelligent Robots and Systems*, pp 783-788, August 2005.

[17] Y. Li and X. Chen, " Dynamic Control of Multi-robot Formation," P*roc. IEEE International Conference on Mechatronics*, Taipei, Taiwan, pp 352-357, July 2005.

[18] Jaydev P. Desai, Jim Ostrowski, and Vijay Kumar, "Controlling Formations of Multiple Mobile Robots," *Proc. IEEE International Conference on Robotics and Automation*, pp. 2864-2869, Leuven, Belgium, May 1998.

[19] F.L. Lewis, S. Jagannathan, and A. Yesilderek, "*Neural Network Control of Robot Manipulators and Nonlinear Systems*," Taylor and Francis, London, UK, 1999.

[20] O. Khatib, “Real-time obstacle avoidance for manipulators and mobile robots,” *Intl. Journal of Robotics Research*, vol. 5, no. 1, pp. 90–98, 1986.

[21] T. Dierks, and S. Jagannathan, "Control of Nonholonomic Mobile Robot Formations: Backstepping Kinematics into Dynamics" to appear in IEEE Multi-conference on Systems and Control, Singapore, 2007.

[22] T. Dierks, "Nonlinear Control of Nonholonomic Mobile Robot Formations", MS Thesis, at the University of Missouri-Rolla, 2007. Available via the internet: (URL: http://www.umr.edu/~tad5x4/RFC_paper1.pdf)

SECTION

2. CONCLUSIONS AND FUTURE WORK

In this thesis, a combined kinematic/torque controller was developed for controlling formations of nonholonomic robots under two scenarios. First, an asymptotically stable controller was developed under the assumption that all robot dynamics were known and available to each robot. The asymptotic stability was shown using Lyapunov methods and numerical results were presented supporting the theoretical conjecture and exposing the flaws in ignoring the dynamics of the mobile robots. Dynamics, like the centripetal/coriolis terms, become an influence on the robots during maneuvers as simple as turning, and the path the robots take when the dynamics are modeled is different than the path the robots take when the dynamics are ignored.

In the second scenario, the assumption of full information about the robot dynamics is removed by introducing a neural network (NN). The universal approximation property of the NN is utilized to learn the complete dynamics of the robot formation including terms like friction, and it was shown using Lyapunov theory that the errors for the entire formation are uniformly ultimately bounded. Numerical results were provided supporting the theoretical conjecture and revealing the flaws associated with perfect velocity tracking assumptions. It was shown that even when the dynamics of the robots are known perfect velocity tracking assumptions do not hold in presence of dynamics and the formation failed to form correctly.

Additionally, a stable tracking controller was presented which allows each follower robot to navigate around obstacles while simultaneously tracking its leader. The control was shown to be effective in both a static and dynamic obstacle environment. The

stability of the system was verified, and the simulation results verified the theoretical conjecture.

In future work, the NN controller developed here can be extended to utilize a NN with multiple layers of tunable weights since a multilayer NN possesses better approximation properties than a NN with a single layer of tunable weights. However, the closed-loop stability is more involved using a multi-layer NN. Additionally, a NN controller can be combined with the robust integral of the sign of the error (RISE) feedback. By incorporating the RISE feedback, it is possible to show that the errors for the entire formation are asymptotically stable and the NN weights are bounded using Lyapunov theory as opposed to uniformly ultimately bounded (UUB) stability which is typical with most NN controllers. It is important to notice that asymptotic stability is a more powerful result than UUB.

VITA

Travis Dierks was born in Chester, Illinois on December 22, 1982. He earned a Bachelor of Science degree in Electrical Engineering while attending the University of Missouri-Rolla in December of 2005. Supported by a GAANN fellowship, he earned a Master of Science degree in Electrical Engineering in August of 2007 while attending the University of Missouri-Rolla.